

Calibration of Material Models for Estimating Impact of Construction Quality on Life Cycle Performance of Pavements

Research Report Number 0-4046-3

TxDOT Project Number 0-4046

**Conducted for:
Texas Department of Transportation &
Federal Highway Administration**

February 2006

**Center for Transportation Infrastructure Systems
The University of Texas at El Paso
El Paso, TX 79968
(915) 747-6925
<http://ctis.utep.edu>**

TECHNICAL REPORT STANDARD TITLE PAGE

1. Report No. FHWA/TX-06/0-4046-3		2. Government Accession No.		3. Recipient's Catalog No.	
4. Title and Subtitle Calibration of Material Models for Estimating Impact of Construction Quality on Life Cycle Performance of Pavements				5. Report Date February 2006	
				6. Performing Organization Code	
7. Authors Brett. T. Haggerty, Imad Abdallah and S. Nazarian				8. Performing Organization Report No. Research Report 0-4046-3	
9. Performing Organization Name and Address Center for Transportation Infrastructure Systems The University of Texas at El Paso El Paso, Texas 79968-0516				10. Work Unit No.	
				11. Contract or Grant No. Project No. 0-4046	
12. Sponsoring Agency Name and Address Texas Department of Transportation Office of Research and Technology Implementation P.O. Box 5080 Austin, Texas 78763-5080				13. Type of Report and Period Covered Technical Report 9/02- 1/05	
				14. Sponsoring Agency Code	
15. Supplementary Notes Project performed in cooperation with the Texas Department of Transportation and the Federal Highway Administration Research Study Title: Impacts of Construction Quality on Life Cycle Performance of Pavements Using Mechanistic Analysis					
16. Abstract Constructing a pavement that will perform well throughout its expected design life is the main goal of any highway agency. The relationship between construction parameters and pavement life, defined by structural models, can be described using material models. An algorithm that can model the complexity and identify construction parameters that affect the stiffness and consequently remaining life of the pavement system has been developed. Such an algorithm can provide contractors with the ability to concentrate on the parameters that can significantly improve the quality of the pavement. By reducing variability of construction parameters and by improving the material stiffness, one can thereby statistically minimize the impact of construction activities on pavement deterioration. In this report, the process used to calibrate material models that relate the construction parameters to moduli has been carried out.					
17. Key Words Construction parameters, Material models, Pavement Performance, Statistical analysis, Variability			18. Distribution Statement No restrictions. This document is available to the public through the National Technical Information Service, 5285 Port Royal Road, Springfield, Virginia 22161, www.ntis.gov .		
19. Security Classified (of this report) Unclassified		20. Security Classified (of this page) Unclassified		21. No. of Pages 109	22. Price

Calibration of Material Models for Estimating Impact of Construction Quality on Life Cycle Performance of Pavements

by

**Brett Haggerty, MSCE
Imad Abdallah, MSCE
and
Soheil Nazarian, Ph.D., P.E.**

Research Project TX-0-4046

**Impacts of construction Quality on the Life-Cycle
Performance of Pavements Using Mechanistic Analysis**

Performed in cooperation with the

**Texas Department of Transportation
and the Federal Highway Administration**

Research Report 0-4046-3

**The Center for Transportation Infrastructure Systems
The University of Texas at El Paso
El Paso, TX 79968-0516
February 2006**

DISCLAIMER

The contents of this report reflect the view of the authors, who are responsible for the facts and the accuracy of the data presented herein. The contents do not necessarily reflect the official views or policies of the Texas Department of Transportation or the Federal Highway Administration. This report does not constitute a standard, specification, or regulation.

The material contained in this report is experimental in nature and is published for informational purposes only. Any discrepancies with official views or policies of the Texas Department of Transportation or the Federal Highway Administration should be discussed with the appropriate Austin Division prior to implementation of the procedures or results.

NOT INTENDED FOR CONSTRUCTION, BIDDING, OR PERMIT PURPOSES

Brett Timothy Haggerty, MSCE
Imad Abdallah, MSCE
Soheil Nazarian, Ph.D., P.E. (69263)

ACKNOWLEDGMENTS

The successful progress of this project could not have happened without the help and input of many personnel of TxDOT. The authors acknowledge Mr. Steve Smith, the project PD and David Head, the project PC for facilitating the collaboration and with TxDOT Districts. They have also provided valuable guidance and input.

Special thanks to the PAs, Ms. Lisa Lukefahr, and Mr. Tomas Saenz whom were involved in development of the protocol for data collection and have helped in the success of the product being developed under this project.

There was extensive field and laboratory work involved with this project and several districts were visited. The authors would like to thank all the TxDOT personal that helped in the data collection process. Special appreciation to the following people who were very instrumental in the process: Karl Bednarz (Director of Construction, San Angelo), Gary Humes (Director of Construction, Brownwood), Luis Peralez (Transportation Engineer, Pharr), Mohammad Moabed (Area Office Engineer, Fort Stockton), Richard Williammee (Laboratory Engineer, Fort Worth), and Alan Easterling (Laboratory Supervisor, Fort Worth).

EXECUTIVE SUMMARY

The ability of a flexible or rigid pavement to perform adequately throughout its design life is one of the biggest challenges that transportation agencies face. One factor that has a large impact on the performance of a pavement is the quality of construction. The implementation of an effective performance-based construction quality management program is one way of ensuring that pavements are meeting their expected service life. As a part of that program a tool for determining impact of construction quality on life-cycle performance of pavements is required.

Ideally, if a pavement section is designed with the same cross section and constructed with the same materials, its performance should be uniform throughout the section. This is not the case in the real world. Almost every constructed road develops distresses randomly in different subsections of the pavement. One reason for the random development of distress is the variability in construction quality. As such the goal in this project is to devise a tool that can be used to identify and minimize variability in material properties that impact the performance of the pavement to ensure a performance period compatible with the expected life of the pavement. With that framework, structural models that predict performance of pavements and material models that relate construction parameters to primary design parameters were identified. Finally, a statistical algorithm that relates the impact of each construction parameter to the performance of a pavement is incorporated into the algorithm.

To arrive at realistic conclusions, the material models have to be calibrated to the local conditions. This report contains the information and process necessary for calibrating such models.

IMPLEMENTATION STATEMENT

At this stage of the project the tools developed can be used for limited implementation. The software has undergone major changes to increase its flexibility and expand its ability to identify and minimize variability in material properties that impact the performance of the pavement to ensure a performance period compatible with the expected life of the pavement. The software is called Rational Estimation of Construction Impact on Pavement Performance (RECIPPE). It can be used to reconcile the results from realistic pavement-performance models used in the state of practice, or those widely accepted by state agencies, with statistical process control techniques and uncertainty analysis methods, to determine project-specific parameters that should be used in construction quality management

TABLE OF CONTENTS

CHAPTER ONE - INTRODUCTION	1
PROBLEM STATEMENT	1
OBJECTIVE	2
ORGANIZATION	2
CHAPTER TWO - BACKGROUND	3
BACKGROUND	3
Methodology	4
PROTOTYPE DESCRIPTION.....	6
Material Models	6
Performance Models	8
Impact Charts	9
CHAPTER THREE - ILLUSTRATIVE EXAMPLE USING ACP PARAMETERS	15
INTRODUCTION	15
CHAPTER FOUR - ALGORITHM OPTIMIZATION	23
INTRODUCTION	23
EFFICIENCY OF TIME.....	23
Reduction Of Parameters	24
Reduction Of Simulations	25
Improving Amount Of Necessary Computer Memory	25
UNCERTAINTY ANALYSIS, AUTOMATION & CUSTOMIZATION	25
Uncertainty Analysis In Performance Models	25
Automation Of Reduction Process	28
<i>Largest Impact Value Reduction</i>	28
<i>N-Largest Impact Value Reduction</i>	28
<i>Setting Limitations for the Input COV</i>	29
Adjustment Of Models	29
Customization Of Material And Performance Models	29
Generation Of New Models	30
Model Calibration	30
QA/QC METHODS	32
Number Of Samples	32

Control Charts	36
Cost Analysis.....	41
CHAPTER FIVE - CALIBRATION OF AC, BASE AND SUBGRADE MODULUS MODELS.....	43
INTRODUCTION	43
DATA COLLECTION.....	43
Literature	43
In-Situ & Laboratory Data	45
ASPHALT CONCRETE MATERIAL MODEL CALIBRATION.....	45
Single Variable Linear Regression.....	50
Modifying Coefficients Of Witczak Equation	50
Multivariable-Nonlinear Regression	51
BASE & SUBGRADE MATERIAL MODEL CALIBRATION.....	53
Base Material Model Calibration	57
Subgrade Material Model Calibration.....	61
CHAPTER SIX - CASE STUDY.....	65
CASE STUDY	65
Problem Statement	65
Manual Procedure	66
Manual Results.....	67
Automation Results.....	70
Post-Construction Analysis.....	71
Cost Analysis.....	74
CHAPTER SEVEN - CONCLUSIONS AND RECOMMENDATIONS	77
SUMMARY	77
CONCLUSIONS.....	77
RECOMMENDATIONS FOR FUTURE STUDY	78
REFERENCES.....	79
APPENDIX A - RESULTS OF THE SENSITIVITY STUDY FOR OF ASPHALT CONTENT OF AC LAYER.....	81
APPENDIX B - RESULTS OF THE SENSITIVITY STUDY FOR AIR VOIDS OF AC LAYER.....	89

LIST OF TABLES

Table 3.1 – Values of ACP Material model Parameters Used in Case Study	15
Table 3.2 – Matrix of Pavement Sections Used for Illustrating RECIPE	16
Table 4.1 – Insensitive Parameters Removed from Simulation.....	24
Table 4.2 – Input Parameters to Material Models.....	25
Table 4.3 – Reliability Example for Determining Acceptable Levels of a Parameter	28
Table 4.4 – Sample Size Example Inputs	35
Table 4.5 – Calculation of Subgroup Means	37
Table 4.6 – Popular Sensitizing Rules Currently in Practice.....	39
Table 4.7 – Sample COV Subgroup’s for Control Chart Example.....	40
Table 4.8 – Typical Inspection Tests & Costs for Texas Pavements.....	42
Table 5.1 – Filtered Data Extracted from LTPP Database for AC Layer.....	46
Table 5.2 – LTPP Data Used in Calibration of ACP Model.....	47
Table 5.3 – Testing Techniques for Base and Subgrade Parameters.....	48
Table 5.4 – Texas Test Sites Visited for Limited Calibration of Models.....	48
Table 5.5 – Summary of Laboratory and In-Situ Data Collected for Calibration of Base Subgrade Models	49
Table 5.6 – Correlation Matrix of Base Construction Parameters Used for Material Model Calibration.....	55
Table 5.7 – Correlation Matrix of Subgrade Construction Parameters Used for Material Model Calibration	56
Table 5.8 – Resulting Correlation Matrix of Simulated Base Construction Parameters Used for Material Model Calibration.....	58
Table 5.9 – Resulting Correlation Matrix of Simulated Subgrade Construction Parameters Used for Material Model Calibration.....	59
Table 6.1 – Darrington Road Design Parameters from Specifications.....	66
Table 6.2 – Darrington Road Base Construction Parameters from Historical Data	66
Table 6.3 – Change in Construction Parameter COV for Final Pavement Performance Results	70
Table 6.4 – Measured Optimum Moisture Content for the first 24,000 yd. ³ of Darrington Road.....	71

Table 6.5 – Initial and Calculated Construction Parameter Sample Sizes.....	75
Table 6.6 – Cost Analysis for Guide Schedule and RECIPPE Sample Sizes.....	76

LIST OF FIGURES

Figure 2.1 – Conceptual Framework for Optimization of Construction Parameters through Mechanistic Analysis.....	4
Figure 2.2 – General Flow of Methodology	5
Figure 2.3 – Theoretical Continuous Curve for Base Thickness.....	10
Figure 2.4 – TPM Simulated Curve for Base Thickness with Normal Distribution.....	10
Figure 2.5 – Impact Chart.....	12
Figure 2.6 – RECIPPE Methodology with Specification of Statistical Algorithm Flow	13
Figure 3.1 – Impact of Variability in Asphalt Content on Remaining Lives.....	17
Figure 3.2 – Results of Impact of Variability of Asphalt Content on Remaining Life for Four Typical Pavement Sections.....	18
Figure 3.3 – Results of Impact of Variability of Air Voids on Remaining Life Varying AC Modulus.....	19
Figure 3.4 – Results of Impact of Variability of Air Voids on Remaining Life for Four Typical Pavement Sections.....	21
Figure 4.1 – Probability Density Function for Continuous Functions.....	27
Figure 4.2 – Customization of Models	30
Figure 4.3 – Generation of New Models	31
Figure 4.4 – Model Calibration.....	31
Figure 4.5 – Statistical Rejection and Acceptance.....	33
Figure 4.6 – Probability of Type II Error.....	34
Figure 4.7 – Typical X-Bar Chart.....	38
Figure 4.8 – Sample X-Bar Chart	39
Figure 4.9 – Sample COV Control Chart.....	41
Figure 5.1 – Results of Calibration of Witczak Model Using Single-Variable Regression	51
Figure 5.2 – Results of Modifying Coefficients of Witczak Model	52
Figure 5.3 – Results of New AC Material Model Using LTPP Database	53
Figure 5.4 – Expected Deflection of a Cantilever under a Point Load	54
Figure 5.5 – Erroneously Simulated Deflections.....	57
Figure 5.6 – Results of Granular Material Model for k_1	60

Figure 5.7 – Results of Granular Material Model for k_2	60
Figure 5.8 – Results of Granular Material Model for k_3	61
Figure 5.9 – Results of Cohesive Material Model for k_1	62
Figure 5.10 – Results of Cohesive Material Model for k_3	62
Figure 6.1 – Constraints & Design Parameter Input.....	67
Figure 6.2 – Construction Parameter Inputs.....	68
Figure 6.3 – Initial Pavement Performance Results for Manual Optimization.....	68
Figure 6.4 – Impact Chart for Initial Manual Optimization.....	69
Figure 6.5 – Secondary Pavement Performance Results from Manual Reduction.....	69
Figure 6.6 – Final Pavement Performance Results from Automated Optimization.....	70
Figure 6.7 – Optimum Moisture Content Mean Control Chart for first 48,000 yd ³ of Darrington Road.....	72
Figure 6.8 – Optimum Moisture Content COV Control Chart for first 48,000 yd ³ of Darrington Road.....	73
Figure 6.9 – Impact Chart Used to Identify the Construction Parameters to Sample.....	76

CHAPTER ONE

INTRODUCTION

PROBLEM STATEMENT

Constructing a pavement that will perform well throughout its expected design life is the main goal of any highway agency. Hence, it becomes necessary to develop a process that reflects the effect of construction on the life of a pavement. This process, in practice, can show the impact of construction quality on how a pavement performs. As a result, cost incentive/disincentive can be quantitatively implemented that incorporates future expenditures due to rehabilitation costs for a poorly constructed pavement.

The relationship between construction parameters and pavement life, defined by structural models, can be described using material models. Material models are created to show connections between construction parameters and quality of pavement materials. For example, if a layer of asphalt concrete pavement (ACP) is completely uniform in properties, no change in its modulus is expected at any location. However, in real world situations this layer will not be completely uniform. This non-uniformity can be attributed to a number of construction parameters, such as aggregate gradation, or binder stiffness or compaction efforts.

Fortunately, the complexities of relating the material stiffness to different constituents can be modeled by applying a statistical analysis. The statistical analysis estimates the average and variance in stiffness for the entire section of an AC layer by considering variability in the constituents. By introducing multiple layers and a larger number of relevant construction parameters, the relationship becomes more complex. Part of this research effort is the development of an algorithm that can model this complexity and identify construction parameters that affect the stiffness, and consequently remaining life of the pavement system.

The goal of this algorithm is to identify, in a quantitative matter, construction parameters that are important to the remaining life of a pavement. Such an algorithm can provide contractors with the ability to concentrate on the parameters that can significantly improve the quality of the

pavement. By reducing the variability of construction parameters and by improving the material stiffness, one can thereby statistically minimize the impact of construction activities on pavement deterioration.

This type of algorithm provides a tool that can determine project-specific parameters that should be used in construction quality management based on statistical process control techniques and uncertainty analysis methods.

OBJECTIVE

The first objective of this study is the development of rational algorithms to reconcile the results from several pavement-performance models used in the state of practice to determine project-specific parameters that should be the focus of the construction quality management. The algorithms incorporate systematic statistical process control techniques and uncertainty analysis methods.

The research effort presented is a continuation of previous work documented by Abdallah et al. (2002). They demonstrated the feasibility of such an algorithm and prototyped it in a program using MS Excel. The work presented in this report describes the optimization of that work. Since several material models found in the literature are used in the algorithm, the second objective is to validate the appropriateness of these models and algorithms, and when necessary, to develop new material models.

The third objective is to improve the prototype program that was developed by Abdallah et al. to be used in practice for the construction of pavements. Once important construction parameters are identified, contractors and inspectors can focus their efforts on those parameters to ensure optimal construction quality.

ORGANIZATION

Chapter 2 of this report introduces information on existing methods, presents an overview of performance-based methodologies, and provides a background on some of the mathematical and analysis tools used in this project. In Chapter 3, an illustration of the algorithm's statistical theory is presented, showing the credibility of the process. Chapter 4 describes adjustments made to the previous prototype to provide optimal results. Also included in Chapter 4 are the additions to the prototype process, including: a) Reliability Analysis, b) Automation of Prototype, c) Sample Size Calculations, d) Control Chart Analysis, and e) Cost Allocation. Chapter 5 describes the calibration of the current material models using regression analysis based upon empirical information. Chapter 6 presents a case study that demonstrates the use of the analysis tool and how the impact of variability of construction parameters impacts variability of performance. Chapter 7, the final chapter, includes the summary of the work accomplished, conclusions based on the results, and future recommendations.

CHAPTER TWO

BACKGROUND

BACKGROUND

Abdallah et al. (2002) showed that a statistics-based algorithm may provide project-specific parameters for construction quality management that may lead to a more efficient use of funds and resources. The basic concept of the process is to first quantify relevant construction parameters for their ideal values and corresponding variances. Once each value has been defined, a mechanistic analysis is employed to estimate the resulting probabilistic remaining life, or performance. The purpose of the developed algorithm is to provide the contractors and designers with the necessary resource to measure the impact of the construction activities on the performance of a project. Ultimately, the production and inspection costs can be optimized and the quality of road can be improved, if the guidelines provided by the algorithm are followed.

Other than Abdallah et al.'s work, several major studies have been carried out relating quality of constructed materials to pavement performance. Weed (1998) describes a conceptual method that utilizes the AASHTO 1993 design procedure with the statistical quality control to predict the as-built life of the pavement, and to tie it to a value using engineering economy principles.

Patel and Thompson (1998) also provide a comprehensive probabilistic-based method for estimating the as-built performance of a pavement using statistical quality control. Unlike Weed (1998), they used a calibrated mechanistic-empirical model developed for the Illinois Department of Transportation.

Ferregut et al. (1999) summarize a large number of mechanistic or mechanistic-empirical models that can be used to predict the remaining lives of pavements based on pavement layer stiffness parameters. The authors also developed a systematic approach to assess the impact of variability of these parameters on the variability of the pavement remaining life.

Ayres and Witczak (1998) describe a probabilistic mechanistic performance model very similar to the one used in the newly-developed mechanistic-empirical design program (Witczak, 2003). The model comprehensively considers a large number of parameters that can impact the performance. For example, moduli of layers and their variations with time and temperature are

the primary parameters used in the predictive models. However, all moduli are predicted from surrogate parameters using regression equations.

The approach that Abdallah et al. (2002) developed is the basis for this report and is summarized below.

Methodology

The general methodology described by Abdallah et al. (2002), as shown in Figure 2.1, is divided into several phases. The first phase is the determination of the construction parameters (represented by the inner circle). The second phase is the selection of the material characteristics models (represented by the middle circle), which is the link between the construction parameters and the pavement performance (represented by the outer circle). These phases form the mechanistic process, and are used in a tool to estimate the impact of construction variability on performance. Once the parameters and models from the three phases are established, the probabilistic algorithms allow pavement engineers to maximize the effectiveness of inspection and to optimize the testing resources during the construction process.

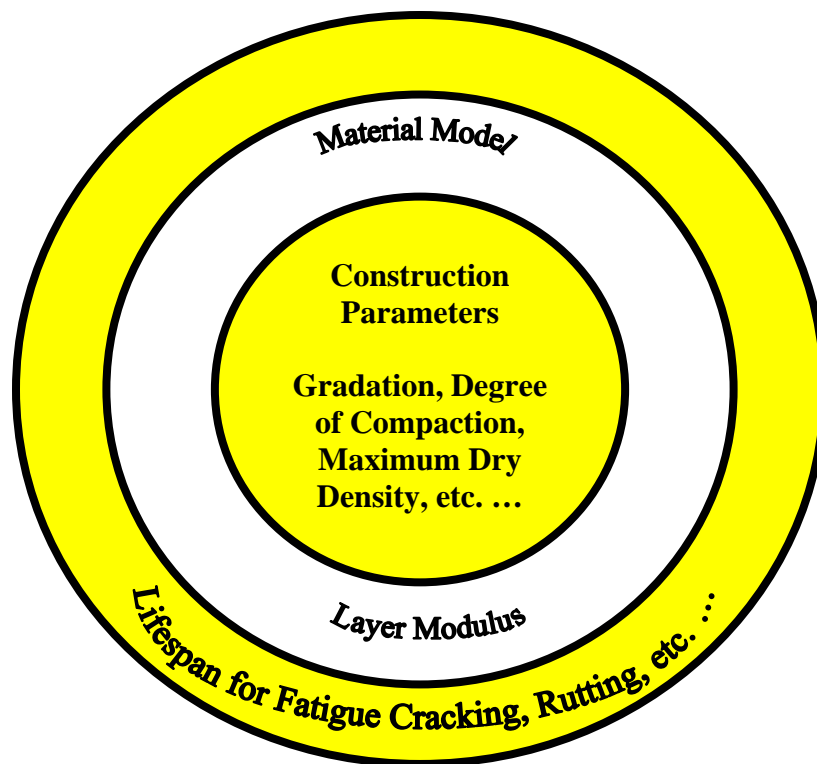


Figure 2.1 - Conceptual Framework for Optimization of Construction Parameters through Mechanistic Analysis

In practical terms, the contractor is trying to achieve acceptable limits for pavement life (with respect to fatigue cracking, rutting, etc. ...) as specified by the designer. The only way the contractor can hope to meet the designer's specifications is by manipulating elements within the

contractor’s control (the construction parameters). Hence, the conceptual framework, as depicted in Figure 2.1, shows how the contractor can accomplish the designer’s specifications.

This methodology can also be utilized as an iterative process that adjusts construction parameter variability until acceptable pavement performance variability is achieved. To be specific, Figure 2.2 shows how this methodology can be used to obtain the desired performance by focusing on the most important construction parameters.

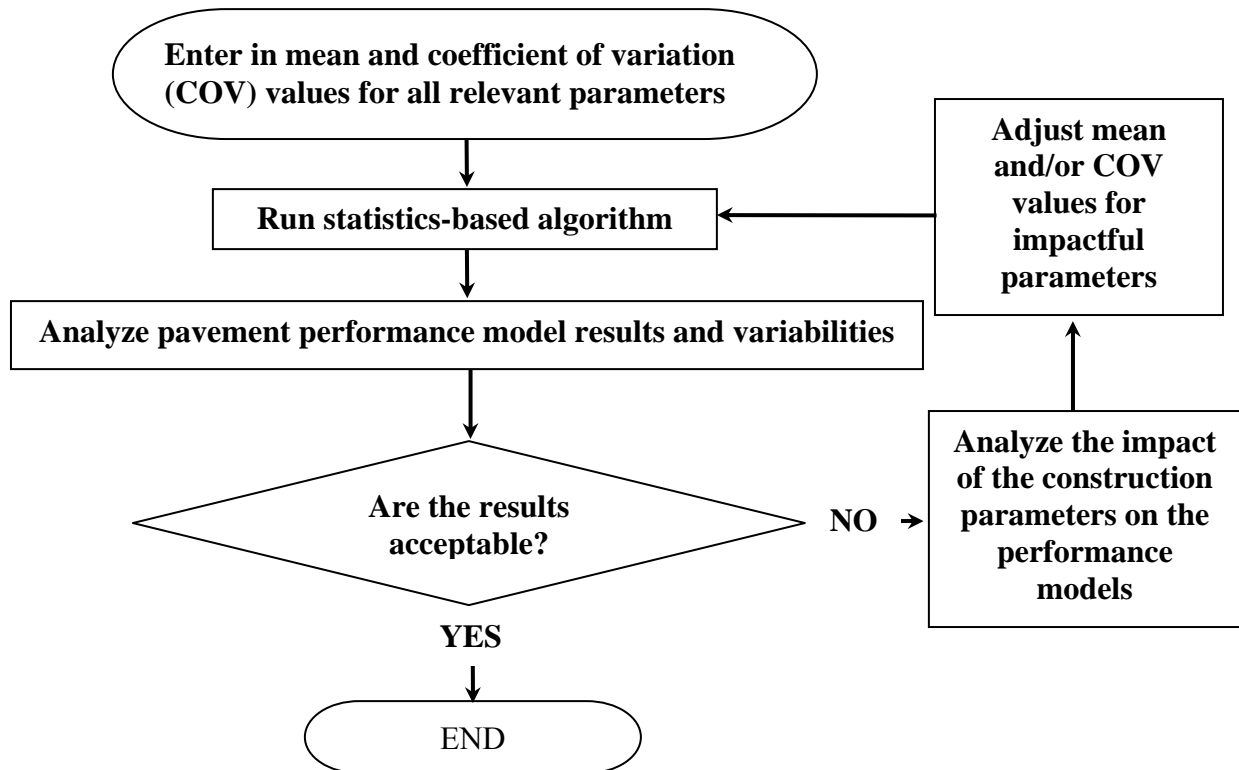


Figure 2.2 – General Flow of Methodology

The initial input, shown in Figure 2.2, is based on the mean and variance of each construction constituent found either in historical data or required specifications. These constituents are then simulated in the statistics-based algorithm by varying the inputs according to a normal distribution and placing the simulations into the material models. The results from the material models are, in turn, entered into the performance equations to estimate the pavement life and pavement life variance. If the simulated pavement life meets the design specifications, the algorithm can provide the contractor with the necessary construction parameter mean and coefficient of variation (COV) values. If the results are not acceptable, the user can adjust COV and/or mean values of relevant construction parameters until the pavement performance specifications are met.

The result of this iterative process is a statistics-based algorithm that provides viable information to improve the quality of pavement through quality assurance/quality control (QA/QC) techniques. The goal of this approach is to minimize the variability in material properties that

impact the performance of the pavement. This effort will promote a pavement that develops distress uniformly.

Abdallah et al. (2002) developed a prototype of an algorithm called “Rational Estimation of Construction Impact on Pavement Performance (RECIPPE).” The prototype was equipped with features that include:

- Material Models
- Performance Models
- Impact Charts

PROTOTYPE DESCRIPTION

The features utilized by the prototype program are detailed by Abdallah et al., but a brief summary is provided within this section.

Material Models

Figure 2.1 showed that material models tie construction parameters to performance models. Material models provide the modulus for individual layers that can be established through the construction parameters. In the initial prototype, a three-layer system could be calculated with an asphalt concrete pavement (ACP) layer, a base layer and a layer of subgrade.

A popular model, known as the “Witczak” model, (see Patel and Thompson, 1998, or Ayers and Witczak, 1998) is a regression-based equation used to determine the modulus of the ACP layer. This equation is shown below:

$$\begin{aligned} \log E_{AC} = & 5.553833 + 0.028829 \frac{P_{200}}{f^{0.17033}} - 0.03476 V_v \\ & + 0.070377 \eta + 0.000005 t_p^{(1.3+0.49825 \log f)} P_{ac}^{0.5} - \\ & 0.00189 t_p^{(1.3+0.49825 \log f)} \frac{P_{ac}^{0.5}}{f^{1.1}} + 0.931757 f^{-0.02774} + \epsilon \end{aligned} \quad (2.1)$$

where E_{AC} is the dynamic modulus of AC mix (in 10^5 psi), η is bitumen viscosity (in 10^6 poise) at 70°F, f is the load frequency (in Hz), V_v is percent air voids in the mix by volume, P_{ac} is percent effective bitumen content by volume, and P_{200} is percent passing No. 200 sieve by total aggregate weight.

Material models for base and subgrade layers are separated for granular and cohesive soils. The popular universal constitutive equation (Barksdale et al., 1997), was adopted for this study. The general form of the universal equation is:

$$M_R = k_1 \theta^{k_2} \sigma_d^{k_3} \quad (2.2)$$

where $\theta = \sigma_1 + \sigma_2 + \sigma_3 =$ bulk stress, and $\sigma_d = \sigma_1 - \sigma_3 =$ deviator stress (σ_1 , σ_2 and σ_3 are the three principal stresses). Parameter M_R represents the resilient modulus of a specimen.

Parameters k_1 , k_2 and k_3 are material and physical parameters that are obtained from equations developed from a multiple regression procedure (Santha, 1994). These parameters are defined separately for granular soils, including the base, and cohesive soils. For granular materials, these parameters are found using:

$$\begin{aligned} \text{Log}(k_1) = & 3.479 - 0.07 * MC + 0.24 * MCR + 3.681 \\ & * COMP + 0.011 * SLT + 0.006 * CLY - 0.025 * \\ & SW - 0.039 * DEN + 0.004 * \left(\frac{SW^2}{CLY} \right) + 0.003 * \left(\frac{DEN^2}{S40} \right) \end{aligned} \quad (2.3)$$

$$\begin{aligned} k_2 = & 6.044 - 0.053 * MOIST - 2.076 * COMP + 0.0053 \\ & * SATU - 0.0056 * CLY + 0.0088 * SW - 0.0069 * SH \\ & - 0.027 * DEN + 0.012 * CBR + 0.003 * \left(\frac{SW^2}{CLY} \right) - 0.31 * \frac{(SW + SH)}{CLY} \end{aligned} \quad (2.4)$$

$$\begin{aligned} k_3 = & 3.752 - 0.068 * MC + 0.309 * MCR - 0.006 * SLT \\ & + 0.0053 * CLY + 0.026 * SH - 0.033 * DEN \\ & - 0.0009 * \left(\frac{SW^2}{CLY} \right) + 0.00004 * \left(\frac{SATU^2}{SH} \right) - 0.0026 * CBR * SH \end{aligned} \quad (2.5)$$

In Equations 2.3 through 2.5, MCR represents the ratio of moisture content (MC) to optimum moisture content (MOIST), COMP is the degree of compaction and SATU is the degree of saturation. Also, S40 represents the percent passing sieve #40, SLT is the percent of silt, CLY is the percent of clay in the layer, SW is the percent of swell value, SH is the percent of shrinkage, DEN is the maximum dry density (in pcf) and CBR is the California bearing ratio.

For cohesive materials, the following set of equations is used:

$$\begin{aligned} \text{Log}(k_1) = & 19.813 - 0.045 * MOIST - 0.131 * MC - 9.171 \\ & * COMP + 0.0037 * SLT + 0.015 * LL - 0.016 * PI \\ & - 0.021 * SW - 0.052 * DEN + 0.00001 * S40 * SATU \end{aligned} \quad (2.6)$$

$$k_2 = 0 \quad (2.7)$$

$$\begin{aligned} k_3 = & 10.274 - 0.097 * MOIST - 1.06 * MCR - 3.471 \\ & * COMP + 0.0088 * S40 - 0.0087 * PI + 0.014 * SH \\ & - 0.046 * DEN \end{aligned} \quad (2.8)$$

The dependent parameters used in Equations 2.6 through 2.8 are the same as described for the granular materials, except for the PI and LL values, which stand for the plasticity index and liquid limit, respectively.

Performance Models

Once the modulus of each layer has been determined, it can be translated to the remaining life of the pavement through pavement performance models. To benchmark similar analyses, four performance models that represent possible modes of failure for flexible pavements have been used.

The first model, which deals with the permanent deformation in the ACP layer, is (Finn et al., 1984):

$$\log RR = -5.617 + 4.343 \log w_0 - 0.167 \log(N_{18}) - 1.118 \log \sigma_c \quad (2.9)$$

Equation 2.9 is applicable to ACP layers that are less than 6 in. thick. For full-depth asphalt pavement with ACP equal to or greater than 6 in. in thickness:

$$\log RR = -1.173 + 0.717 \log w_0 - 0.658 \log(N_{18}) + 0.666 \log \sigma_c \quad (2.10)$$

where RR is the rate of rutting in micro-inches (1 $\mu\text{in.} = 10^{-6}$ in.) per axle load repetition, w_0 is the surface deflection in mil (1 mil = 10^{-3} in.), σ_c is the vertical compressive stress under the ACP in psi, and N_{18} is the equivalent 18-kip single-axle load in 10^5 ESALS. Since the pavement has not been constructed, the surface deflection, w_0 , is obtained by executing the forward model with the mean values for the pavement layer properties under 9000 lb load.

The second pavement performance method concentrates on finding permanent deformation in the subgrade, as defined in Equation 2.11 (Huang, 1993).

$$N_d = f_4 (\varepsilon_c)^{-f_5} \quad (2.11)$$

In addition to permanent deformation, pavement failure may also result from cracking. This particular type of pavement failure is calculated using the following equation (Huang, 1993):

$$N_f = f_1 (\varepsilon_t)^{-f_2} (E_1)^{-f_3} \quad (2.12)$$

where N_f and N_d are the allowable number of load repetitions to prevent fatigue cracking and rutting respectively, ε_t is the tensile strain at the bottom of the ACP layer, E_1 is the elastic modulus of asphalt-concrete layer (in psi), ε_c is the compressive strain at the top of subgrade and parameters f_1 through f_5 are design constants derived from field and laboratory testing. Commonly used coefficients are based on the Asphalt Institute equation where f_1 through f_5 are 0.0796, 3.291, 0.854, 1.365×10^{-9} and 4.477, respectively (Huang, 1993).

The final model was developed by the American Association of State Highway and Transportation Officials (AASHTO) for flexible pavements to estimate the cumulative expected

18-kip equivalent single-axle load. This model was developed to consider environmental, serviceability and reliability factors, in the form of:

$$\log_{10}(W_{18}) = Z_R \times S_0 + 9.36 \times \log_{10}(SN + 1) - 0.20 + \frac{\log_{10}\left[\frac{\Delta PSI}{4.2 - 1.5}\right]}{0.4 + \frac{1094}{(SN + 1)^{5.19}}} + 2.32 \times \log_{10} M_R - 8.07 \quad (2.13)$$

$$SN = a_1 D_1 + a_2 D_2 \quad (2.14)$$

where W_{18} is the number of 18-kip equivalent single axle load repetitions to failure, ΔPSI is the design serviceability loss, Z_R is the reliability factor, S_0 is the overall standard deviation, SN is the structural number of pavement. Parameters a_1 and a_2 are layer coefficients for the surface and base layers, respectively; and D_1 and D_2 are the thicknesses of the surface and base layers, respectively. Parameter M_R is the effective roadbed soil resilient modulus.

In the AASHTO model for flexible pavements, the only parameters that can be related to design or construction are SN and M_R . Parameter SN is a function of layer coefficients and layer thicknesses. AASHTO design guide proposes a relationship between layer coefficients and the resilient modulus of the corresponding layer approximated by:

$$a_1 = -0.0012E_1^4 + 0.0174E_1^3 - 0.0967E_1^2 + 0.295E_1 - 0.02787 \quad (2.15)$$

where E_1 is modulus of top layer. Similarly, layer coefficient for granular base, a_2 , can be related to its modulus, E_2 , using:

$$a_2 = 0.249(\log E_2) - 0.977 \quad (2.16)$$

The AASHTO equation, although empirically developed, was incorporated into the analysis for completeness. The methodology developed provides flexibility to incorporate several types of performance models as long as the parameters of the equation can be tied into the layer properties.

Impact Charts

Through the models and methodology discussed above, it is possible to estimate the performance for each of the failure modes based on the mean value of the construction parameters (also referred to as deterministic remaining lives). However, in real-world situations, no construction parameter can be constant, and (some variability needs to be considered) consequently, the performance models will also carry variabilities. Hence, for each performance model, the COV is found through a statistical algorithm. The impact charts compare the influence of each construction parameter's corresponding COV on the remaining life COV values. The COV of remaining life is estimated based on two types of probabilistic analysis: 1) Monte Carlo Simulation and 2) Two Point Mass (TPM) Simulation.

Monte Carlo simulations randomly generated values for uncertain variables. In this case, the construction parameters are randomly created multiple times to simulate a continuous model. For example, if the base thickness would vary according to a normal distribution with a mean of 6 inches and a COV of 2%, a continuous curve can be created, as shown in Figure 2.3.

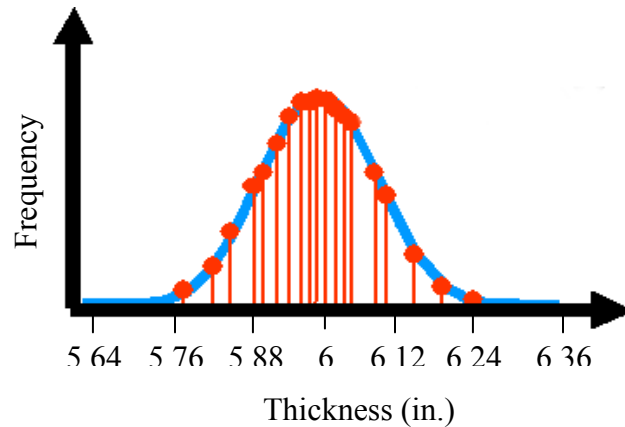


Figure 2.3 – Theoretical Continuous Curve for Base Thickness

Similarly, the TPM simulation is used to approximate low-order moments of functions for construction parameters (Rosenblueth, 1981). This is achieved by replacing continuously randomly generated values with a few discrete values. In this case, the base thickness continuous random variable (represented by a mean, a COV and a skewness coefficient) is replaced by two discrete variables that provide the same mean, COV and skewness coefficient as the continuous distribution. The result is a simulated curve similar to the one shown in Figure 2.4.

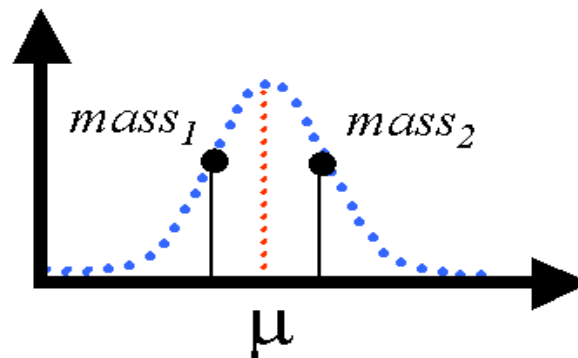


Figure 2.4 – TPM Simulated Curve for Base Thickness with Normal Distribution

The methodology described accounts can handle several different distributions and not just normal. However, the normal distribution was implemented here to simplify the process, since many distributions such as the chi-square can be derived from the normal distribution. Also, RECIPE is developed to accommodate new material models and perhaps new construction parameters and therefore it would be much easier at this time to assume a single distribution. At a later date and depending on the successful use of this program, the selection of the distribution for each parameter can be implemented as part of the input. With the current assumption that all

parameters follow a normal distribution, the skewness coefficient has an equal weight of 0.5 for each mass in the TPM simulation. In the event that the parameter in question does not follow a normal distribution, both the Monte Carlo and Two Point Mass approximations would have to be altered. This occurrence will not be discussed in this study.

The major difference between the Monte Carlo and TPM simulations is the number of iterations it takes to complete a simulation. With a Monte Carlo simulation, 500 simulations are considered adequate enough to model a normal distribution (Abdallah et al., 2002), while the number of iterations for TPM varies with the number of random variables represented by:

$$\text{Iterations}_{\text{TPM}} = 2^{\text{Number of Random Variables}} \quad (2.17)$$

For all material and performance models used, two types of statistical analyzes are performed: 1) varying values for a single construction parameter and 2) varying all parameters at once. In this project, the TPM and Monte Carlo simulations can be used independently or in unison.

For the two types of statistical analyses, 31 construction and design parameters are used. In the first type of statistical simulation, the point of interest is varying 31 parameters independently to show how the life of the pavement will vary when only a single parameter is varied. Consequently, using the 31 defined parameters in the Monte Carlo simulation would generate 500 iterations for each parameter. The result would be 15,500 total iterations (31 parameters times 500 simulations for each parameter). With the TPM, the number of iterations is reduced to 62 (31 times 2), while still maintaining a high level of accuracy when compared to a continuous function.

The TPM is a more efficient use of simulation time, but only when varying a small number of parameters at a time. Because Equation 2.17 is used to find the number of simulations for all of the parameters in question, only two simulations are needed for each parameter. However, when all of the parameters are changed simultaneously, the number of calculations using TPM increases exponentially. For example, if one was interested in finding how the material model would vary when all of the construction parameters changed, using TPM would require 231 simulations. This is why the Monte Carlo simulation is a good replacement for this situation, with 500 iterations.

This does not imply, however, that one is limited to using only the Monte Carlo or TPM simulations alone, they can also be run in unison. Due to the modularity of the material and pavement performance equations, the TPM simulations can be used to calculate the variance of the remaining life when one parameter changes, and the Monte Carlo simulations can be used when all of the construction parameters are simulated together. This results in 2062 total simulations; 62 TPM simulations, 500 simulations when only varying ACP parameters, 500 when only varying base parameters, 500 when only varying subgrade parameters and 500 when varying all parameters together. These simulations provide users with the pavement performance variance when one parameter is run, when only the layer moduli changes and when all parameters vary at once.

When the simulation is carried out for a single construction parameter, it is possible to create pie charts showing how each parameter impacts the variability of a performance model with respect to the other construction parameters. The values that are entered into the pie charts are called normalized impact values, shown in Equation 2.18:

$$NIV_i = \frac{\frac{COV_i}{COV_{ALL}}}{\sum_{i=1}^n \frac{COV_i}{COV_{ALL}}} \quad (2.18)$$

where NIV is the normalized impact value for construction parameter i , the COV_i is the coefficient of variation of the pavement performance model for construction parameter i and the COV_{ALL} represents the coefficient of variation for the same pavement performance model when all input parameters, for a single layer, are simultaneously varied.

By placing all of the NIVs in a pie chart, a new definition for the impact of construction parameters on the variability of a remaining life model, or material model, can be created called an impact chart. Figure 2.5 is an example of an impact chart that exhibits the relative impact values of six parameters labeled P_1 to P_6 . In this example, P_1 is very significant and impacts the performance indicator the most, while parameters P_3 and P_6 have negligible impact on the performance indicator. If one is interested in changing the mean and COV of the performance indicator associated with these parameters, she/he should focus on P_1 . By reducing the COV for this parameter, not only will the model COV reduce, but so will the parameter's NIV.

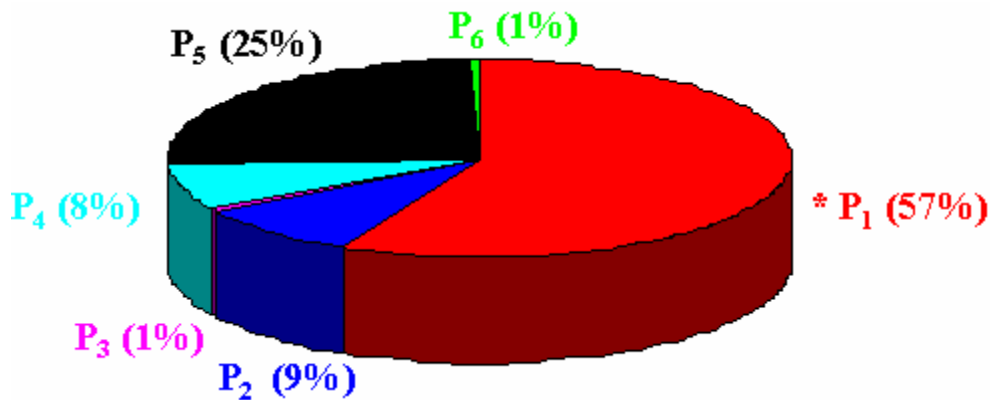


Figure 2.5 – Impact Chart

The material models, pavement performance models and impact charts comprise the statistical algorithm mentioned in Figure 2.2. Now that these processes have been described in detail, the updated flow can be shown in Figure 2.6. Figure 2.6 follows the same flow as the general method, depicted in Figure 2.2. However, the statistical based process, shown in Figure 2.2, has been changed in order to show how impact charts and pavement performance are estimated.

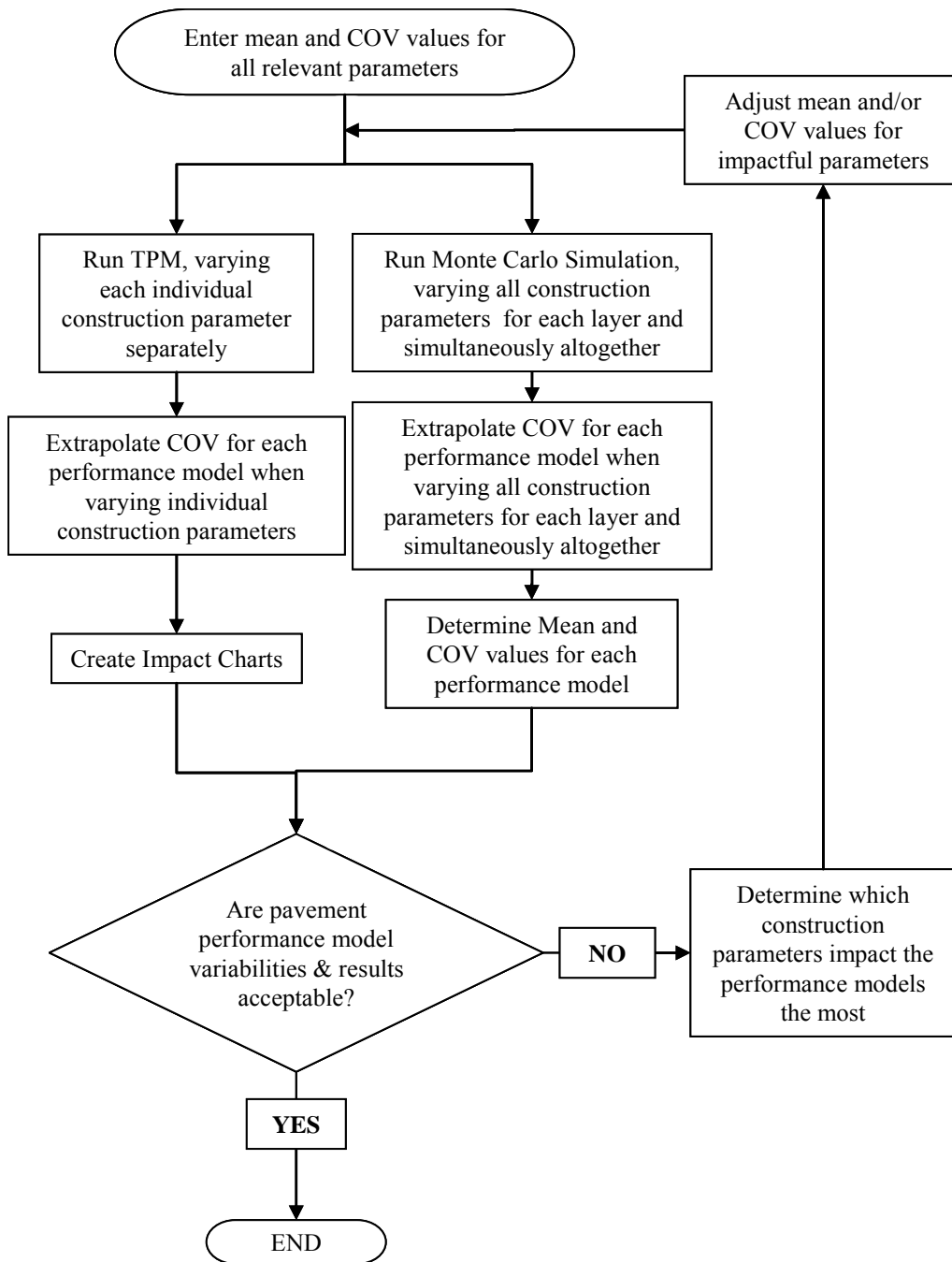


Figure 2.6 – RECIPPE Methodology with Specification of Statistical Algorithm Flow

CHAPTER THREE

ILLUSTRATIVE EXAMPLE USING ACP PARAMETERS

INTRODUCTION

In this chapter, a limited implementation of the algorithms is presented to illustrate the consequence of variability in construction. This process will also demonstrate the use of RECIPPE to identify the impact of construction variability on the pavement performance. In this sample case, the focus will be on the ACP layer. The moduli for the base and subgrade layer are assumed constant with values of 50 ksi and 10 ksi, respectively.

The parameters used in the ACP layer simulation are based on the material model presented in Chapter 2 (Equation 2.1). The model is a function of the following parameters: viscosity of binder, load frequency, percent air voids, percent asphalt content, and percent passing No. 200 sieve. Table 3.1 contains three sets of values for the parameters used in analyzing the ACP layer. Two of the parameters, temperature and loading frequency, are not controlled by the contractor during construction, and as such, these parameters are fixed as illustrated in Table 3.1. The remaining four parameters are controlled by the contractor and the variability of these parameters could change due to construction practices. In this study two parameters (asphalt content and air voids) were selected to illustrate their impacts on pavement performance. The performance models selected for illustrating the methodology were fatigue cracking, subgrade rutting and ACP rutting.

Table 3.1 - Values of ACP Material model Parameters Used in Case Study

Case	% Aggregate. Passing Sieve No. 200	Air Voids, %	Asphalt Content, %	Asphalt Viscosity, 10 ⁶ poise	Temperature,* °F	Loading Frequency*, Hz
1	5	12	5	0.0022	77	18
2	10	8	5	0.0022		
3	15	4	5	0.0022		

* - contractor does not have control over these parameters.

To show the response of the analysis on a wide range of pavement sections, four typical pavements are used in this study. The sections have an ACP thickness varying from 2 in. to 6 in. and for the base layer varying from 6 in. to 12 in. The matrix presented in Table 3.2 contains the combination of cases that were analyzed.

Table 3.2 - Matrix of Pavement Sections Used for illustrating RECIPPE

Modulus (ksi)		Pavement Sections			
		Thin-Thin	Thin-Thick	Thick-Thin	Thick-Thick
Base /Subgrade	ACP*	2in. - 6in.	2in. - 12in.	6in. - 6in.	6in. - 12in.
50 / 10	240	Case 1	Case 1	Case 1	Case 1
	400	Case 2	Case 2	Case 2	Case 2
	680	Case 3	Case 3	Case 3	Case 3

* - ACP moduli are determined from AC material model.

As an example, the variations in the COV of the remaining life, as a function of the COV for the AC content in thin AC and thick base pavements for the three cases in Table 3.1, are presented in Figure 3.1. The mean value of the asphalt content is fixed at 5%. In all three cases, the performance indicator that is impacted the most is fatigue cracking. In Case 1, where the mean air voids is 12%, the COV due to fatigue cracking is 81% for a 50% COV for the AC content. As the mean air voids decrease to 8% and 4%, the COVs of the remaining life due to fatigue cracking decrease to 39% and 19%, respectively.

The variability of the asphalt content on the variability of the performance in terms of subgrade rutting and ACP rutting are small in all three cases. With an AC content COV of 50%, the variability in remaining life due to subgrade rutting increased from 14% to 15% to 19% for Cases 1, 2 and 3, respectively. For remaining life due to ACP rutting, the variability was less than 13%.

The variations in performance indicators, as a function of the COV of AC content at a mean air voids of 8% for the four typical pavement sections, are shown in Figure 3.2. The most sensitive performance indicator changes depending on the thickness of the layers. For the thin ACP pavements (Figures 3.2a and 3.2b), the fatigue cracking is the most sensitive parameter; while for the thick ACP pavements (Figures 3.2c and 3.2d), the subgrade rutting is the most sensitive. In the case of thin ACP pavements, the subgrade rutting and ACP rutting performance indicators show little sensitivity to the COV of the asphalt content. As the thickness of the ACP layer increases, the sensitivity of the subgrade rutting and ACP rutting performance indicators also increases. This trend shows that as the ACP layer thickness increases and the base layer thickness decreases the impact of variability of asphalt content on pavement performance becomes more pronounced. The results of all twelve cases depicted in Table 3.2, for the impact of varying asphalt content, are graphically presented and summarized in a tabular form in Appendix A.

In part 2 of the case study, the variations in the COV of the remaining lives are analyzed as a function of the COV of the air void contents. The air void contents of the ACP layer were changed from 12% to 8% to 4%. As an example, the results from the thin ACP-thin base section are shown in Figure 3.3.

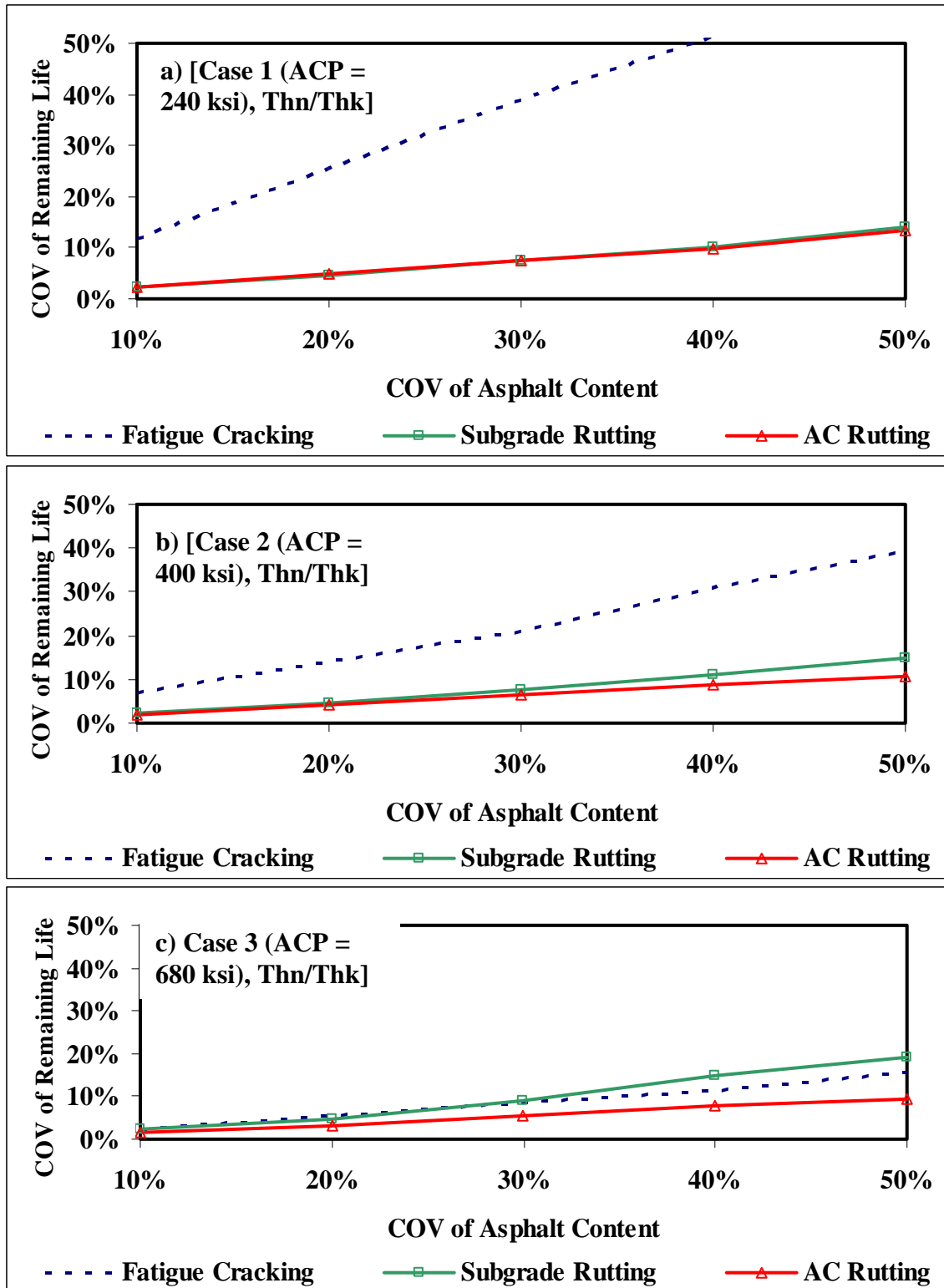


Figure 3.1 - Impact of Variability in Asphalt Content on Remaining Lives

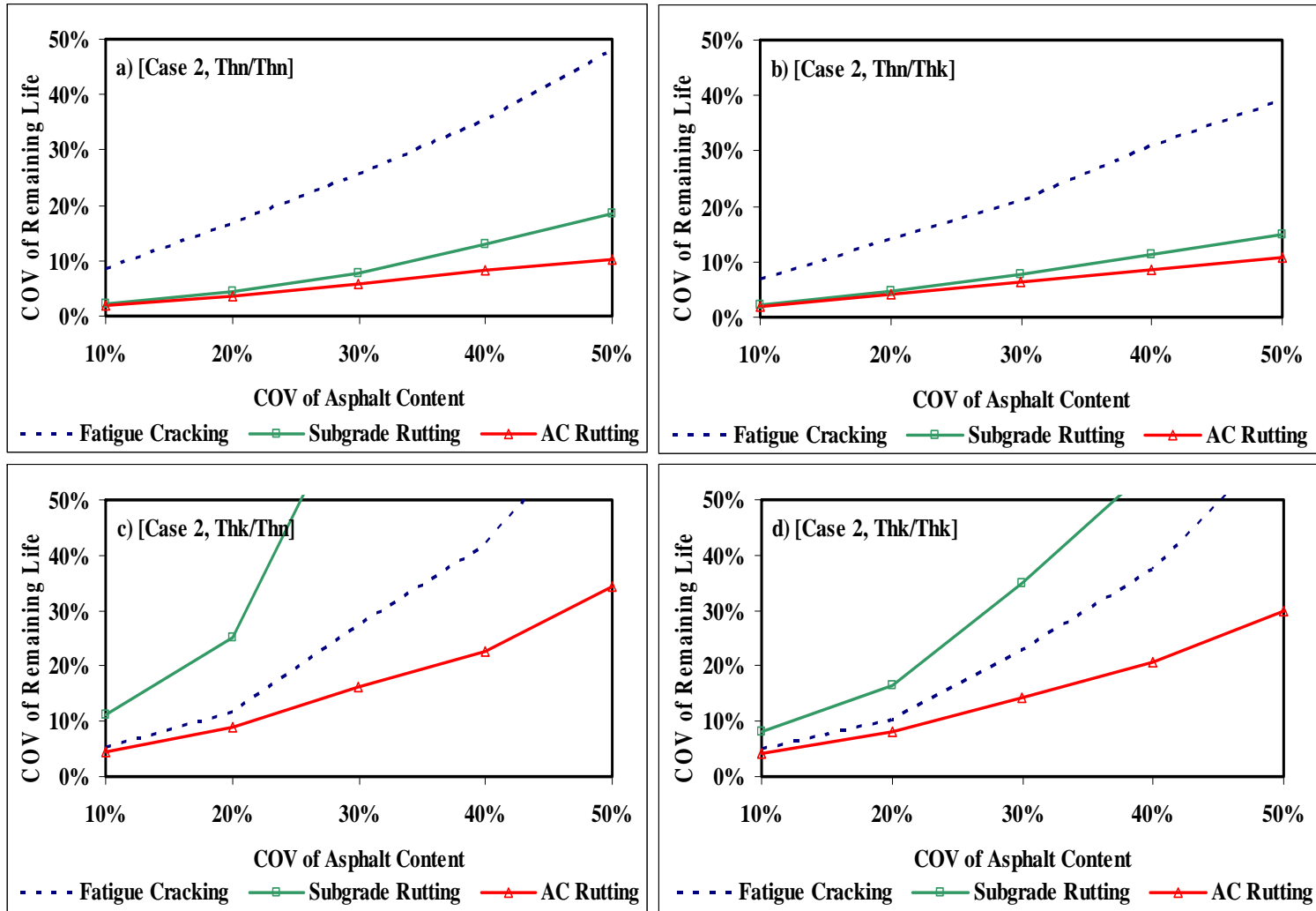


Figure 3.2 - Results of Impact of Variability of Asphalt Content on Remaining Life for Four Typical Pavement Sections

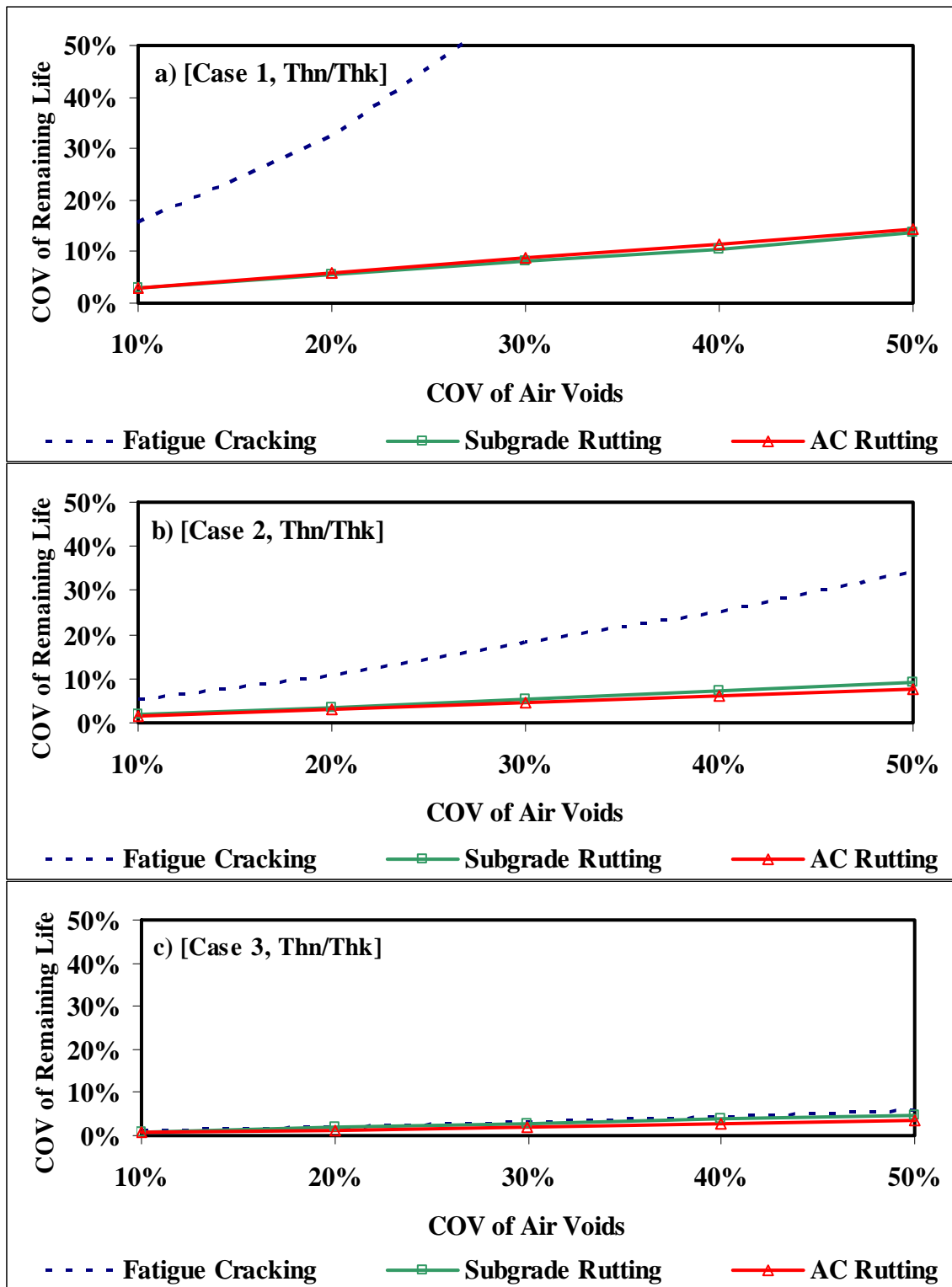


Figure 3.3 – Results of Impact of Variability of Air Voids on Remaining Life Varying AC Modulus

As in the previous case, the variability of each performance indicator increases with increasing the variability in this construction parameter. Comparing the three graphs, the impact of construction variability on performance is less significant as the air void contents get smaller. The largest impact is for the air voids of 12%. Another observation is that the fatigue cracking as a performance indicator is much more sensitive to the variability in air void content than the other two performance indicators.

The variations in the variability of the performance indicators as a function of the variability in air void content for the four typical pavement sections are shown in Figure 3.4. The same trends observed in Figure 3.2 are present here. The fatigue cracking as a performance indicator is more sensitive to the variability of air void content for the thin AC pavements as compared to the thick AC pavements. Also, as in Figure 3.2, the subgrade rutting criterion is more impacted by the variability in the air void content for the thick AC pavements than for the thin AC pavements. The results of all twelve cases depicted in Table 3.2, for investigating the impact of varying percent air voids, are graphically presented in Appendix B.

The overall results of these experiments illustrate the versatility of the algorithm in RECIPPE to analyze different flexible pavement sections. This case study showed two situations where the effect of one parameter is varied. However, for actual field data, the number of construction parameters that are variable is more, and the combining effect of their variability increases the complexity of the analysis. The algorithm incorporated in RECIPPE is able to handle such complexities.

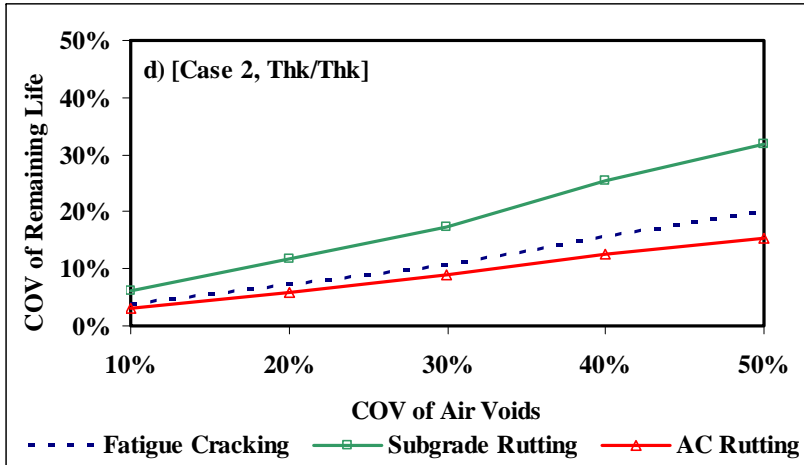
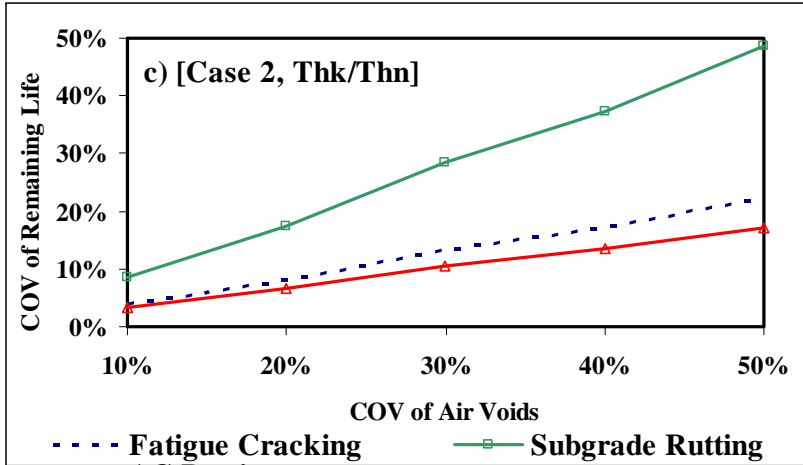
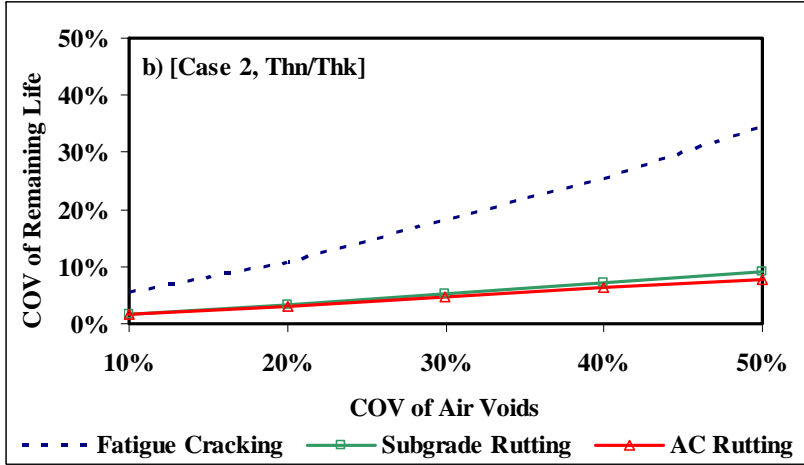
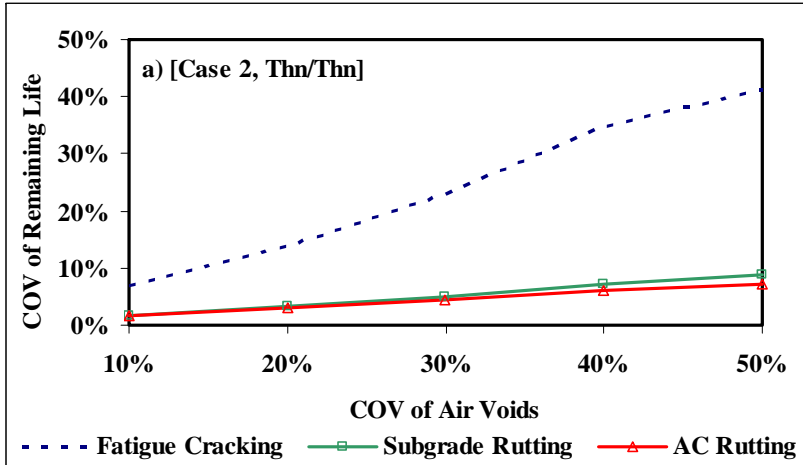


Figure 3.4 - Results of Impact of Variability of Air Voids on Remaining Life for Four Typical Pavement Sections

CHAPTER FOUR

IMPROVEMENTS TO ALGORITHM

INTRODUCTION

A framework detailing the impact of construction parameters on the remaining life of pavements was established from the prototype of RECIPE. The next stage in the development of RECIPE was to expand the program to a comprehensive and flexible tool that would be of practical use to a state highway agency. The following general modifications were made to the prototype:

- 1) The impact value was calculated more efficiently by using fewer simulations
- 2) The interface was modified to allow the following items:
 - a) Uncertainty analysis in the performance predictions
 - b) Automation of the optimization process
 - c) Customization of material and performance models
- 3) Quality control methods, based on control charts, was implemented

These changes provided a more practical algorithm.

EFFICIENCY OF TIME

Based on test trials, a limitation with the RECIPE prototype was the duration of time needed to execute the simulations. Due to the large number of statistical simulations (using the Monte Carlo and TPM simulations), the execution time was more than 30 minutes on a 500 MHz computer with over 380 MB of RAM. To reduce this processing time, three methods were used:

- Reduction of the number of construction parameters
- Reduction of the number of simulations
- Improvement in necessary computer memory

Reduction of Parameters

The first step in accelerating the simulation of the impact of construction variability on performance variability was to reduce the number of parameters. This is accomplished by: 1) removing the insensitive parameters in the material models from the probabilistic analysis, and 2) considering the interdependency among some of the parameters.

Abdallah et al. (2002) conducted a sensitivity analysis with the RECIPPE prototype to quantify the impact of each construction parameter on the four pavement performance equations. They showed that some parameters had no significant impact on any of the performance models. As a result, these parameters were replaced with constants in the material models. Table 4.1 lists the parameters that were considered constant.

Table 4.1 – Insensitive Parameters Removed from Simulation

Layer	Parameter	Assumed Constant Values*
Base	Shrinkage	2%
	Swell	2%
Subgrade	Shrinkage	4%
	Swell	10%

* - Values are extracted from Abdallah et al. (2002)

The second method used to reduce the number of input parameters was to consider the relationships that existed between the inputs parameters. Specifically, the degree of saturation and California Bearing Ratio (CBR) showed a direct correlation with the other parameters.

The degree of saturation is actually a value that can be determined from some of the other parameters in the models, as opposed to being measured. This is depicted below (Coduto, 1999):

$$S = \frac{wG_s}{\frac{G_s \gamma_w}{Comp(\gamma_{d \max})} - 1} \quad (4.1)$$

Where S is the degree of saturation, w is the field moisture content, G_s is the specific gravity of soil (estimated as 2.7), γ_w is the density of water (62.4 pcf), Comp is the degree of compaction and $\gamma_{d \max}$ is the maximum dry density. The CBR value measured in the field or based on Equation 4.2, as shown below, is a good approximation for stiff and soft soils (Webster et al., 1992).

$$CBR = \left(\frac{E_{soil}}{2.55} \right)^{1.5625} \quad (4.2)$$

In Equation 4.2, E_{soil} is the modulus of the soil in question, measured in ksi. A list of all the input parameters is shown in Table 4.2. By removing eight parameters, the 31 initial inputs were reduced to 23.

Reduction of Simulations

To further reduce the processing time, an analysis was conducted on the calculations being performed. The analysis demonstrated that Equation 2.18 could be reduced to:

$$NIV_i = \frac{COV_i}{\sum_{i=1}^n COV_i} \quad (4.3)$$

The change in the equation was a result of a simple algebraic relationship that existed between the COV when all input parameters, for a single layer, are simultaneously varied (COV_{ALL}). In Equation 2.18, the COV_{ALL} values are cancelled out, rendering the calculation of this parameter useless. Hence, there is no need for individual layers to be simulated. As a result, the number of calculations is reduced from 2,062 to 546 (46 TPM simulations and 500 Monte Carlo simulations).

Improving Amount of Necessary Computer Memory

The amount of time needed to run RECIPPE was further reduced by placing the material models into a dynamic link library (DLL). DLL's, which are executable files that are loaded into memory when the algorithm is executed, substantially reduce the amount of memory necessary for the actual execution. This also allows for modularization, so that the DLL can be accessed multiple times from the same algorithm without relinquishing memory that can be allocated elsewhere.

Consequently, these three adjustments reduced the process time from thirty minutes to about two minutes on the same computer.

UNCERTAINTY ANALYSIS, AUTOMATION & CUSTOMIZATION

Uncertainty Analysis in Performance Models

To improve the user interface, and provide more flexibility, an additional enhancement was added to the program to offer users the ability to perform uncertainty analysis. As depicted in RECIPPE's flow chart in Figure 2.6, the users have to decide if the pavement performance values and associated variabilities are acceptable. However, the levels of acceptability were never identified. By introducing a reliability factor, the users are allowed to incorporate the level of confidence desired.

Table 4.2 – Input Parameters to Material Models

Layer	Parameter
Asphalt/Concrete Layer	Thickness
	Modulus
	Aggregate Passing No.200
	AC Mix Air Void
	Asphalt Viscosity
	Asphalt Content
	Loading Frequency
	Temperature
Base Layer	Thickness
	Modulus
	Maximum Dry Density
	Optimum Moisture Content
	Moisture Content
	Degree of Compaction
	Aggregate Passing No.40
	Percent of Clay
Percent of Silt	
Subgrade Layer	Thickness
	Modulus
	Maximum Dry Density
	Optimum Moisture Content
	Moisture Content
	Degree of Compaction
	Aggregate Passing No.40
	Percent of Clay
	Percent of Silt
	Liquid Limit
	Plastic Index
AASHTO Design Coefficients	Load in 105
	Standard Normal Deviate, ZR
	Overall Standard Deviation, S0
	The Drainage Coefficient of Second Layer , m2
	ΔPSI

To be specific, a normal distribution was assumed for all of the input and output values. Therefore, it was possible to supply the confidence level as a function of the required remaining life specifications. For example, if the mean and COV for the remaining life due to fatigue cracking were 24×10^6 ESALs and 20%, respectively, then a probability density function could be generated. To determine the acceptable confidence level, where the pavement would not fail due to fatigue cracking before 25×10^6 ESALs, one simply must find the area under the curve, as shown below.

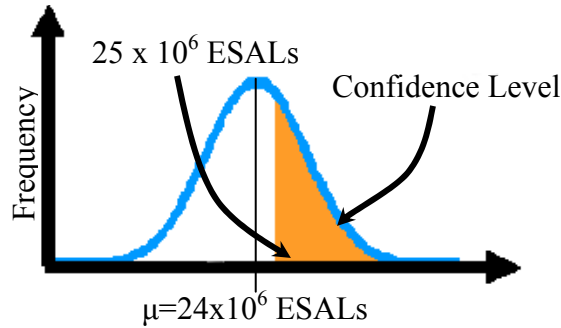


Figure 4.1 – Probability Density Function for Continuous Functions

Figure 4.1 depicts a one-tailed test, indicating that it is only necessary to analyze minimum thresholds of pavement performance. The confidence level shows the percentage of pavement that will not fail before 24×10^6 ESALs. Furthermore, Figure 4.1 follows a continuous curve, which is based upon a mean and standard deviation. If the mean (μ) and standard deviation (σ) are known, then the acceptable failure level (x), at a given confidence level can be found using:

$$x = \mu + Z_{\alpha} \sigma \quad (4.4)$$

In Equation 4.4, Z_{α} represents the standard normal variable at a given significance level, α . The significance level value is calculated from the confidence level (p), using:

$$\alpha = 1 - p \quad (4.5)$$

The following is a brief example that only depicts the uncertainty analysis process to find if a value meets the levels of acceptability for a one tailed test. These values are arbitrarily selected, and not based on an actual project.

Given:

$\mu_{AC} = 5\%$	$\mu_{Mt} = 50\text{kg}$
$\sigma_{AC} = 0.1\%$	$\sigma_{Mt} = 0\text{kg}$

where, AC is the asphalt content for the ACP layer and M_t represents the total mass of HMA to be sampled during production. The standard deviation for the asphalt content is indicative of 99.7% of all samples lying $\pm 0.3\%$ from the expected value. Since during the process control, the mass of the binder, M_b , is used, the following equation was used to calculate that quantity:

$$M_b = AC \times M_t \quad (4.6)$$

Find: The inspector is interested in finding if 90% of the binder mass is greater than 2.4 kg using the Monte Carlo simulations.

Solution: The results for 500 Monte Carlo simulations are shown in Table 4.3. The table shows the average and COV values for the simulated mass of binder. For a confidence level of $\alpha = 90\%$, the acceptable failure level can be calculated, using Equation 4.4:

$$x = Z_{1-\alpha} \sigma + \mu = -1.28(0.05) + 2.5 = 2.44 \text{ kg}$$

Table 4.3 – Reliability Example for Determining Acceptable Levels of a Parameter

Measurement	AC Content	M _b
Average	5%	2.5 (kg)
Std. Dev.	0.1%	0.05 (kg)
COV	2%	2 %

This shows that 90% of the binder mass is greater than 2.44 kg. Therefore, because this value is greater than the level specified, 2.4 kg at 90% confidence, the inspector finds that the simulated values does meet the levels of acceptability.

Automation of Reduction Process

The flow chart of RECIPPE, as depicted in Figure 2.6, shows an iterative loop that continues until acceptable levels of pavement performance are met. With the prototype, this process was repeated manually based on the user's decision. However, this loop can be automated for the pavement performance variance, using the reliability calculations mentioned above. Assuming that the mean values for the construction and design parameters are constant, the designer becomes concerned only with reducing the variability of the pavement life. This section of the report describes four automatic reduction options:

- Largest Impact Value
- N-Largest Impact Values
- Set Minimum Level of COV
- Manual

Largest Impact Value Reduction

The RECIPPE prototype had the capability to provide users with a mean and standard deviation for a specified pavement performance model. Based on the reliability calculations mentioned previously, the users should also specify an acceptable confidence level for a pavement performance. The pavement performance in RECIPPE is defined as the number of ESALs a pavement can withstand before failure, with respect to each pavement performance model.

The program has been modified to identify the construction parameter that contributes to the pavement performance COV the most (from the Impact Charts), and reduce the variance of the parameter that most impacts the performance by a specified amount. The program continues to reduce the COV of the largest impacting construction parameters until the acceptable pavement performance limits have been met.

N-Largest Impact Value Reduction

Using the methodology discussed in the previous section, the process can be modified to incorporate the N parameters that impact the performance the most. This should provide pavement performance values that meet the level of acceptability more rapidly. In the Largest

Impact Value Reduction method, only one parameter is selected to be reduced, which may take more processing time than using multiple parameters. This may be especially true if the reduction factor that is used to reduce the most impacting input parameter COV after each iteration is very small. Hence, it seems practical to expand the theory for reducing the single most significant parameter COV to the Nth most significant ones.

Unfortunately, there is a drawback to this method. By considering N parameters simultaneously, it is possible that the reduction of the COVs of the construction parameters may become unstable. Due to the high degree of nonlinearity that exists in the program, some of the COV parameters will reduce more quickly than others. Hence, some input parameter COV's may be reduced below a practical threshold. When selecting this option, one should be careful in interpreting the results.

Setting Limitations for the Input COV

Furthermore, the users may not wish to reduce the COV of construction parameters below a certain level. The goal of reducing the COV of a construction parameter is to reduce the impact of that construction parameter on pavement performance variance. However, reducing a construction parameter COV past a certain point may not be practical. For example, the air void content for the ACP layer will usually vary; hence, having variability close to zero may not be achievable by a contractor. Therefore, constraining the input COV within a certain range allows the automation process to provide more practical results.

Adjustment of Models

The models in RECIPPE have been described as being modular in form. This means that an individual equation for material and/or performance can be adjusted separately. Because the equations can be adjusted individually, no model is required to be hard coded into RECIPPE. Hence, if a specific model needs to be changed or a new model needs to be entered, an interface needs to be incorporated to allow for the future adjustments. This section describes three types of adjustments that may occur:

- Customization
- Generation
- Calibration

Customization of Material and Performance Models

The algorithms used in the prototype program were specific for each material and performance type; however, it may not be completely necessary to change the entire equation for a certain model, but only the trend that certain parameters exhibit. For example, the material model discussed for the ACP layer (Equation 2.1) currently has a value of 1 for the coefficient associated with the parameter associated with the aggregates passing sieve No. 200. However, if alternate studies show that this coefficient should change to a value of 400, then an adjustment can be made to the AC Modulus equation, as shown in Figure 4.2.

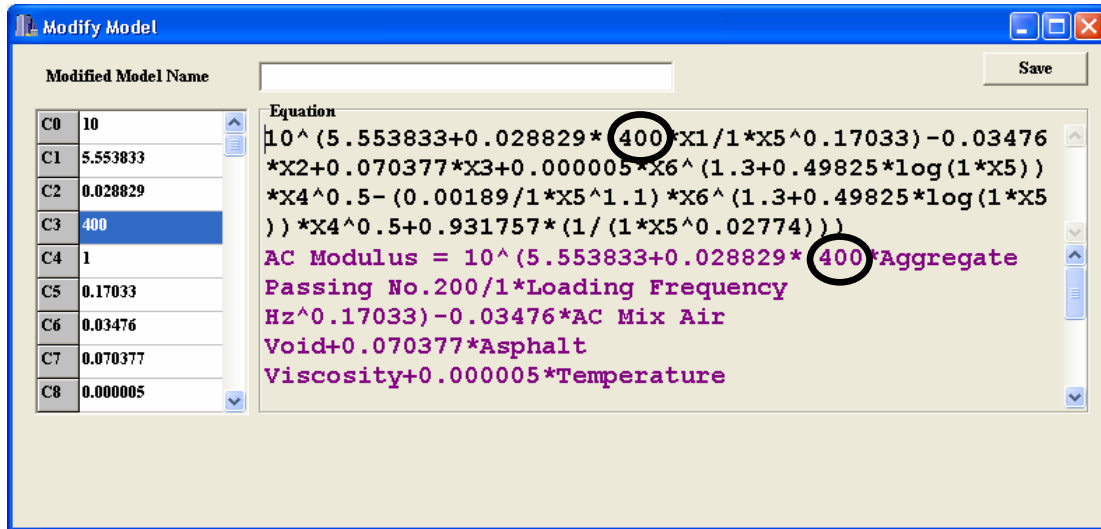


Figure 4.2 – Customization of Models

The left hand side of the interface shown in Figure 4.2 displays the constants that are used in the material model. The relevant equation is shown with the constants and variable name in black, and again with the constants and variable abbreviation in purple. In this example, the constant, C3, is replaced with the number 400, which automatically updates in the equation on the right hand side of the form. With the implementation of this option, the users can change the model coefficients as needed.

Generation of New Models

The creation of completely new models is also possible. To create a new model, the users do not have to use the parameters or mathematical operators that are specified in the material models described in Chapter Two, but an equation, such as that shown in Figure 4.3, can be easily entered into the graphical users interface.

The interface shown in Figure 4.3 allows users to specify a current or new input parameter, as shown on the left hand side. These input parameters are then used in the equation that users provide, as shown on the right hand side. The entire equation is updated and shown in the box at the top of the figure. This option allows the program to become more adjustable and easy to use with new models.

Model Calibration

RECIPPE would also permit users to calibrate any material model and/or performance model. This calibration is based upon a simple linear regression between the values calculated by the model and those that are measured in the field. Once the relationship has been found, it can be entered into the program. This technique is very similar to the customization of material and performance models process, but because calibration follows a different concept, it allows for easier entry into the program, as shown in Figure 4.4.

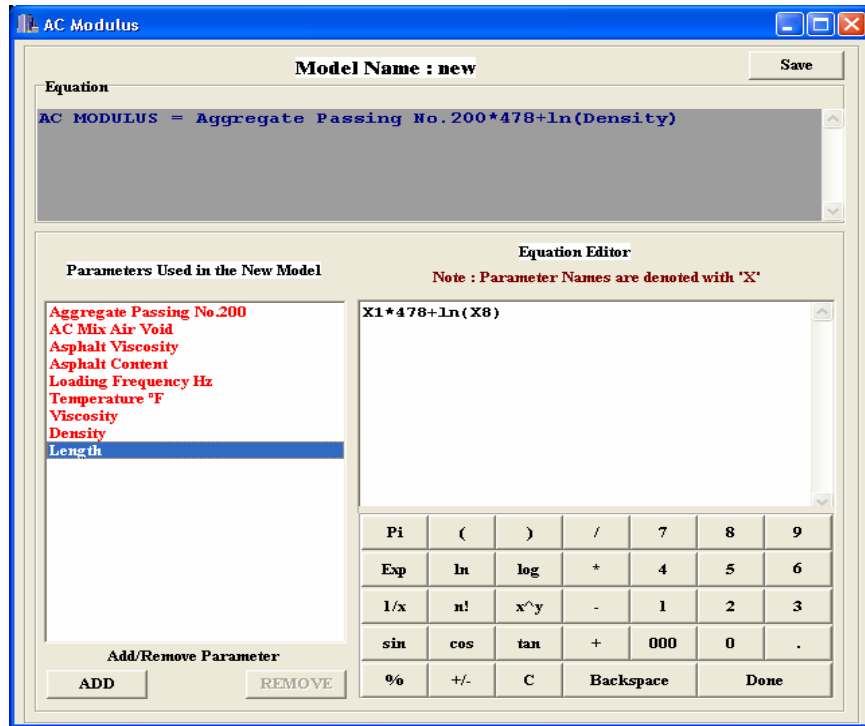


Figure 4.3 – Generation of New Models

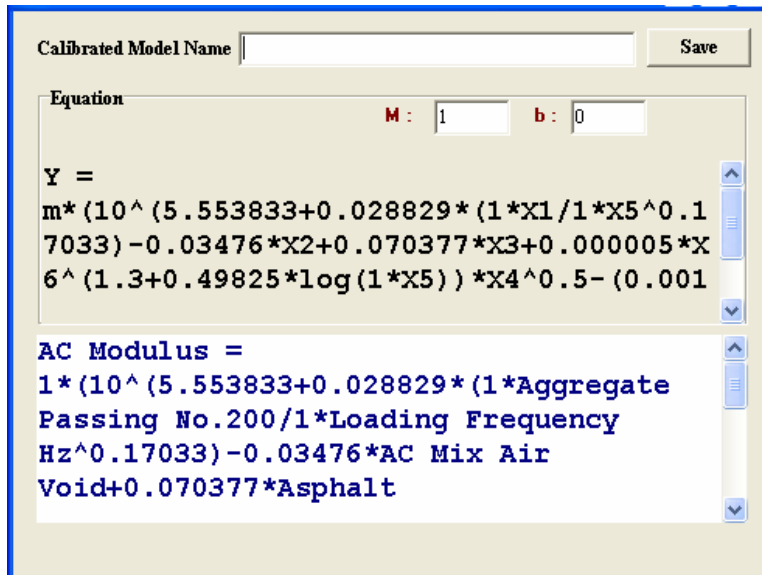


Figure 4.4 – Model Calibration

RECIPPE displays the current equation and how the equation looks after it has been calibrated. Also shown in this calibration process is the requirement for the slope, m , and intercept, b , as shown in Figure 4.4. However, the process of finding these values will be discussed in detail in Chapter 5, where an explanation of regression capabilities will be given.

QA/QC METHODS

Number of Samples

Because RECIPPE is designed for a practical, statistical analysis of a mechanistic algorithm based on construction parameters, it will become necessary to gather empirical information from lab and/or in-situ testing methods. The problem, however, is predicting the number of samples needed for each parameter so that statistical reliability is maintained while minimizing the costs for obtaining the data.

Based on the previously mentioned assumptions that all parameters follow a normal distribution, it can be deduced that all parameters have a mean of μ (μ is the mean value) and a variance of σ^2 (σ^2 is the parameter variance) (Devore, 1995). Hence, the sampling distribution for any parameter is normal with a mean of μ and a variance of σ^2/n , as shown below:

$$\bar{x} \cong N\left(\mu, \frac{\sigma^2}{n}\right) \quad (4.7)$$

This model can then be implemented in a cumulative distribution function to replicate the standard normal distribution:

$$P(x) = \Phi(Z_\alpha) = \Phi\left(\frac{x - \mu}{\sigma}\right) \quad (4.8)$$

where x represents some random number, $P(x)$ is the probability of some random number x that defines a discrete point on a continuous normal distribution curve, Z defines the normalized standard deviation value based upon the level of significant (α), and Φ is the cumulative distribution function of the standard normal distribution. By combining the sampling distribution with the standard normal distribution, the resulting equation is:

$$P(x) = \Phi(Z_\alpha) = \Phi\left(\frac{x - \mu}{\sigma/\sqrt{n}}\right) \quad (4.9)$$

However, the interest is in determining whether the sampled data follows the specifications previously set, rather than merely replicating the distribution. In other words, it is necessary to verify that the data gathered for an input parameter gives a mean, μ_1 , that equals the mean set by the designer, μ_0 :

$$\mu_0 \stackrel{?}{=} \mu_1$$

This type of analysis is called hypothesis testing. A statistical hypothesis is a statement about the values of the parameters of a probability distribution (Montgomery, 2001). For example, in this analysis, the null hypothesis is defined as H_0 and the complement of this occurrence is called the alternative hypothesis, H_1 , as shown below.

$$\begin{aligned} H_0 : & \quad \mu_0 \geq \mu_1 \\ H_1 : & \quad \mu_0 < \mu_1 \end{aligned} \quad (4.10)$$

This indicates a one-tailed test, where the alternative hypothesis implies that the sampled mean can only be less than the true mean.

In hypothesis testing, another parameter that must be specified is the test statistic, α . This statistical test, also referred to as the probability of type I error, provides information to either reject or accept the null hypothesis. As shown graphically in Figure 4.5, the equation for a standard normal distribution is used. If the sample mean falls within the rejection region, the null hypothesis is rejected and the alternative is selected as true.

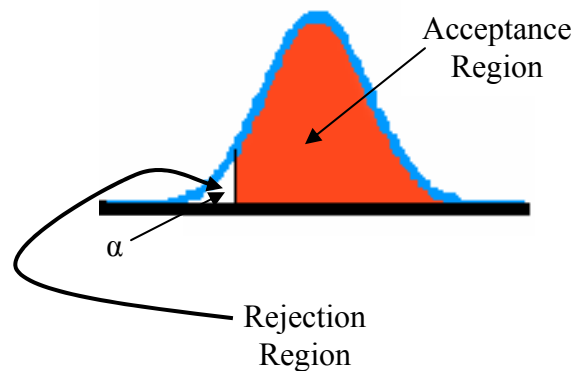


Figure 4.5 – Statistical Rejection and Acceptance

The null hypothesis tests the contractor’s level of confidence in the parameter’s variability. The alternative hypothesis tests for the owner’s level of confidence in the quality of the product. Because the two confidence levels are based upon the amount of risk each contractor or owner is willing to take, there is an inherent probability that the mean is wrong. This is called Type I error for contractors and Type II error for owners.

$$\begin{aligned} \alpha &= \text{Probability \{Type I Error\}} = \text{Probability \{reject } H_0 \mid H_0 \text{ is true\}} \\ \beta &= \text{Probability \{Type II Error\}} = \text{Probability \{failure to reject } H_0 \mid H_0 \text{ is true\}} \end{aligned}$$

The contractor and owner, in this case, are interested only in the stiffness of the pavement. The pavement can be stiffer than designed (to be able to withstand more traffic), but it should not be less stiff. This is where the probabilities of Type I and Type II errors need to be considered. Parameter β , as described above, is the probability that the users fail to reject the null hypothesis, given that it is true. Put another way, β is the probability of failure to accept the alternative hypothesis, given that it is false, an example of which is represented in Figure 4.6.

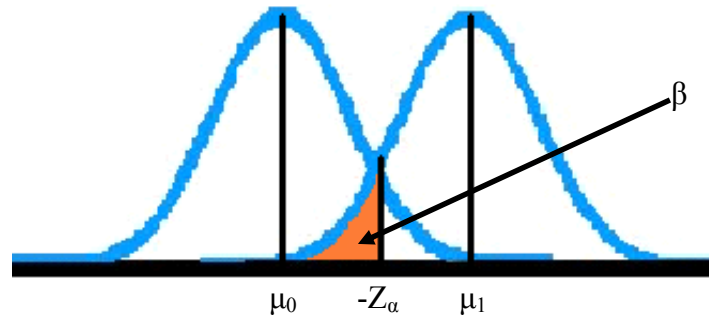


Figure 4.6 – Probability of Type II Error

The calculation of the probability of Type II error can be equated in terms of the standard normal distribution, as shown below (Zhang et al., 2001):

$$\beta = \Phi\left(-Z_{\alpha} + \frac{(\mu_1 - \mu_0)\sqrt{n}}{\sigma}\right) \quad (4.11)$$

By readjusting this equation, an algorithm can be derived to determine the sample size needed to find the measurements reliably.

$$n = \left(\frac{(Z_{\alpha} + Z_{\beta})\sigma}{\mu_1 - \mu_0}\right)^2 \quad (4.12)$$

Because the material model is to be a reflection of each construction parameter, the mean value should be changed so that it can be interpreted in relative terms. This will allow the tolerable error for each construction parameter to be inferred from the layer modulus, and vice versa. The tolerable error, then, is a relative value in terms of the mean value.

$$e = \frac{\mu_1 - \mu_0}{\mu_0} \quad (4.13)$$

where e represents the tolerable error. This tolerable error for a single construction parameter can now be applied to Equation 4.12, leading to the following sample size equation.

$$n = \left(\frac{(Z_{\alpha} + Z_{\beta}) \times COV}{e}\right)^2 \quad (4.14)$$

where, COV represents the coefficient of variation for an individual construction parameter, found as the standard deviation divided by the mean, σ / μ_0 . This procedure is important from a production quality point of view.

Sometimes it is necessary to consider a failure whenever a test result is above or below the mean value, and not only one sided. For example, when testing for air voids in asphalt pavement, very high and very low values are considered unacceptable. In these cases, the probability of the known sample mean may fall between two equi-distant intervals from the mean, also called a two tailed test. In situations where this may occur, Equation 4.15 is recommended.

$$n = \left(\frac{(Z_{\alpha/2} + Z_{\beta}) \times COV}{e} \right)^2 \quad (4.15)$$

For another perspective, consider the following example.

Given: The interest is in finding the number of asphalt content samples needed so that the asphalt content can be reliably characterized. The following information is provided:

$$\begin{aligned} \mu_{AC} &= 5\% \\ \sigma_{AC} &= 0.15\% \end{aligned}$$

Assume that the contractor is 95% confident (i.e. $\alpha = 0.05$) and that the consumer needs to be 80% ($\beta = 0.2$) confident in the binder content. Also, assume the mean for the mass of the binder is 5% and that the sampled asphalt content is within 2% of the mean value. An analysis would provide the following:

$$\begin{aligned} Z_{\alpha/2=2.5\%} &= 1.96 \\ Z_{\beta=20\%} &= 0.84 \\ e &= 0.03 \end{aligned}$$

With this information, a Monte Carlo simulation would be able to generate the results listed in Table 4.4.

Table 4.4 – Sample Size Example Inputs

MEASUREMENT	AC	M _b
MEAN	5%	2.5 kg
STD. DEV.	0.1%	0.05 kg
COV	2.0%	2 %

$$n = \left(\frac{(1.96 + 0.84) * 0.02}{0.02} \right)^2 = 7.84 \approx \underline{8 \text{ samples}}$$

The number of samples is rounded up to provide a more liberal value that will successfully achieve the Type I, Type II and/or tolerable error.

Control Charts

Due to the fact that this analysis should be available for the contractor as well as the owner, a device providing practical quality control should also be considered. One way of conducting this type of inspection is through control charts. Usually used for diagnostic techniques for monitoring in manufacturing industries, control charts can identify instability and unusual circumstances in production processes. This implies that, based upon allowable variances, inspectors can randomly sample road specimens and determine whether or not the pavement, statistically, will be stable over time (in-control or out-of-control, respectively). Control charts have become increasingly popular for five major reasons:

- Control charts are a proven technique for improving productivity by reducing rework.
- Control charts are effective in defect prevention. The charts help keep the process in-control initially, preventing the need to rehabilitate when defects are detected.
- Control charts prevent unnecessary process adjustments. The charts allow for distinguishing between background noise and abnormal variation, which means that they are effective in determining whether variations are randomly occurring or the result of some continuous event.
- Control charts provide diagnostic information. They present patterns on the history of the process, thus predicting trends over time.
- Control charts provide information about process capability. They are used to identify whether the process can adequately meet the process limits, which will be described later.

The first step in generating control charts is acquiring an adequate set of random variables and placing them into a subgroup. Subgroups are sets of empirical information that represent a time order for construction processes. Time order determines the frequency for collecting subgroup sizes. This is important because the previous section described the method for determining the number of samples that would be required to conduct a hypothesis test, but did not describe when the subgroups should be sampled. The sample size was a function of the coefficient of variation and tolerable error, which in turn signified the time order for sampling the subgroup, or the amount of time between lots. To be specific, if the tolerable error and coefficient of variation were functions of a day's production or linear travel way, then so would the time order. This definition of time order allows for consecutive units to be measured so that the chance of variability due to assignable causes within sample is minimized, while the variability between samples are maximized if assignable causes are present.

For instance, in the asphalt binder problem mentioned previously, it was determined that eight samples should be taken. It is given that the subgroups are measured on a daily basis. The empirical mean data points would then be placed into a control chart, which can be calculated as shown in Table 4.5.

Table 4.5 – Calculation of Subgroup Means

Measurement	Subgroup (Day)				
	1	2	3	4	5
1	4.91%	4.97%	5.05%	5.17%	5.04%
2	5.08%	4.96%	4.93%	5.06%	5.02%
3	5.01%	4.88%	4.84%	4.89%	4.75%
4	4.87%	5.15%	5.07%	4.77%	4.89%
5	4.85%	4.93%	4.97%	5.08%	5.01%
6	5.01%	4.88%	4.83%	4.83%	5.01%
7	4.81%	5.07%	4.94%	5.02%	4.94%
8	5.08%	5.08%	5.03%	5.02%	4.91%
Mean	4.95%	4.99%	4.96%	4.98%	4.95%

To create the control chart for sample mean, the limits and center lines must be specified. The center line represents the average value of the quality characteristics corresponding to the in-control state. In this case, the center line will be the mean value for the parameter in question. The upper and lower control limits are selected so that, if the process is in-control, then nearly all of the sample points will fall between them and can be assumed to be in-control. This done, a general model for the mean, or x-bar, chart can be generated using:

$$UCL_{xi} = \mu_i + L\sigma_i \quad (4.16)$$

$$CL_{xi} = \mu_i \quad (4.17)$$

$$LCL_{xi} = \mu_i - L\sigma_i \quad (4.18)$$

where UCL_{xi} is the upper control limit for construction parameter i , the CL_{xi} value represents the center line for construction parameter i . LCL_{xi} is the lower control limit value for construction parameter i , μ_i is the mean for construction parameter i , σ_i defines the standard deviation for construction parameter i , and L is the distance of the control limits from the center line, expressed in standard deviation units.

Because interest lies in the contractor's and owner's risk in modeling the pavement, L will be based upon the Type I and Type II errors as shown in Equation 4.19 for one tailed tests.

$$L = Z_\alpha + Z_\beta \quad (4.19)$$

and for two tailed tests Equation 4.20 will be used.

$$L = Z_{\alpha/2} + Z_\beta \quad (4.20)$$

The x-bar chart shows variation of the mean, and thus graphically illustrates whether the alternative hypothesis should be chosen for certain time orders. For example, using the same asphalt binder problem, an x-bar chart for the asphalt content can be created, given the following.

$$\begin{aligned}
 Z_{\alpha=2.5\%} &= 1.96 \\
 Z_{\beta=20\%} &= 0.84 \\
 \mu_{AC} &= 5\% \\
 \sigma_{AC} &= 0.1\% \\
 LCL_x &= 5 - (1.96 + 0.84) \times 0.1 = \underline{4.7\%} \\
 CL &= \underline{5.0\%} \\
 UCL_x &= 5 + (1.96 + 0.84) \times 0.1 = \underline{5.3\%}
 \end{aligned}$$

With the construction of this control chart, it can be graphically determined whether the sample values of the mean fall within the control limits and exhibit no systematic pattern. Hence, it can be deduced whether the process is in-control at the level indicated by the chart. This level of control, however, is not the sole indicator for out-of-control systems. For example, consider the x-bar chart in Figure 4.8, which is based on the data from Table 4.5. While all five points shown in Figure 4.8 fall within the control limits, the points do not indicate statistical control because their pattern is not random. To be specific, all five points are below the center line. If this control chart were to be indicative of random variance, a more even distribution of points could be expected above and below the center line.

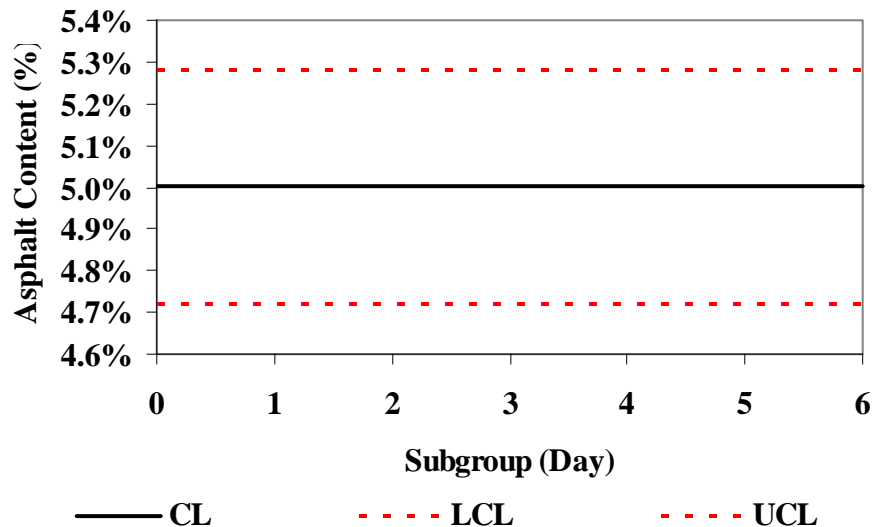


Figure 4.7 – Typical X-Bar Chart

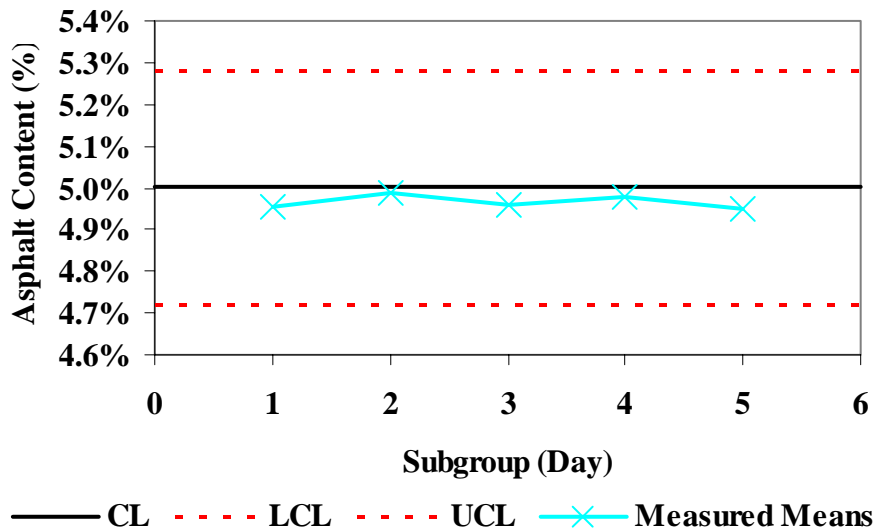


Figure 4.8 – Sample X-Bar Chart

The basic criteria to determine whether a control chart is out-of-control can be shown by plotting points outside of the control limit. However, supplementary criteria can sometimes be used to increase the sensitivity of the control charts so that inspectors can respond more quickly to assignable causes. The top five rules that are widely used in practice are shown in Table 4.6. These rules were extrapolated from Western Electric (Montgomery, 2001).

In addition, changes in the mean the variance of the construction parameters must also be controlled so that the road may become more uniform. For this purpose, a control chart for the sample variation can be provided in terms of the coefficient of variation (COV) of empirical measurements. Using the same data as before, the sample coefficient of variation, COV, can be calculated using Equation 4.21.

$$COV = \frac{\sqrt{\frac{\sum_{i=1}^n (x_i - \bar{x})^2}{n-1}}}{\bar{x}} \quad (4.21)$$

where COV is the subgroup coefficient of variation, x_i represents the i^{th} measured value for the subgroup in question, \bar{x} defines the subgroup mean, and n is the subgroup sample size.

Table 4.6 – Popular Sensitizing Rules Currently in Practice (Montgomery, 2001)

1. One or more points outside of the control limits
2. A run of eight consecutive points on one side of the center line
3. Six points in a row steadily increasing or decreasing
4. Fourteen points in a row alternating up and down
5. An unusual or not random pattern in data

Using the data in Table 4.5, the sample COV can be determined as shown in Table 4.7. These values can then be graphed in a COV control chart with center line and control limits described in Equations 4.22 through 4.24.

$$UCL_{COVi} = COV + \frac{4L(n-1)COV}{4n-3} \sqrt{1 - \left(\frac{4(n-1)}{4n-3}\right)} \quad (4.22)$$

$$CL_{COVi} = COV \quad (4.23)$$

$$LCL_{COVi} = 0 \quad (4.24)$$

where UCL_{COVi} is the upper control limit for construction parameter i , CL_{COVi} defines the center line for construction parameter i , LCL_{COVi} represents the lower control limit for construction parameter i , and n is the sample size. The resulting COV control chart limits can be calculated as follows:

$$Z_{\alpha=2.5\%} = 1.96$$

$$Z_{\beta=20\%} = 0.84$$

$$\mu_{AC} = 5\%$$

$$\sigma_{AC} = 0.1\%$$

$$n = 8$$

$$LCL_x \% = 0\%$$

$$CL = \frac{0.1\%}{5\%} = 2\%$$

$$UCL_x = 0.02 + \frac{4(1.96 + 0.84)(8-1)(0.02)}{4(8)-3} \sqrt{1 - \left(\frac{4(8-1)}{4(8)-3}\right)} = 3\%$$

Table 4.7 – Sample COV Subgroup’s for Control Chart Example

Measurement	Subgroup (Day)				
	1	2	3	4	5
1	4.91%	4.97%	5.05%	5.17%	5.04%
2	5.08%	4.96%	4.93%	5.06%	5.02%
3	5.01%	4.88%	4.84%	4.89%	4.75%
4	4.87%	5.15%	5.07%	4.77%	4.89%
5	4.85%	4.93%	4.97%	5.08%	5.01%
6	5.01%	4.88%	4.83%	4.83%	5.01%
7	4.81%	5.07%	4.94%	5.02%	4.94%
8	5.08%	5.08%	5.03%	5.02%	4.91%
Mean	4.95%	4.99%	4.96%	4.98%	4.95%
COV	2.16%	2.00%	1.82%	2.73%	1.97%

Similarly, the resulting COV control chart for the data shown in Table 4.7 can be graphically depicted, as shown in Figure 4.9. The data follows a random pattern with data varying above and below the center line, indicative of a process that is completely in control.

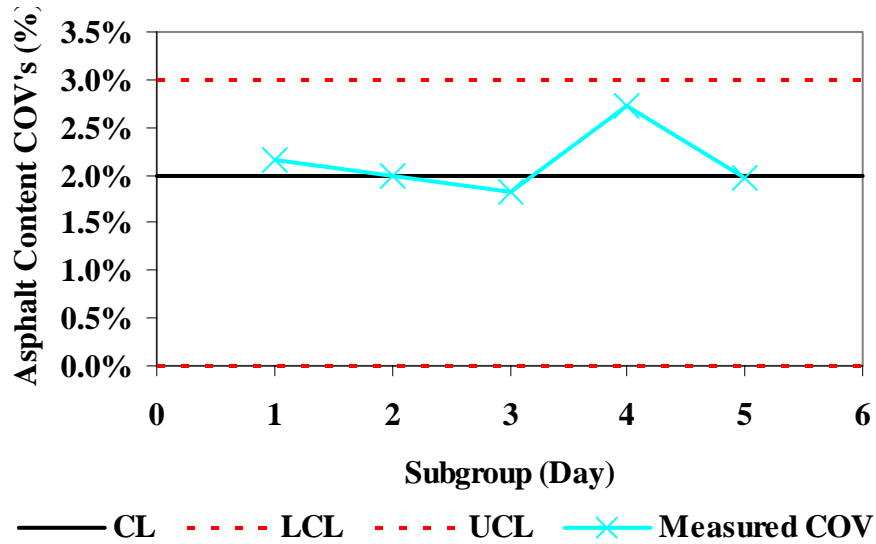


Figure 4.9 – Sample COV Control Chart

Cost Analysis

With the information that has been described, thus far, a quantitative value can be provided for inspection costs, which will be discussed in this section. Production expenditures, due to rehabilitation and maintenance, are intuitively calculated in a qualitative manner, because the basic concept of the RECIPPE is to minimize variability to increase the longevity of pavement. However, due to time constraints, an actual cost/benefit analysis for production expenditures will not be performed in this report.

RECIPPE, as described above, estimates the minimum number of tests to be run for inspecting a single parameter. Hence, for each test run there is a corresponding cost, which can be related as a unit price (i.e. \$10.00/Nuclear Density Gauge). If the unit price is known for each test to be run, then the total inspection costs can be found using a simple mathematical operation:

$$TotalCost_{inspection} = \sum_{i=1}^m C_i n_i \quad (4.25)$$

Where C_i is the unit price for parameter i and n_i is the sample size for parameter i . Typical costs for all of the base and subgrade parameter tests in Texas are shown in Table 4.8. These costs are estimated for the entire state of Texas, and can be easily changed to account for inflation and/or the development of new inspection standards.

Table 4.8 – Typical Inspection Tests & Costs for Texas Pavements

STANDARD		TEST	Unit	STATEWIDE AVG.		2 Year Avg.
				FY 2002	FY 2003	
Tex	103	Moisture Content	each	\$6.00	\$27.00	\$16.50
Tex	106	Plasticity Index	each	\$33.75	\$71.00	\$52.38
Tex	110, Pt1	Gradation	each	\$32.50	\$60.00	\$46.25
Tex	110, Pt2	Gradation	each	-	\$150.00	\$150.00
Tex	113	M-D Curve for Base	each	\$162.50	\$330.00	\$246.25
Tex	114	M-D Curve for Base	each	\$155.00	\$330.00	\$242.50
Tex	115	Nuclear Density	hour	\$31.50	\$37.50	\$34.50
Tex	116	Wet Ball	each	\$135.00	\$200.00	\$167.50

Not shown are the test costs for the ACP layer and the AASHTO design coefficients. AASHTO design coefficients are based upon layer specifications, and do not require testing. Unfortunately, typical tests for the ACP layer were not found prior to the writing of this report. This information will be incorporated in the final report.

CHAPTER FIVE

CALIBRATION OF AC, BASE AND SUBGRADE MODULUS MODELS

INTRODUCTION

The material models presented in Chapter 2 were created from regression analyses on data that was not specifically collected for Texas. It is reasonable to assume that the results from the models are not calibrated for Texas pavements. The focus of this chapter is to obtain data from either literature or field and lab testing for Texas pavements, in order to evaluate existing models and, if necessary, calibrate or generate new material models.

DATA COLLECTION

Literature

When generating new equations through regression analysis, it is important to obtain as much data as possible to represent all possible situations. For this reason, data that have been previously documented can provide an excellent source of information to generate a database. One valuable source for this documented information is the Long Term Pavement Performance (LTPP) database. The LTPP is a 20-year program that was initiated in 1987 as part of the Strategic Highway Research Program (SHRP). With more than 2,400 test sections at over 900 locations throughout North America, the LTPP database is the world's largest pavement performance database (Federal Highway Administration, 2004).

The online LTPP database (www.datapave.com) offers a user-friendly format for exploring, extracting, and organizing the extensive LTPP data. In addition, the website provides the capability to identify the LTPP database tables and fields for data extraction.

A filtering process was used to extract specific data, and to minimize extraction of unnecessary information contained in the multiple tables in the database. The extraction effort was first

focused on Specific Pavement Study (SPS) sites and later expanded to other Texas sections. For the AC layer, the construction parameters that were extracted from the LTPP database were:

- Asphalt content
- Viscosity
- Percent of aggregate passing sieve #200
- Percent air voids
- Elastic Modulus of the ACP layer (from backcalculation)

To illustrate the filtering process for the construction parameters, the example of extracting data for the asphalt content is discussed. The asphalt content can be found in the Inventory IMS module, which contains tables with listings of plant mixed asphalt data. One of the tables, “Plant-mixed asphalt bound layers original mixture properties,” contains information such as the following.

STATE_CODE, LAYER_NO, SHRP_ID, SAMPLE_TYPEHVEEM_COHESIOMETER,
BULK_SPEC_GRAVITY_MEAN, MAX_SPEC_GRAVITY, NUMBER_BLOW,
PCT_AIR_VOIDS_MAX, PCT_AIR_VOIDS_MIN, PCT_AIR_VOIDS_MEAN,
ASPHALT_CONTENT_STD_DEV, RECORD_STATUS, ANTISTRIP_AGENT_TYPE,
ASPHALT_PLANT_TYPE_OTHER, HVEEM_STABILITY, MARSHALL_FLOW,
RETAINED_STRENGTH_INDEX, PERCENT_STRIPPED, HVEEM_STABILITY_NO,
TENSILE_STRENGTH_RATIO, EFFECTIVE_ASPHALT_CONTENT,
NO_SAMP_ASPHALT_CONTENT, ASPHALT_PLANT_TYPE, CONSTRUCTION_NO,
ASPHALT_CONTENT_MAX, ASPHALT_CONTENT_MIN, ASPHALT_CONTENT_MEAN,
BULK_SPEC_GRAVITY_STD_DEV, BULK_SPEC_GRAVITY_MIN,
MARSHALL_STABILITY, BULK_SPEC_GRAVITY_MAX, VOIDS_MINERAL_AGGR,
NO_SAMP_PCT_AIR_VOIDS, PCT_AIR_VOIDS_STD_DEV,
MOISTURE_SUSCEPT_TEST, ANTISTRIP_AGENT_AMOUNT,
ANTISTRIP_AGENT_CODE, ANTISTRIP_AGENT_TYPE_OTHER,
MOISTURE_SUSCEPT_TEST_OTHER

This list contains a large amount of information to filter through in order to obtain the asphalt content. Identification keys are used to link the variety of tables together for a given site. Crucial identification keys such as SHRP ID, the road identification key, are used to extract, link, and match the appropriate data that is required. Few of the other identification keys that were used are:

SHRP_ID, LAYER_NO, RECORD_STATUS, ASPHALT_GRADE, CONSTRUCTION_NO,
and ASPHALT_SPECIFIC_GRAVITY.

The LTPP database provided thirty complete Texas sites, as shown in Table 5.1. However, when the backcalculated moduli are compared to the estimated moduli from Equation 2.1, some of the values were clearly different. Hence, to remove data that may have inaccuracies, further data

mining using cluster techniques was used to remove outlier sites. Equation 5.1 defines the cluster values as:

$$ClusterValue\% = \frac{abs(M_{backcalculated} - M_{Wiczak})}{M_{backcalculated}} \quad (5.1)$$

By calculating the cluster value for each site, three groups of data can be identified: 1) cluster values less than 20%, 2) cluster values between 20% and 80%, and 3) cluster value greater than 80%. These three groups represent cluster sets of data that show similar trends between the FWD moduli and the calculated moduli from the Wiczak equation, as shown in Table 5.2. The largest cluster set is between 20% and 80%. Therefore, this set was used in the calibration process.

In-Situ and Laboratory Data

Unfortunately, extensive literature search did not reveal adequate amounts of information for base and subgrade layers. As such a matrix of test sections that represents flexible pavements in Texas was developed. With the help of TxDOT personnel, a protocol was developed to allow for a comprehensive data collection scheme from Texas sites. Data were collected according to an adjusted guide schedule that specifies the frequency and location for gathering sample information for each required construction parameter. The adjustments to the guide schedule were developed by UTEP and TxDOT personnel for more practical testing frequencies. The protocol was appended in Appendix A of Research Report 0-4046-2. For the most part the protocol was followed. As a result field and laboratory tests were performed on eleven sites and the results are summarized next.

According to Table 4.2, nineteen parameters for the base and subgrade layers are required for each site. A list of all pertinent tests is shown in Table 5.3. The eleven sites were located in six different counties, representative of the major climate differences of the environments found within the state of Texas. The location and pertinent information for the sites are shown in Table 5.4. The tests listed in Table 5.3 were performed either in-situ or in the laboratory on materials at each site. The results are summarized in Table 5.5.

ASPHALT CONCRETE MATERIAL MODEL CALIBRATION

Calibration is the adjustment of an existing equation by comparing it with measured information. The calibration process assumes that there is a direct proportionality between all of the independent parameters and the parameters that are being predicted. Hence, the calibration process can be considered as a shift between what is currently practiced and what is actually occurring.

This calibration process is carried out using regression analysis. Regression is the measure of the association between one variable (the dependent variable) and one or more other variables (the independent variables). With this in mind, it can be assumed that the Wiczak model for the AC modulus will be nonlinear and multivariable. This section of the report will provide a step-by-step procedure on formulating the multivariable-nonlinear regression

Table 5.1 – Filtered Data Extracted from LTPP Database for AC Layer

No.	SHRP ID	County	AC Material Model Parameters						Backcalculated Modulus (psi)
			V _v (%)	P _{AC} (%)	P ₂₀₀ (%)	η(poise)	F (Hz)	T (°F)	
1	1	TRAVIS	9.9	5	2	0.002139	18	70	1089450
2	1047	CARSON	7	5	5	0.00118	18	58.6	1004921
3	1048	ECTOR	4.5	5.6	3	0.00056	18	69.4	1188200
4	1049	NACOGDOCHES	3.9	7.4	6	0.00206	18	61.3	1470466
5	1050	GRIMES	3.9	5.8	4	0.00198	18	70	1673964
6	1060	REFUGIO	4.7	5.4	1	0.00205	18	81.8	1600674
7	1061	SHERMAN	7	6.6	3	0.000858	18	70	123367
8	1065	OLDHAM	2.1	5.4	3	0.0012	18	76.4	866992
9	1068	LAMAR	7.9	5.4	6	0.00198	18	54.3	662867
10	1076	TERRY	2.1	6.4	3	0.000895	18	70	238458
11	1077	HALL	3.6	4.2	1	0.00102	18	92.2	1015125
12	1092	MEDINA	3	5.2	2	0.00202	18	86.5	1425218
13	1094	BEXAR	3.2	26	2	0.001094	18	70	1845473
14	1096	MEDINA	4.7	4.5	8	0.00113	18	74.7	1281383
15	1109	WALKER	5	5.2	3	0.0018	18	70	1618405
16	1122	WILSON	2.8	4	6	0.00099	18	82	817177
17	1130	GUADALUPE	4.4	4.5	4	0.001008	18	70	1114637
18	1169	RUSK	3.7	5	4	0.00187	18	70	1100145
19	1178	BURLESON	3.2	5.9	7	0.002037	18	70	7490028
20	1181	LIVE OAK	2.4	4.3	3	0.00093	18	89.5	517531
21	1183	GARZA	10.8	6.9	3	0.00092	18	70.8	1074224
22	2133	BELL	6.3	5.3	3	0.002133	18	70	1760070
23	3559	WALKER	5.9	6.5	7	0.0025	18	78.3	2347916
24	3579	VAN ZANDT	5.3	5.8	1	0.002119	18	70	1059546
25	3629	COLORADO	2.4	5.7	4	0.001854	18	70	1337024
26	3669	ANGELINA	4.1	8.5	6	0.00211	18	55.3	1887475
27	3679	ANGELINA	3.3	6.6	5	0.0021	18	61.7	236279
28	3689	POLK	3.7	7.5	5	0.00197	18	66.9	1185704
29	3835	BRAZOS	3.4	5.7	3	0.00176	18	70.5	1273637
30	9005	BEXAR	7.2	4.7	4	0.00111	18	70.7	2399228

* V_v=Air Void Content P_{AC}=% Asphalt Content P₂₀₀=% Aggregate Passing Sieve #200 =Viscosity @ 70°F
F=Loading Frequency T=Temperature

Table 5.2 – LTPP Data Used in Calibration of ACP Model

No.	Site ID	AC Material Model Parameters						M _B [*] (psi)	M _W ^{**} (psi)	Cluster value
		V _V (%)	P _{AC} (%)	P ₂₀₀ (%)	η (poise)	F (Hz)	T (°F)			
1	1068	7.9	5.4	6.0	0.00198	18	54.3	662867	741162	12%
2	1047	7.0	5.0	5.0	0.00118	18	58.6	1004921	694742	31%
3	1122	2.8	4.0	6.0	0.00099	18	82.0	817177	511980	37%
4	1181	2.4	4.3	3.0	0.00093	18	89.5	517531	322365	38%
5	1065	2.1	5.4	3.0	0.0012	18	76.4	866992	468589	46%
6	1130	4.4	4.5	4	0.001008	18	70	1114637	593957	47%
7	1169	3.7	5	4	0.00187	18	70	1100145	586114	47%
8	1049	3.9	7.4	6.0	0.00206	18	61.3	1470466	676469	54%
9	1096	4.7	4.5	8.0	0.00113	18	74.7	1281383	574762	55%
10	3629	2.4	5.7	4	0.001854	18	70	1337024	593430	56%
11	3689	3.7	7.5	5.0	0.00197	18	66.9	1185704	517165	56%
12	1048	4.5	5.6	3.0	0.00056	18	69.4	1188200	499365	58%
13	3669	4.1	8.5	6.0	0.00211	18	55.3	1887475	776873	59%
14	3835	3.4	5.7	3.0	0.00176	18	70.5	1273637	515611	60%
15	3579	5.3	5.8	1	0.002119	18	70	1059546	411378	61%
16	1050	3.9	5.8	4	0.00198	18	70	1673964	519705	69%
17	1109	5.0	5.2	3.0	0.0018	18	70.0	1618405	493774	69%
18	1	9.9	5	2	0.002139	18	70	1089450	329040	70%
19	2133	6.3	5.3	3	0.002133	18	70	1760070	439164	75%
20	1077	3.6	4.2	1.0	0.00102	18	92.2	1015125	245871	76%
21	1183	10.8	6.9	3.0	0.00092	18	70.8	1074224	242947	77%
22	1092	3.0	5.2	2.0	0.00202	18	86.5	1425218	277885	81%
23	9005	7.2	4.7	4.0	0.00111	18	70.7	2399228	449937	81%
24	1060	4.7	5.4	1.0	0.00205	18	81.8	1600674	277737	83%
25	3559	5.9	6.5	7.0	0.0025	18	78.3	2347916	316691	87%
26	1178	3.2	5.9	7	0.002037	18	70	7490028	613084	92%
27	1094	3.2	26	2	0.001094	18	70	1845473	99415	95%
28	1076	2.1	6.4	3	0.000895	18	70	238458	535411	125%
29	1061	7	6.6	3	0.000858	18	70	123367	353223	186%
30	3679	3.3	6.6	5.0	0.0021	18	61.7	236279	720591	205%

* M_B=Backcalculated modulus from the Falling Weight Deflectometer device

** M_W=Witczak modulus calculated using Equation 2.1

Table 5.3 – Testing Techniques for Base and Subgrade Parameters

Parameter	Test
Thickness	Dynamic Cone Penetration Test
Resilient Modulus	Resilient Modulus Test
Maximum Dry Density	Field/Laboratory Method for Determining In-Place Density of Soils and Base Materials (Tex-115-E & Tex-113-E, respectively)
Optimum Moisture Content	
Moisture Content	Determining Moisture Content in Soil Materials (Tex-103-E)
Degree of Compaction	Field Method for Determining In-Place Density of Soils and Base Materials (Tex-115-E)
Aggregate Passing No.40	Particle Size Analysis of Soils (Tex-110-E)
Percent of Clay	
Percent of Silt	
Liquid Limit	Determining Plastic Limit (Section 7. Tex.-105-E) of Soils and Calculating the Plasticity Index (Section 8. Tex-106-E) of Soils
Plastic Index	

Table 5.4 – Texas Test Sites Visited for Limited Calibration of Models

Layer	County	Roadway	Material	Date of Testing
Base	El Paso	Darrington	Silty or Clayey Sand (A-2-4)	Feb-04
	Terrel	US90 (Old Base)	Silty or Clayey Sand (A-2-6)	Apr-04
	Terrel	US90 (New Base)	Silty or Clayey Sand (A-2-6)	May-04
	Hidalgo	US281	Silty or Clayey Sand (A-2-4)	Jun-04
	Hidalgo	FM2220	Silty or Clayey Sand (A-2-4)	Jun-04
	Brown	FM45	Silty or Clayey Sand (A-2-4)	Aug-04
	Dallas	FM1187	Silty or Clayey Sand (A-2-4)	Aug-04
Subgrade	Hidalgo	Loop 499	Silty or Clayey Sand (A-2-6)	Jun-04
	Hidalgo	FM1016	Silty or Clayey Sand (A-2-7)	Jun-04
	Brown	FM45	Silty or Clayey Sand (A-2-6)	Aug-04
	Tom Green	FM2288	Crushed Limestone, Silty or Clayey Sand (A-2-4)	Jun-04

Table 5.5 – Summary of Laboratory and In-Situ Data Collected for Calibration of Base Subgrade Models

Layer	Location	Max. Dry Density (pcf)	Opt. Moist. Content (%)	Moist. Content (%)	Degree of Comp. (%)	Agg. Passing No.40 (%)	% of Clay	% of Silt	LL (%)	PI (%)	Resilient Modulus		
											k1 (ksi)	k2	k3
BASE	DARRINGTON	135.9	6.9	3.5	102.4	14.0	3.4	1.0	N/A	N/A	12.0	0.5	0.0
	US90 NEW BASE	128.9	8.8	7.0	101.3	17.3	4.0	1.6	N/A	N/A	19.7	0.5	-0.2
	US90 OLD BASE	128.4	8.6	8.5	98.8	41.4	0.9	0.3	N/A	N/A	54.8	0.5	-0.4
	US281	110.2	15.3	10.4	95.5	13.8	1.0	0.0	N/A	N/A	53.3	0.3	-0.2
	FM 45 BASE	137.1	6.8	3.5	100.9	9.4	2.9	0.7	N/A	N/A	28.0	0.4	-0.1
	FM2220	108.0	17.0	12.7	96.6	17.1	2.9	0.5	N/A	N/A	16.6	0.1	0.0
	FM1187	132.1	8.1	8.0	101.9	18.9	6.5	3.8	N/A	N/A	85.7	-0.1	-0.2
SG	LOOP 499	95.4	23.5	16.9	106.7	71.9	21.1	15.4	40.7	28.0	14.0	0.3	-0.1
	FM 1016	100.1	20.8	19.6	101.5	79.2	54.3	5.9	42.0	20.0	38.0	0.3	-0.3
	FM 45 SG	124.0	8.0	3.8	100.6	21.5	6.3	1.6	23.7	12.0	47.0	0.2	-0.4
	US281	128.5	9.2	5.8	102.9	24.8	7.1	2.2	29.0	9.6	34.0	0.0	-0.2

Single Variable Linear Regression

As stated before, calibration can be described as a direct proportionality between dependent and independent parameters. In this case, even though a number of models could have been used for the calibration of the ACP model, the Witczak equation was selected. This model has been currently practiced as a method for finding dynamic modulus based on multiple input parameters. In order to calibrate this equation for Texas, first, the relevant parameters were inputted into the Witczak equation to calculate the predicted modulus of the ACP layer. These values were then compared to the actual measured moduli.

The first step in calibration is to fit the following linear equation to the data:

$$Y = mx + b + \varepsilon \quad (5.2)$$

Where x is the independent variable (measured modulus), m is the slope of the line, b is the intercept for the dependent variable and Y represents that dependent variable (estimated modulus). Parameter ε represents random analogous elements that are not considered or cannot be measured following a normal distribution with $N(0, \sigma^2)$.

Once the form of the equation has been generated, the next step is to use actual measured results that can be placed into the form of the equation as dependent and independent variables. Single variable linear regression is contingent on having more than one set of empirical data points. Subsequently, a linear equation that is representative of the measured data can easily be generated

Based on the unshaded LTPP cluster points shown in Table 5.2, this linear regression analysis can be performed for the modulus of the ACP layer. Where the backcalculated modulus represents the dependent variable (Y) and the modulus from Witczak equation represents the independent variable (x). Figure 5.1 shows the results of the calibration based on Equation 5.2, with a slope of 2.34 and an intercept of 0. The data used in curve fitting are presented by the solid points, and the data in the other clusters are presented with the hollow points. Unfortunately, the linearly calibrated model is highly uncorrelated, as shown by the R^2 value of 0.21 in Figure 5.1.

Modifying Coefficients of Witczak Equation

The next step for the calibration process consisted of adjusting the coefficients of the Witczak equation based on the data in Table 5.2. Data from the middle cluster was used for that analysis as well. Out of the twenty points available, seventeen were used for developing the equation and three randomly selected points were saved for validation. Equation 5.2 is rewritten as follows:

$$\begin{aligned} \log(E_{ac}) = & C^1 + (C^2) \left(\frac{P_{200}}{F^{0.17033}} \right) + (C^3) V_v + (C^4) \eta \\ & + (C^5) t_p^{(1.3+0.49825 \log(F))} P_{ac}^{0.5} + \frac{(C^6)}{F^{1.1}} t_p^{(1.3+0.49825 \log(F))} P_{ac}^{0.5} \end{aligned} \quad (5.3)$$

where C^1 to C^6 are the coefficients to be determined. The remaining terms were left unadjusted. Also, the last term in the initial Witczak equation, Equation 2.1, was combined into C^1 since this

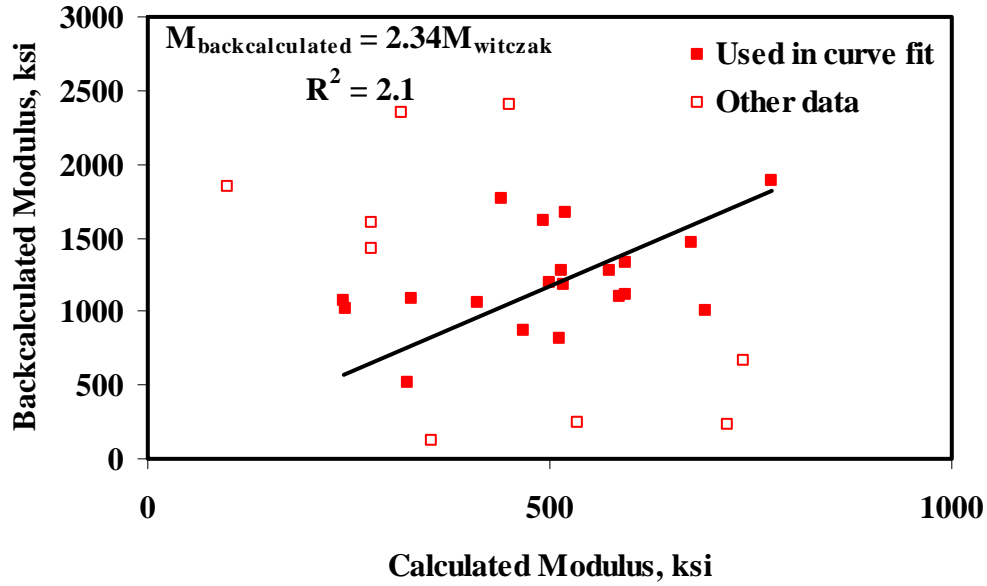


Figure 5.1 - Results of Calibration of Witczak Model Using Single-Variable Regression

term is related to frequency. The frequency for all points in the database was set to a constant value of 18 Hz. This process is more complicated than the single variable regression. However, since the form of the equation is fixed, the determination of the coefficients was straight forward. Equation 5.4 presents the results of the estimation process, while Figure 5.2 presents the model.

$$\begin{aligned} \log(E_{ac}) = & 5.560 + 0.43 \left(\frac{P_{200}}{F^{0.17033}} \right) + .004V_v \\ & + 140.953\eta + 21.280t_p^{(1.3+0.49825\log(F))} P_{ac}^{0.5} \\ & - \frac{511.418}{F^{1.1}} t_p^{(1.3+0.49825\log F)} P_{ac}^{0.5} \end{aligned} \quad (5.4)$$

Even though the new model can predict the moduli better, given the low R^2 value, a more appropriate model is desirable.

Multivariable-Nonlinear Regression

The development of a new ACP material model based on n independent variables requires a multivariable nonlinear estimation algorithm. In general the form of the equation is:

$$Y = C^1 + C^2(x_1) + C^3(x_2) + \dots + C^n(x_n) \quad (5.5)$$

where C^1 to C^n are model coefficients, X_1 to X_n are independent model variables (n is an integer from 1 to number of variables available) and Y is the dependent variable. The complexity of this equation is in the model variables. Each variable in Equation 5.5 can be a function of several parameters. This complicates the process since an endless number of possible combinations

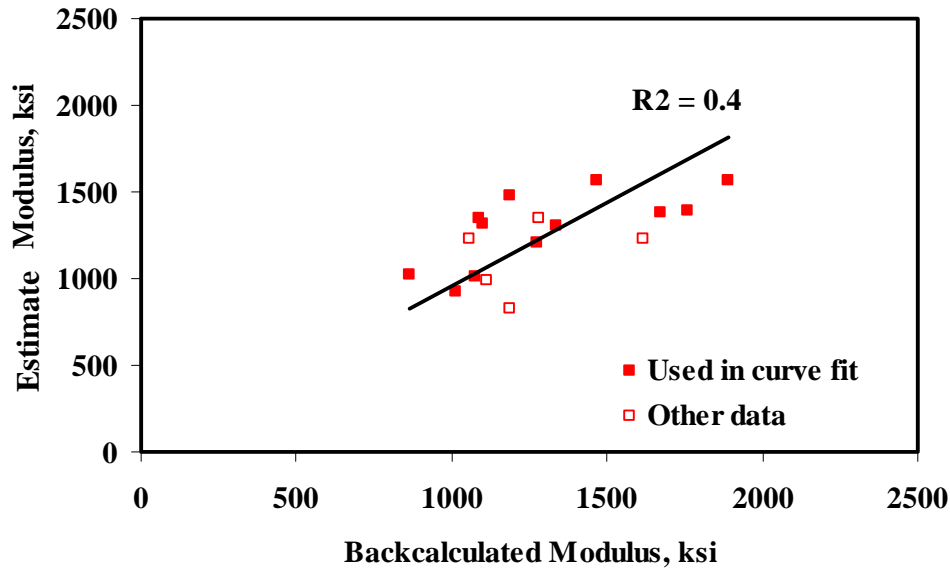


Figure 5.2 - Results of Modifying Coefficients of Witzak Model

exist. In order to solve this problem and determine a feasible solution, the possible number of combinations was reduced. First, all trigonometric functions were eliminated based on the nature and current status of the ACP material models. Common functions such as addition, subtraction, multiplication, division, logarithms, natural logarithms, and exponentials were used in the regression analysis. Through an iterative process, resulting coefficients for each of the possible independent variable equations were determined. The combination with the lowest least squares error was selected.

Based on the assumptions discussed, a regression analysis process with four independent variables was carried out. The analysis differed slightly from linear regression in the fact that each of these four variables can also be multiplied, divided, taken the logarithm of, etc. The result is a nonlinear, multivariable regression equation based on the measured parameters from the LTPP database. In this case, as in the previous methods, data from the middle clusters was used (seventeen used for generating the model and three for testing and validating the model). Equation 5.6 presents the results of the best model.

$$\begin{aligned}
 E_{AC} = & -64342 + 169 \ln(V_v)(t_p^2) + 1.25(e^{P_{ac}})(e^{P_{200}}) \\
 & - 2.44(P_{200}^3)(e^{V_v}) - 7.38 \times 10^{-26}(\eta^3)(e^{t_p}) \\
 & + 109.7(f)(V_v^3) - 157.3\sqrt{t_p}(P_{200}^3)
 \end{aligned} \tag{5.6}$$

As depicted in Figure 5.3, the predicted moduli were fairly reasonable, with a much better R^2 value of 0.68 when compared to the single variable linear regression keeping in mind that Equation 5.6 was derived with a very limited number of points. The validation data points, plotted as hollow points, exhibited higher errors than the rest of the data.

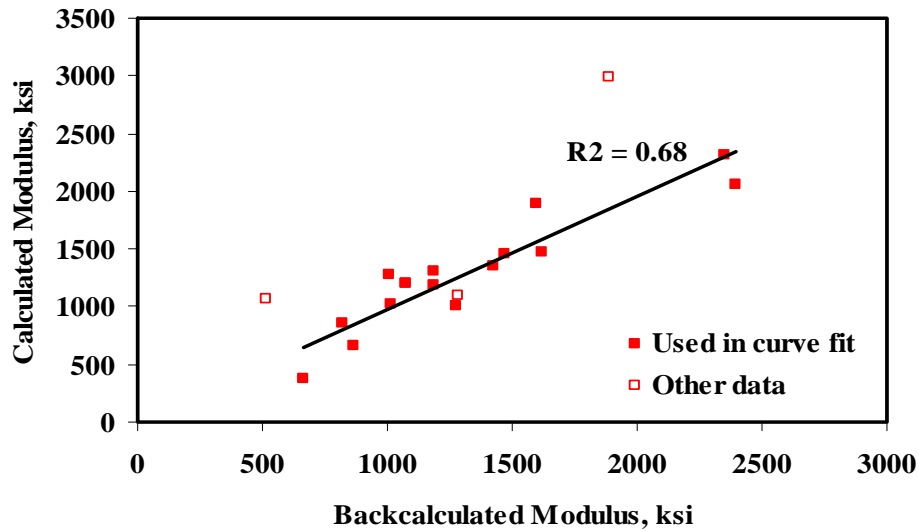


Figure 5.3 - Results of New AC Material Model Using LTPP Database

Overall, the models generated are reasonable, keeping in mind the limited data that was available and used. Four material models for the ACP layer are now available and can be used in the RECIPPE. Also, the calibration and model development algorithms developed here are being incorporated into RECIPPE in the case that more data becomes available.

BASE & SUBGRADE MATERIAL MODEL CALIBRATION

The correlation, represented by the R^2 value, for the multivariable nonlinear regression of the ACP modulus equation was considerably better than the other regression analyses discussed. For this reason, the multivariable nonlinear regression is the only calibration performed for the base and subgrade material models. The material models for base and subgrade layers, as discussed in Chapter 2, are based on the constitutive equation as presented in Equation 2.2. Equation 2.2 can be used for both granular and cohesive soils. The main distinctions for these two materials using the model are the k_1 , k_2 and k_3 material parameters. As stated in Chapter 2, parameters k_1 , k_2 and k_3 are obtained from equations developed from a multiple regression procedure. Equations 2.3 through 2.8 provide the k parameters as a function of construction parameters as a result of a study by Santha (1994). The study was for pavement sections in Georgia. Since these equations were based on empirical data, similar types of equations (estimating the k parameters based on construction measures) would have to be generated for pavement sections in Texas. Unfortunately, the LTPP database cannot be used to for this task. As discussed previously, the parameters required for base and subgrade materials were not comprehensively available in the LTPP database. The best solution was to use the data from the sections previously intended for model calibration to develop new models (summarized in Table 5.5). When developing regression equations based on empirical data a large database is preferable. Unfortunately,

because the database of samples obtained for these layers is only for eleven sites, an innovative technique was used to populate the database. The process is presented next.

The technique used in populating the database involved utilizing the values of the parameters collected from the sites and simulating hundreds of possible values for those parameters with similar attributes. To capture the attributes for each pavement layer, correlation matrices shown in Tables 5.6 and 5.7 were developed. Table 5.6 is for the base layer and Table 5.7 is for the subgrade layer. Once the correlation of the parameters is established, the next step is to use a technique to simulate the variables. The main assumption was to represent each variable with a distribution. In this case, each variable was assumed normal with a mean and standard deviation equal to the values obtained from the field data for each parameter.

For example, by obtaining the statistical information for each parameter from Table 5.5 (e.g. the mean for the maximum dry density is 124.7 pcf with a COV of 10%, moisture content is 10.6% with a COV of 42%, and so on) numerous simulations can be made that fit a normal distribution for each parameter. These simulated values will provide a wider range of base and subgrade stiffness parameters that can be used in the regression analysis. Thus the material model is not limited to just the specific sites, but any range of values that fall within the parameter statistics.

The next step is to simulate each variable depending on its distribution while insuring that the correlation of that variable with the other variables is maintained.

To illustrate the concept a simplistic example of predicting the deflections of a cantilever beam under a point load is presented. It is expected that the deflections should follow a continuous curve, as shown in Figure 5.4. In other words, the correlation between the deflection points shows that as the deflection point moves closer to the load, the deflection should increase monotonically in the beam. Hence, if the Monte Carlo simulation was carried out to simulate the deflections, the simulated deflections should increase monotonically with the deflection points as opposed to following completely random events within the normal distribution, as shown in Figure 5.5. For this reason, the correlation was included in the simulation for the base and subgrade parameters.

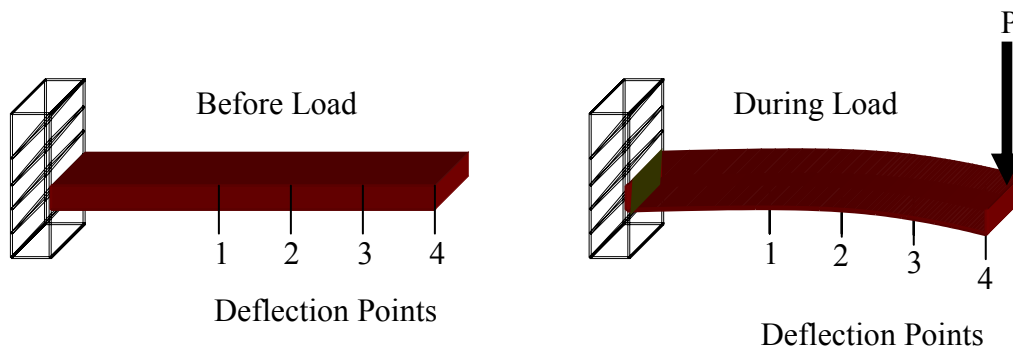


Figure 5.4 – Expected Deflection of a Cantilever under a Point Load

Table 5.6 - Correlation Matrix of Base Construction Parameters Used for Material Model Calibration

	Max. Dry Density	Opt. Moist. Content	Moist. Content	Degree of Comp.	Agg. Passing No.40	% of Clay	% of Silt	k1	k2	k3
Max. Dry Density	1.00	-0.99	-0.94	0.92	-0.01	0.37	0.54	-0.25	0.76	-0.16
Opt. Moist. Content		1.00	0.92	-0.90	-0.07	-0.31	-0.53	0.16	-0.83	0.26
Moist. Content			1.00	-0.88	0.28	-0.41	-0.49	0.31	-0.68	-0.03
Degree of Comp.				1.00	-0.16	0.67	0.79	-0.56	0.67	0.09
Agg. Passing No.40					1.00	-0.60	-0.30	0.57	0.26	-0.71
% of Clay						1.00	0.90	-0.93	0.04	0.61
% of Silt							1.00	-0.72	0.41	0.22
k1								1.00	0.17	-0.81
k2									1.00	-0.57
k3										1.00

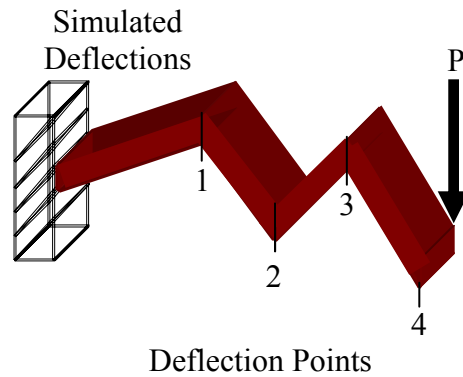


Figure 5.5 – Erroneously Simulated Deflections

The simulated values for this study were created using @RISK, a risk analysis software that performs the desired calculations using the “CORRMAT” macro (Palisade, 1996). This command identifies 1) a matrix of rank correlation coefficients and 2) the location in the matrix of the coefficients used in correlating the distribution function to run the Monte Carlo simulation (Palisade, 1996). For more accurate results, 10,000 simulations were run for each of the k_1 , k_2 and k_3 parameters in cohesive and granular materials. Tables 5.8 and 5.9 show the statistics for the parameters of the base and subgrade layers after the correlated simulation, respectively. As depicted in the table, the statistical information for each parameter is very similar to those shown in tables 5.6 and 5.7. Since a large population of examples exists, the development of the regression equation based on empirical data is performed. The results of the regression equations the k parameters are presented next.

Base Material Model Calibration

Of the seven samples that were collected, six were used for developing the new material models, and one was used for validation. As more field-testing is performed further validation can be carried out.

The initial models for the k_1 , k_2 and k_3 parameters for granular materials are shown in Equations 2.3 through 2.5, respectively. The new calibrated models are shown in Equations 5.7 through 5.9.

$$\begin{aligned}
 k_1 = & 52.84[\ln(DEN)](CLY) - \frac{8.21[\ln(MOIST)]}{\sqrt{MOIST}} + 0.418(\sqrt{MC})(SLT^2) - \\
 & 2.92(COMP)(CLY) - 1.11(\sqrt{S40})[\ln(MOIST)] + 18.21(CLY)(\sqrt{SLT}) \\
 & + 98.35
 \end{aligned} \tag{5.7}$$

Table 5.9 - Resulting Correlation Matrix of Simulated Subgrade Construction Parameters Used for Material Model Calibration

	Max. Dry Density (pcf)	Opt. Moist. Content	Moist. Content	Degree of Comp.	Agg. Passing No.40	% of Clay	% of Silt	LL	PI	k1 (ksi)	k3
Max. Dry Density (pcf)	1.00	-0.98	-0.94	-0.53	-0.96	-0.71	-0.84	-0.92	-0.96	0.62	-0.81
Opt. Moist. Content		1.00	0.96	0.61	0.97	0.69	0.86	0.96	0.95	-0.70	0.70
Moist. Content			1.00	0.40	1.00	0.86	0.69	0.99	0.83	-0.52	0.69
Degree of Comp.				1.00	0.42	-0.08	0.88	0.51	0.71	-0.99	0.09
Agg. Passing No.40					1.00	0.84	0.72	0.98	0.86	-0.53	0.73
% of Clay						1.00	0.26	0.80	0.48	-0.05	0.64
% of Silt							1.00	0.73	0.95	-0.91	0.52
LL								1.00	0.82	-0.62	0.58
PI									1.00	-0.77	0.73
k1 (ksi)										1.00	-0.15
k3											1.00

$$\begin{aligned}
k_2 = & \frac{-1.84[\ln(MC)]}{MOIST^2} + \frac{3.14 \times 10^{-4}(COMP^2)}{\sqrt{CLY}} - \frac{0.176[\ln(S40)]}{e^{SLT}} \\
& - 3.67 \times 10^{-5}(e^{CLY})(MOIST^2) + \frac{0.442[\ln(SLT)]}{S40} \\
& - \frac{0.423[\ln(DEN)]}{\sqrt{CLY}} + 1.93 \times 10^{-5}(MOIST^3)(SLT^3)
\end{aligned} \tag{5.8}$$

$$\begin{aligned}
k_3 = & 9.31 \times 10^{-4}(\sqrt{DEN})(\sqrt{S40}) + 1.44 \times 10^{-2}(MOIST)(CLY) \\
& - 4.83 \times 10^{-2}(MC)(\sqrt{SLT}) - \frac{0.182[\ln(COMP)]}{\ln(S40)} - \frac{2.22 \times 10^{-2}(\sqrt{S40})}{CLY^3} \\
& - \frac{145.83(\sqrt{CLY})}{e^{MOIST}} + \frac{2.03(e^{SLT})}{e^{MC}}
\end{aligned} \tag{5.9}$$

As stated before, the new granular equations are based upon the simulated data. The estimated and measured values (for both the initial and calibrated material models) are compared in Figure 5.6 through 5.8. Using the three calibrated models the resulting correlation for the curve fit samples was considerably better than the results from the initial model.

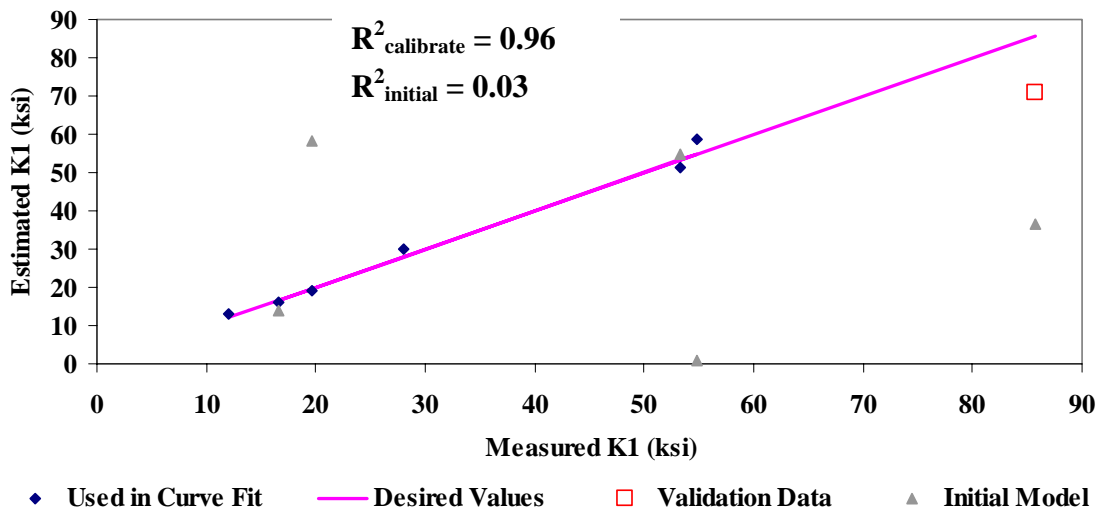


Figure 5.6 – Results of Granular Material Model for k_1

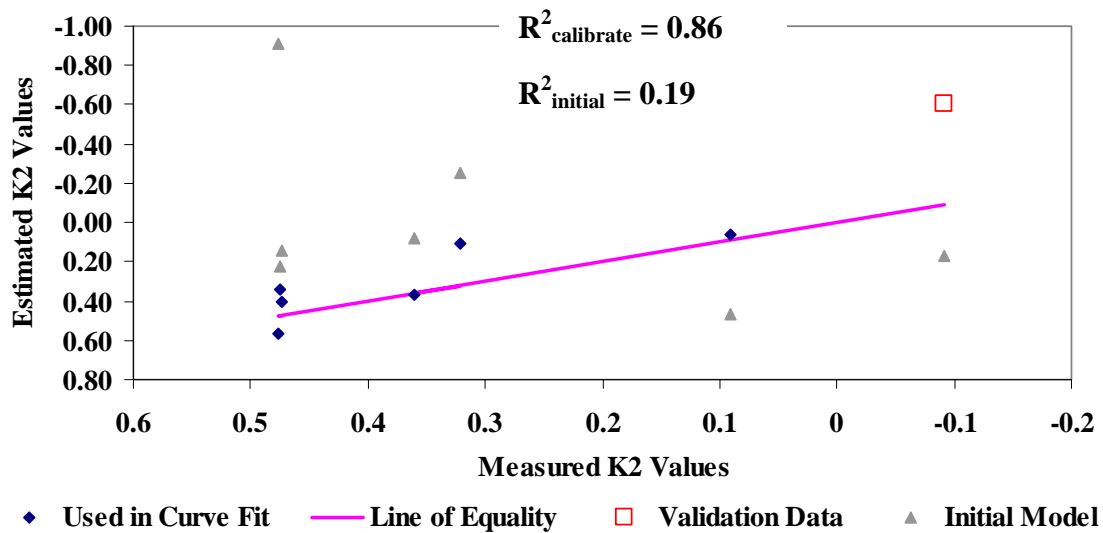


Figure 5.7 – Results of Granular Material Model for k_2

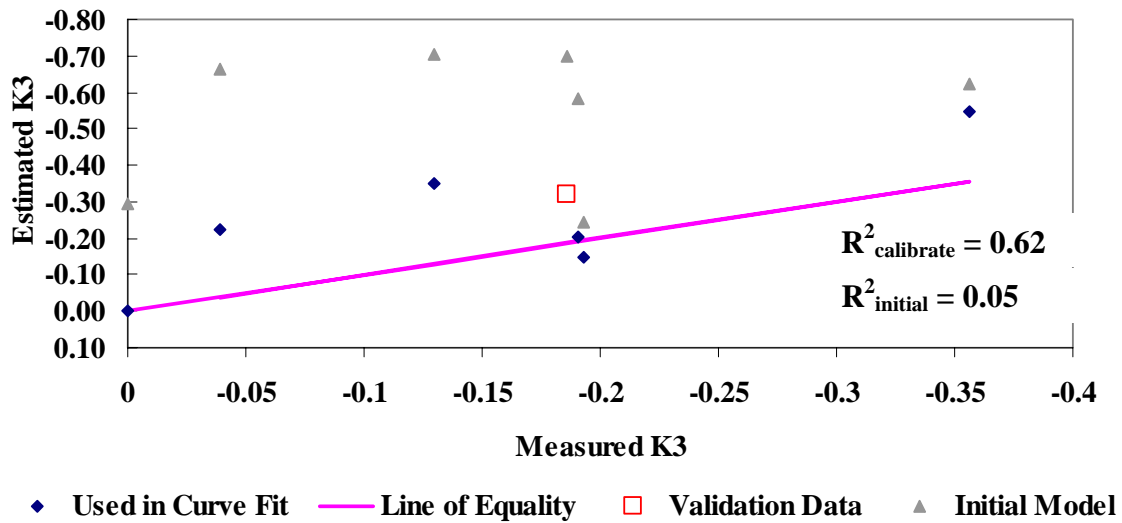


Figure 5.8 – Results of Granular Material Model for k_3

Subgrade Material Model Calibration

Because there are only four samples for the subgrade as shown in Table 5.5, all data points were used to calibrate the models. The models for the k_1 , k_2 and k_3 parameters for cohesive soils, are shown in Equations 2.6 through 2.8, respectively. The results for the calibrated values are shown in Equations 5.10 through 5.12. The measured and estimated parameters (for both initial and calibrated models) are compared in Figures 5.9 and 5.10.

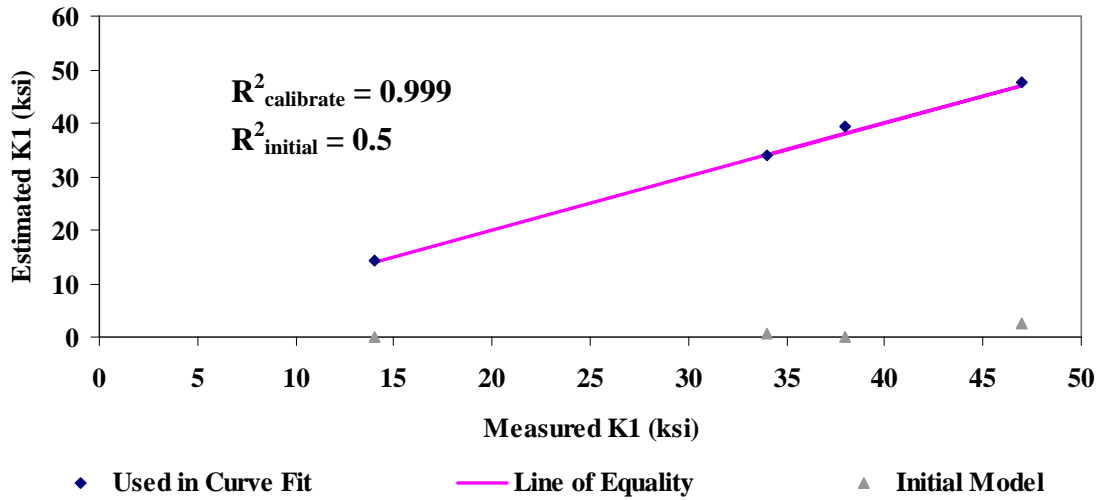


Figure 5.9 – Results of Cohesive Material Model for k_1

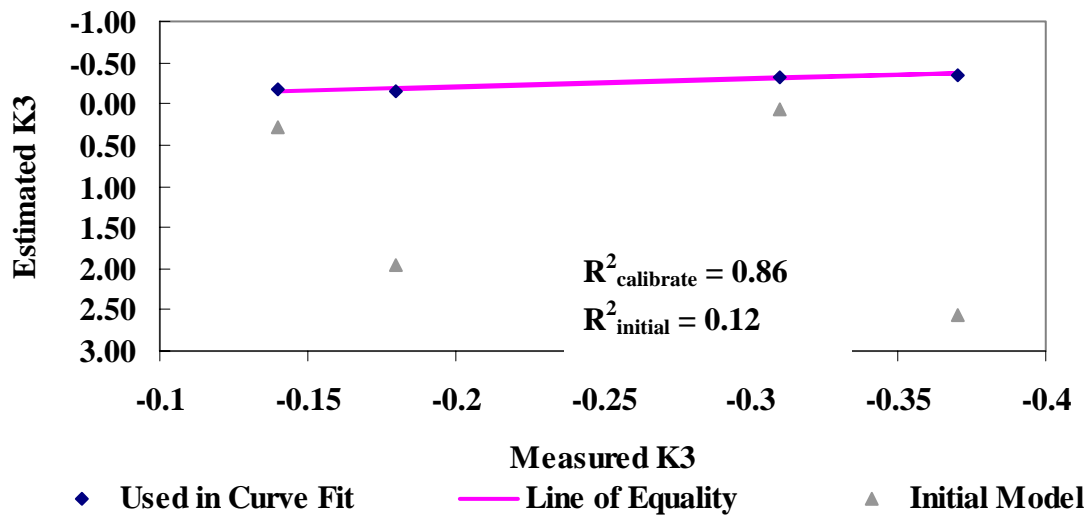


Figure 5.10 – Results of Cohesive Material Model for k_3

$$\begin{aligned}
 k_1 = & 1453 - \frac{1.52 \times 10^7 [\ln(DEN)]}{COMP^3} - \frac{0.683(MOIST^3)}{PI^3} - \frac{133.9(COMP)}{\sqrt{COMP}} \\
 & + \frac{104.7[\ln(S40)]}{LL} + \frac{1.25 \times 10^{39}(CLY^3)}{e^{COMP}} + \frac{42.21[\ln(SLT)]}{e^{MC}} - \quad (5.10)
 \end{aligned}$$

$$\begin{aligned}
 & 7.897 \times 10^{-6} [\log(LL)](CLY^3) - 0.915[\ln(PI)][\ln(MOIST)] \\
 & k_2 = 0 \quad (5.11)
 \end{aligned}$$

$$\begin{aligned}
k_3 = & -3.06 + \frac{1.48 \times 10^{42} (MOIST)}{e^{COMP}} - \frac{194.67 (MC)}{LL^3} + 5.65 \times 10^{-5} (COMP^2) [\ln(DEN)] \\
& + 1.05 \times 10^{-4} (\sqrt{CLY}) (DEN) - \frac{0.668 (\sqrt{SLT})}{MOIST} - \frac{8.29 \times 10^{41} (LL)}{e^{COMP}} + \\
& \frac{0.033 (PI)}{SLT} + 6.04 \times 10^{-8} [\log(DEN)] (CLY^3)
\end{aligned} \tag{5.12}$$

The results for the calibrated base and subgrade models exhibit a better general correlation to the simulated values, when compared to the initial models. However, as more data becomes available the models can be recalibrated and show an even higher level of correlation.

CHAPTER SIX

CASE STUDY

CASE STUDY

With the implementation of new models and QC procedures, RECIPPE can be used for pre-construction and post-construction purposes, as well as quality assurance and quality control. This chapter outlines a brief example that covers all techniques described thus far, and how they can be incorporated into the optimization of pavement performance. More specifically, the problem concentrates on the base layer only, in order to demonstrate the practicality of RECIPPE by simulating an actual construction process; where the subgrade currently exists and the contractor wishes to only focus on the pavement layer currently being built.

Problem Statement

Given: TxDOT has hired a contractor to build a length of road called Darrington Road, in El Paso, Texas. Darrington Road is designed to be 10 miles long and 24 feet wide. From historical records, site specifications for design and construction data have been listed in Table 6.1 and 6.2, respectively. Also included in the tables are the current sampling frequency values, based on TxDOT guide schedule.

Find: A set of construction parameters that meets a minimum performance life of 1,500,000 ESALS with 90% reliability and a COV not greater than 45% for fatigue cracking and subgrade rutting criteria. The frequency of sampling at various points in the post-construction process should also be determined.

Assume: Darrington Road is a three-layer system (5 in. ACP over 12 in. flexible base over subgrade). Also, TxDOT and contractor's confidence level are both 80%, with 5% tolerable error.

Table 6.1 – Darrington Road Design Parameters from Specifications

Parameter	Mean	COV(%)	Current Sample Size
ACP Thickness (in.)	5	0	N/A
Base Thickness (in.)	12	0	N/A
SG Thickness (in.)	225	0	N/A
ACP Modulus (psi)	650000	0	N/A
Base Modulus (psi)	80000	Based Material Information	See Construction Parameters
SG Modulus (psi)	30000	0	N/A

Table 6.2 – Darrington Road Base Construction Parameters from Historical Data

Parameter	Mean	COV(%)	Current Sample Size
Maximum Dry Density (pcf)	136	1	8 sample per 16000 yd. ³
Opt. Moisture Content (%)	6.9	10	8 sample per 16000 yd. ³
Moisture Content (%)	3.5	10	30 samples per 16000 yd. ³
Degree of Compaction (%)	102	0.3	30 samples per 16000 yd. ³
% Aggregate Passing Sieve #40	14	12.5	8 sample per 16000 yd. ³
% Clay	3.4	2	8 sample per 16000 yd. ³
% Silt	1	2	8 sample per 16000 yd. ³

Manual Procedure

The graphical user interface (GUI) for RECIPPE is set up so that the assumptions and inputs can be easily entered. Figure 6.1 shows the input screen for the design parameters and the constraint inputs. The design values for the thicknesses and moduli, located at the top of the image. This design information includes the mean and COV values. The COV's are all equal to zero except for the modulus of the base layer (as listed in Table 6.1). The mean for the modulus of the base layer is actually a priori value that is set as a limitation in the algorithm. The COV of the base is derived from the variance of the construction parameters, which are used to find the modulus variance using the material models, discussed before.

Also shown in Figure 6.1 are the constraints set by the assumptions in the problem statement, displayed in the “Miscellaneous” and “Performance Indicators” frames. For example, the minimum failure limit of 1,500,000 ESALS is called the “Input ESALS”, the reliability for this minimum remaining life of 90% is called the “Reliability Level”, and so on. Most of the “Miscellaneous” inputs are self explanatory. In order to make the reduction process manual (instead of automatic) the “Max # Iterations” value should be set to 1. Similarly, the construction parameter values are inputted as shown below.

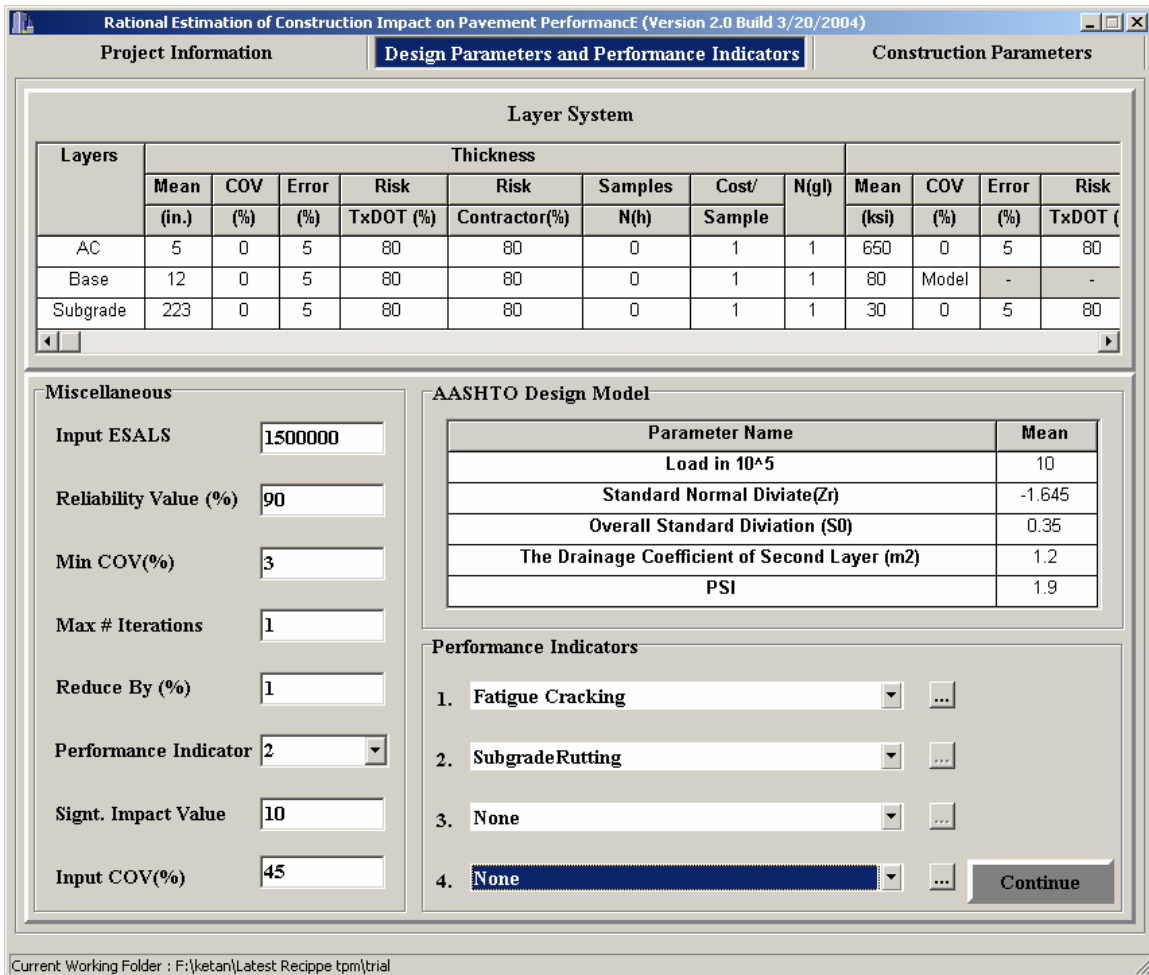


Figure 6.1 – Constraints & Design Parameter Input

Figure 6.2 displays the GUI that allows users to provide the data listed in Table 6.2. That figure also shows the capability for users to provide the data pertaining to sample size and sample size cost estimation. Specifically, the tolerable error, owner (TxDOT) and contractor acceptable confidence (or risk), cost per sample and the current level of sampling are the inputs needed for the frequency of sampling calculations. The “Ngl” value represents the sample size from guidelines, or the sample size that is provided from the TxDOT guide schedule. The cost per sample is set as the same value for each construction parameter so that the importance for the total cost is a function of sample size only.

Manual Results

From the initial execution, remaining life due to subgrade rutting meets the 1,500,000 ESAL limit at 90% reliability, as depicted in Figure 6.3. However, the remaining life due to fatigue cracking, at the 90% confidence interval, is only 1.37 million ESALs, and the COV is greater than 45%. As a result the COV of the construction parameters must be adjusted to improve the

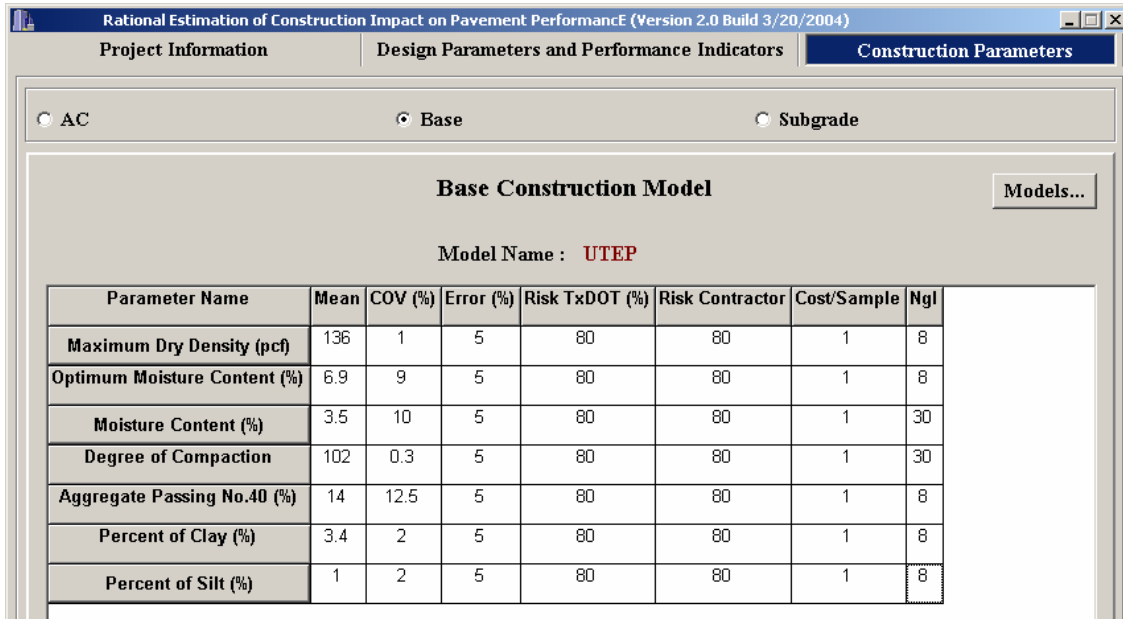


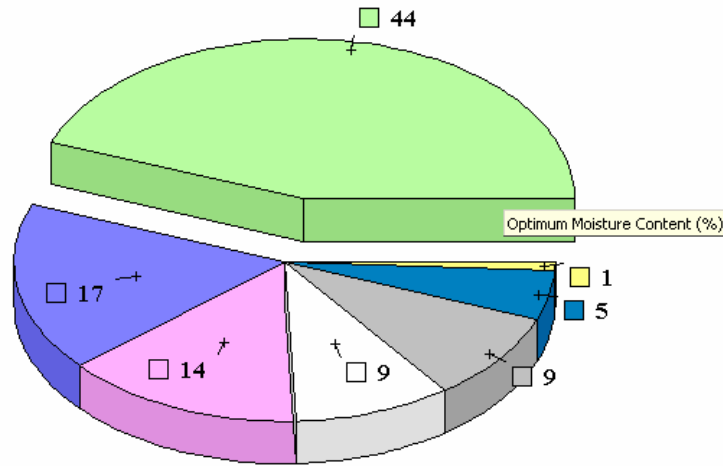
Figure 6.2 – Construction Parameter Inputs

reliability level. In the figure, the remaining life as per 1993 AASHTO design guide is unacceptable at 90% confidence interval because of the large variability in the predicted remaining life. However, since this criterion was not of interest to the user, it was not considered. Once again, it should be emphasized that the AASHTO model is not mechanistic, but it is included in the software for the sake of completeness.

In order to improve the remaining life due to fatigue cracking at the 90% reliability, only the most important construction parameter COV value will be reduced. This value is found using the impact charts, as shown in Figure 6.4.

Method of Analysis		Number of ESALs of Failure (10 ⁶)			
PreConstruction Mode		Fatigue Cracking	Subgrade Rutting	AC Rutting	AASHTO Failure Criterion
Deterministic		3.29	362.95	1074.44	292.93
Probabilistic	Mean	3.50	455.19	1307.24	387.45
	Std.Dev.	1.66	139.25	995.34	328.82
	COV (%)	47.4	30.6	76.1	84.9
	90%	1.37	276.73	31.66	-33.96

Figure 6.3 – Initial Pavement Performance Results for Manual Optimization



Critical Parameters	Mean	COV (%)	Error (%)	Risk TxDOT (%)	Risk Contractor
Maximum Dry Density (pcf)	136	1	105	97	-
Percent of Clay (%)	3.4	2	105	97	-
Optimum Moisture Content (%)	6.9	10	105	97	-
Moisture Content (%)	3.5	10	105	97	-
Percent of Silt (%)	1	2	105	97	-

Figure 6.4 – Impact Chart for Initial Manual Optimization

From impact charts the COV of the optimum moisture content affects the pavement performance variance the most, followed by the field moisture content and the degree of compaction, respectively.

The manual optimization will follow the “Largest Impact Value Reduction” technique, by only reducing the COV of the optimum moisture content from 10% to 9%. The result of this reduction is shown in Figure 6.5.

Method of Analysis		Number of ESALs of Failure (10 ⁶)			
PreConstruction Mode		Fatigue Cracking	Subgrade Rutting	AC Rutting	AASHTO Failure Criterion
Deterministic		3.29	362.95	1074.44	292.93
Probabilistic	Mean	3.50	453.92	1304.82	386.47
	Std.Dev.	1.65	137.89	990.18	327.12
	COV (%)	47.2	30.4	75.9	84.6
	90%	1.38	277.20	35.85	-32.75

Figure 6.5 – Secondary Pavement Performance Results from Manual Reduction

By reducing only the COV of the optimum moisture content, the remaining life due to fatigue cracking at 90% reliability increased from 1.37 million ESALs to 1.38 million ESALs, and the COV decreased from 47.4% to 47.2%. The remaining life due to subgrade rutting at 90% reliability also increased from 276 million ESALs to 277 million ESALs, and the COV reduced from 30.6% to 30.4%.

Automation Results

Unfortunately, the remaining life due to fatigue cracking still does not meet the specifications for reliability bounds mentioned in the problem statement. The next step in the manual procedure would be to continue reducing the COV of the construction parameter with the greatest impact value. However, to accelerate the process the automated feature was used. This process provides the pavement performance results shown in Figure 6.6. The remaining lives due to fatigue cracking and subgrade rutting meet the requirements of the problem statement. The combination of construction parameters used to obtain these results is listed in Table 6.3.

Method of Analysis		Number of ESALs of Failure (10 ⁶)			
PreConstruction Mode <input type="button" value="v"/>		Fatigue Cracking	Subgrade Rutting	AC Rutting	AASHTO Failure Criterion
Deterministic		3.29	362.95	1074.44	292.93
Probabilistic	Mean	3.51	427.13	1293.92	379.86
	Std.Dev.	1.50	109.94	910.44	301.72
	COV (%)	42.9	25.7	70.4	79.4
	90%	1.58	286.24	127.15	-6.81

Figure 6.6 – Final Pavement Performance Results from Automated Optimization

Table 6.3 – Change in Construction Parameter COV for Final Pavement Performance Results

Parameter	Mean	Initial COV(%)	New COV (%)
Maximum Dry Density (pcf)	136	1	1
Opt. Moisture Content (%)	6.9	9	7
Moisture Content (%)	3.5	10	10
Degree of Compaction (%)	102	0.3	0.3
% Aggregate Passing Sieve #40	14	12.5	12.5
% Clay	3.4	2	2
% Silt	1	2	2

Table 6.3 depicts that only the COV of the optimum moisture content is changed, from 10% to 7%. With this new information, the second part of the problem statement can now be addressed for quality control during post-construction.

Post-Construction Analysis

The initial frequency for inspection should follow guide schedule sample sizes, and then changes should be based on the inspection results from control charts.

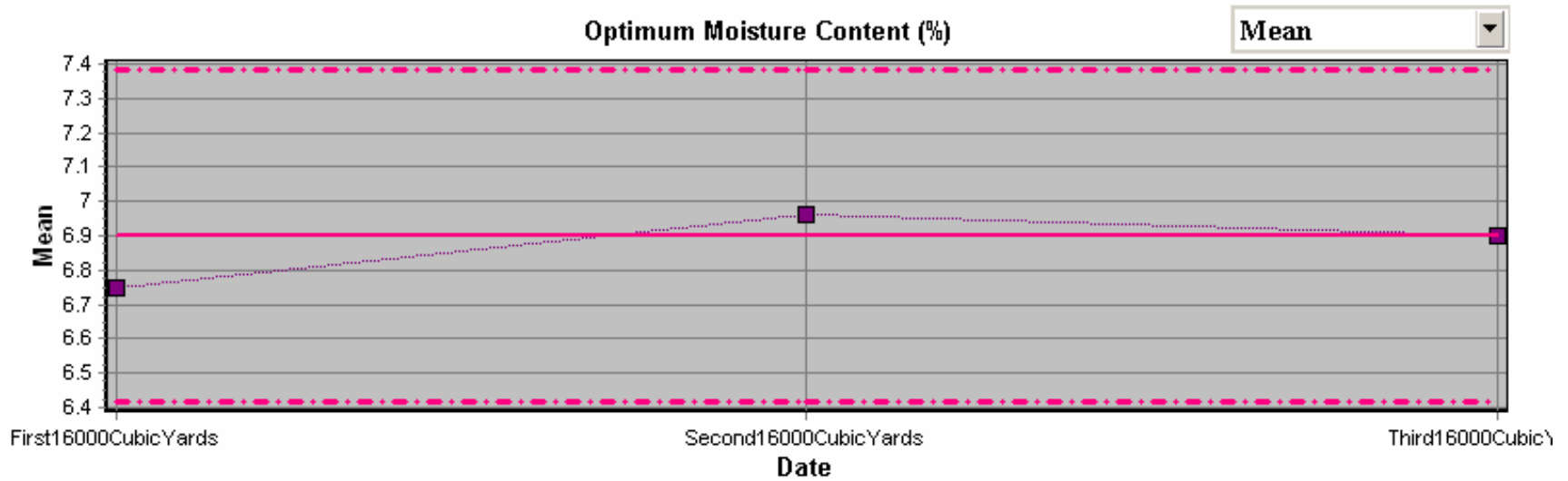
In the case of the optimum moisture content, the inspector should initially take eight random samples for every 16,000 yd³ of base material that is built. Every time a subgroup is sampled, the measurements are entered into RECIPPE to identify changes in the mean and COV. For example, for the first 48,000 yd³, the information shown in Table 6.4 was entered into RECIPPE. The information listed in the table is used to create the mean and COV control charts, shown in Figures 6.7 and 6.8, respectively. The upper and lower control limits for the mean control chart are denoted by the dashed red lines, the center line is represented by the solid red line and the measured means are solid blocks connected by a black line. The same style is used for the COV control chart, however the upper control limit for the COV is too large to be seen (UCL = 9%).

Table 6.4 – Measured Optimum Moisture Content for the first 24,000 yd.³ of Darrington Road

Subgroup	Sample #							
	1	2	3	4	5	6	7	8
First 16,000 yd ³	6.0%	6.9%	7.6%	6.3%	7.8%	6.7%	6.6%	6.1%
Second 16,000 yd ³	6.3%	7.4%	6.8%	6.5%	7.7%	6.3%	7.3%	7.4%
Third 16,000 yd ³	6.7%	7.0%	6.8%	7.1%	6.9%	7.2%	6.8%	6.7%

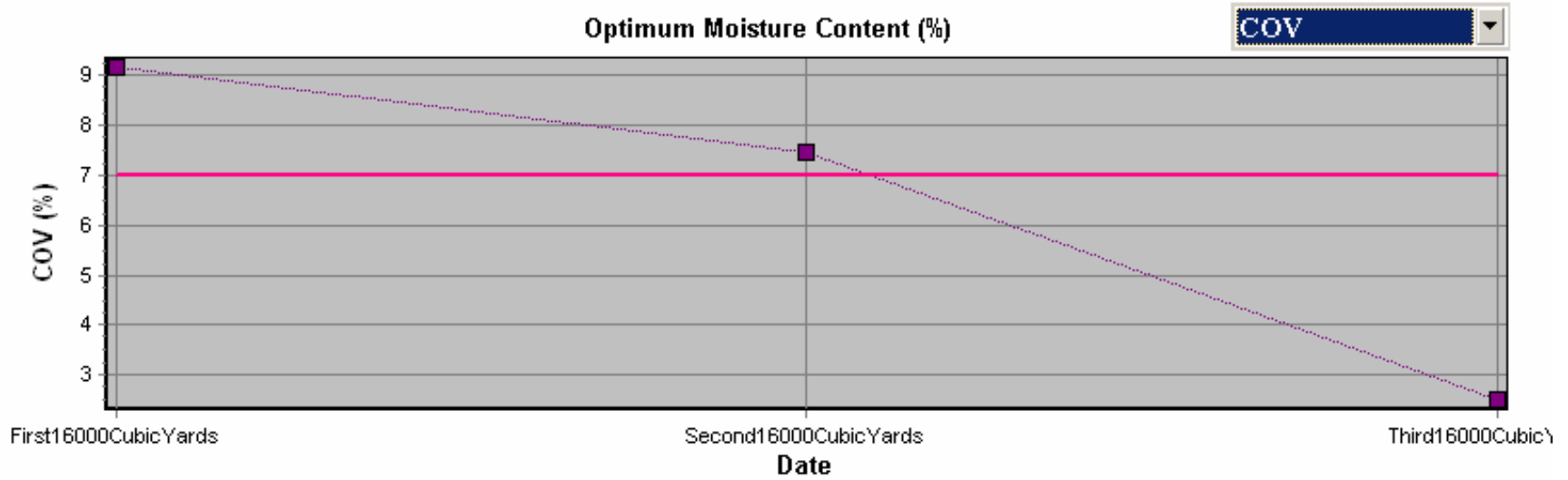
In Figure 6.7, the mean measured optimum moisture contents follow a random pattern and stay within the control limits. Thus, the mean for the optimum moisture content is in-control, and no corrective action needs to be performed for the average values.

For the COV control chart, none of the measured subgroups exceed the upper control limit, plus an encouraging trend is exhibited (see Figure 6.8). The COV of the measured optimum moisture content is continually decreasing, which is the phenomenon that TxDOT and the contractors wish to see. Furthermore, because the COV decreased below the centerline, along a trend that is not random, the control chart depicts that the contractor is exhibiting an increased level of consistency. Hence, continuing to measure the optimum moisture content at the frequency supplied by the guide schedule is excessive. Reducing the sample size to the final suggested sample size, listed in Table 6.5, is adequate enough to ensure that the optimum moisture content is within limits (according to Equation 4.14).



Measured Values for Optimum Moisture Content (%)				
Date	1	2	3	4
First16000CubicYards	6	6.9	7.6	6.3
Second16000CubicYards	6.3	7.4	6.8	6.5
Third16000CubicYards	6.7	7	6.8	7.1

Figure 6.7 – Optimum Moisture Content Mean Control Chart for first 48,000 yd³ of Darrington Road



Measured Values for Optimum Moisture Content (%)				
Date	1	2	3	4
First16000CubicYards	6	6.9	7.6	6.3
Second16000CubicYards	6.3	7.4	6.8	6.5
Third16000CubicYards	6.7	7	6.8	7.1

Figure 6.8 – Optimum Moisture Content COV Control Chart for first 48,000 yd³ of Darrington Road

If the COV had increased, then the guide schedule sample size could no longer be assumed adequate to verify that the optimum moisture content was within limits. As a result, the inspector would be encouraged to increase the sample size to the initial suggested sample size, listed in Table 6.5. If the initial suggested sample size was smaller, or the COV continued to increase, then all construction should cease so that corrective action could be performed to identify and resolve the factors that are leading to an increased COV. Also, if the number of samples becomes excessive, the construction should be stopped for corrective action.

Cost Analysis

The decrease in sampling is a benefit to contractors by reducing the cost of inspection. Just as increasing the sampling is a detriment to the contractors. Therefore, calculation of the cost for sampling provides the cost/benefit results for increasing/decreasing the measurement frequency.

Furthermore, the costs could be additionally reduced by removing the need for sampling of some parameters altogether. The parameters that have no impact on pavement performance can be completely removed from sampling because the RECIPPE program quantitatively identifies the importance of each parameter.

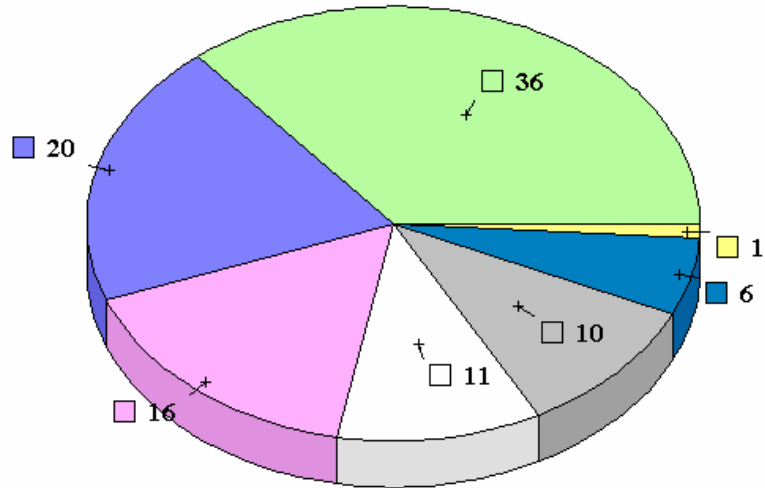
For example, the total cost of sampling only the parameters for the final combination of construction parameters, provided in the Automation Results section, can be compared to the initial cost of sampling according to TxDOT guide schedule sample sizes. The result is a cost/benefit analysis for increasing the quality of pavement performance.

Specifically, to calculate the total sampling cost for the optimized pavement the first step would be to analyze the impact chart and identify the most important parameters that contribute to the variance of the pavement performance. The results from the impact chart, shown in Figure 6.9, identify five parameters to measure: optimum moisture content, moisture content, degree of compaction, maximum dry density, percent of clay, and percent of silt (with the same order of importance). The impact due to percent aggregate passing sieve #40 can be considered negligible.

By taking the final suggested sample sizes for these six parameters and comparing their total costs (based on FY2003 values, shown in Table 4.8) to the seven guide schedule sample sizes (both listed in Table 6.5) provides the results listed in Table 6.6. The cost analysis shows that the initial sample sizes cost over three times as much as the samples provided by RECIPPE, for this situation. However, the general idea shows the incentive of reducing the variability of pavement performance from construction variability.

Table 6.5 – Initial and Calculated Construction Parameter Sample Sizes

Parameter	Mean	Initial COV	Final COV	TxDOT's Confidence	Contractor's Confidence	Tolerable Error	Guide schedule Sample Size per 16000 yd.³	Initial Suggested Sample Size per 16000 yd.³	Final Suggested Sample Size per 16000 yd.³
Maximum Dry Density (pcf)	136	1%	1%	80%	80%	5%	8	1	1
Opt. Moisture Content (%)	6.9	9%	7%				8	12	6
Moisture Content (%)	3.5	10%	10%				30	12	12
Degree of Compaction (%)	102	0.1%	0.1%				30	1	1
% Aggregate Passing Sieve #40	14	13%	13%				8	18	18
% Clay	3.4	2%	2%				8	1	1
% Silt	1	2%	2%				8	1	1



Critical Parameters	Mean	COV(%)	Error (%)	Risk TxDOT (%)
Maximum Dry Density (pcf)	136	1	105	97
Percent of Clay (%)	3.4	2	105	97
Optimum Moisture Content (%)	6.9	7	105	97
Moisture Content (%)	3.5	10	105	97
Percent of Silt (%)	1	2	105	97

Figure 6.9 – Impact Chart Used to Identify the Construction Parameters to Sample

Table 6.6 – Cost Analysis for Guide Schedule and RECIPPE Sample Sizes

Parameter	Guide Schedule Sample Size	Final Suggested Sample Size	Cost per Sample	Cost for Guide Schedule Sample Size	Cost for Final Suggested Sample Size
Maximum Dry Density (pcf)	4	1	\$ 330.00	\$1,320.00	\$330.00
Opt. Moisture Content (%)	4	2	\$ 330.00	\$1,320.00	\$660.00
Moisture Content (%)	30	12	\$ 27.00	\$810.00	\$324.00
Degree of Compaction (%)	30	1	\$ 37.50	\$1,125.00	\$37.50
% Aggregate Passing Sieve #40	4	0	\$ 60.00	\$240.00	\$0.00
% Clay	4	1	\$ 150.00	\$600.00	\$150.00
% Silt	4	1	\$ 150.00	\$600.00	\$150.00
TOTAL COST				\$6,015.00	\$1,651.50

CHAPTER SEVEN

CONCLUSIONS AND RECOMMENDATIONS

SUMMARY

The goal of this report was to develop rational algorithms that reconcile the results from several pavement-performance models, to validate the appropriateness of these models and algorithms, and to create a program that can be used in practice for the construction of pavement.

An overview of performance-based methodologies and a background on some of the mathematical and analysis tools used in this project are included in Chapter 2. A validation of the algorithm's statistical theory was performed to reduce simulation time, described in Chapter 3. Chapter 4 described adjustments made to the previous prototype to provide optimal results. Also included in Chapter 4 were the additions to the prototype process, including: a) Reliability Analysis, b) Automation of Prototype, c) Sample Size Calculations, d) Control Chart Analysis, and e) Cost Allocation. Chapter 5 described the calibration of current material models using regression analysis based upon empirical information. Chapter 6 presented a case study that demonstrated the use of the analysis tool and how the impact of variability of construction parameters impacts variability on performance.

CONCLUSIONS

RECIPPE presents a process that can be used in a practical manner to optimize pavement performance. Furthermore, the latest version of the process is versatile and avails complete modularity, which allows for new material and performance models to be inputted and/or calibrated as needed. Even though a limited number of sites were used to develop calibrated material models the results from RECIPPE and the methodology presented in this study is a step towards a more rational estimation of pavement remaining life from construction parameters.

The current RECIPPE program can be used to:

- Generate constructions parameter values that will meet owner's needs for pavement life
- Identify the construction parameters to focus on, in order to reduce pavement life variance and increase reliability
- Track and identify out of control procedures during construction
- Reduce sampling costs by optimizing the frequency of testing
- Create databases that can be used in future projects
- Lower variability of construction practices
- Provide penalties/bonuses to contractors
- Perform quality control and/or quality assurance of construction practices
- Focus manpower on specific parameters and reduce costs

There are several limitations to the program. As discussed in Chapter 5, the material models were developed with very limited data and as such the models should be used with caution. As more data becomes available and better models are developed, tested and validated using real data, more confidence is can be attain in using the material models in RECIPPE. The performance models are not calibrated either since it was outside the scope of this project. The performance models are being calibrated under other TxDOT projects.

RECOMMENDATIONS FOR FUTURE STUDY

Now that the proposed methodology for predicting pavement performance, and its corresponding variation, has been completed and calibrated and it is ready for shadow implementation. Shadow implementation would allow for RECIPPE to be validated by comparing its results to current methods. The results from the shadow implementation would provide the limitations/advantages of practically using the program in the real world.

Also, an additional cost/benefit analysis can be incorporated to show the life cycle cost analysis, based on the results from RECIPPE. To be specific, the present cost/benefit analysis concentrates on only the price of sampling and not the cost of future rehabilitation. Due to the fact that RECIPPE finds the amount of pavement that will withstand a set number of ESALs (in the form of the reliability), it could be expanded to find the amount of pavement that will not withstand a set number of ESALs. Hence, predicting how much pavement will need to be rehabilitated before the expected design life.

REFERENCES

1. Ayres M. Jr., and M.W. Witzak, (1998), "AYMA - A Mechanistic Probabilistic System to Evaluate Flexible Pavement Performance," Transportation Research Record 1629, Washington, D.C., pp 137-48.
2. Barksdale R.D., J. Alba, P.N. Khosla, R. Kim, P.C. Lambe, and M.S. Rahman, (1997), "Laboratory Determination of Resilient Modulus for Flexible Pavement Design," Federal Highway Administration.
3. Coduto, P.D., (1999), "*Geotechnical Engineering*," Prentice Hall.
4. Devore, J. L., (1995), "*Probability and Statistics for Engineering and the Sciences. 4th Edition*," Brooks/Cole Publishing Co.
5. Federal Highway Administration, (2004), Available: <http://www.datapave.com>.
6. Ferregut C., I. Abdallah, O. Melchor-Lucero, and S. Nazarian, (1999), "*Artificial Neural Network-Based Methodologies for Rational Assessment of Remaining Life of Existing Pavements*," El Paso, TX: Center for Highway Materials Research.
7. Finn F.N., and C.L. Monismith, (1984), "*Asphalt Overlay Design Procedures*," National Cooperative Highway Research Program.
8. Huang, Y.H., (1993), "*Pavement Analysis and Design*," Englewood Cliffs, New Jersey 07632: Prentice Hall.
9. Montgomery, C. D., (2001), "*Introduction to Statistical Quality Control*," Vol. 4th Edition. New York, New York 10158-0012: John Wiley & Sons.
10. Palisade Corporation, (1996), "Guide to Using @Risk," Newfield, NY 14867.
11. Patel A.J., and M.R. Thompson, (1998), "Consideration and Characterization of Pavement Construction Variability," Transportation Research Record 1632, Washington D.C. pp 40-50.

12. Rosenblueth, E., (1981), "Two-Point Estimates in Probabilities," D.F. Mexico, Universidad Nacional Autonoma de Mexico.
13. Santha, L. B., (1994), "Resilient Modulus of Subgrade Soils: Comparison of Two Constitutive Equations," Transportation Research Record 1462, Washington D.C., pp 79-90.
14. Webster S.L., R. H. Grau, and T.P. Williams, (1992), "Description and Application of Dual Mass Dynamic Cone Penetrometer," US Army Corps of Engineers.
15. Weed, R.M., (1998), "A Rational Method for Relating as-Built Quality to Pavement Performance Value," Transportation Research Record 1632, Washington D.C., pp 32-39.
16. Witczak, M.W., (2003), "Development of the 2002 Guide for the Design of New and Rehabilitated Pavement Structures," NCHRP 1-37A.
17. Abdallah I., H. Yin, S. Nazarian, C. Ferregut, (2002), "Optimizing Construction Quality Management of Pavements Using Mechanistic Performance Analysis," El Paso, TX.: Center for Highway Materials Research.
18. Zhang Z.F., W. Fowler, W.R. Hudson, and R. Ceballos, (2001), "Development of a Methodology to Determine the Appropriate Minimum Testing Frequencies for the Construction and Maintenance of Highway Infrastructure," Austin, TX., Center for Transportation Research.

APPENDIX A

RESULTS OF THE SENSITIVITY STUDY FOR ASPHALT CONTENT OF AC LAYER

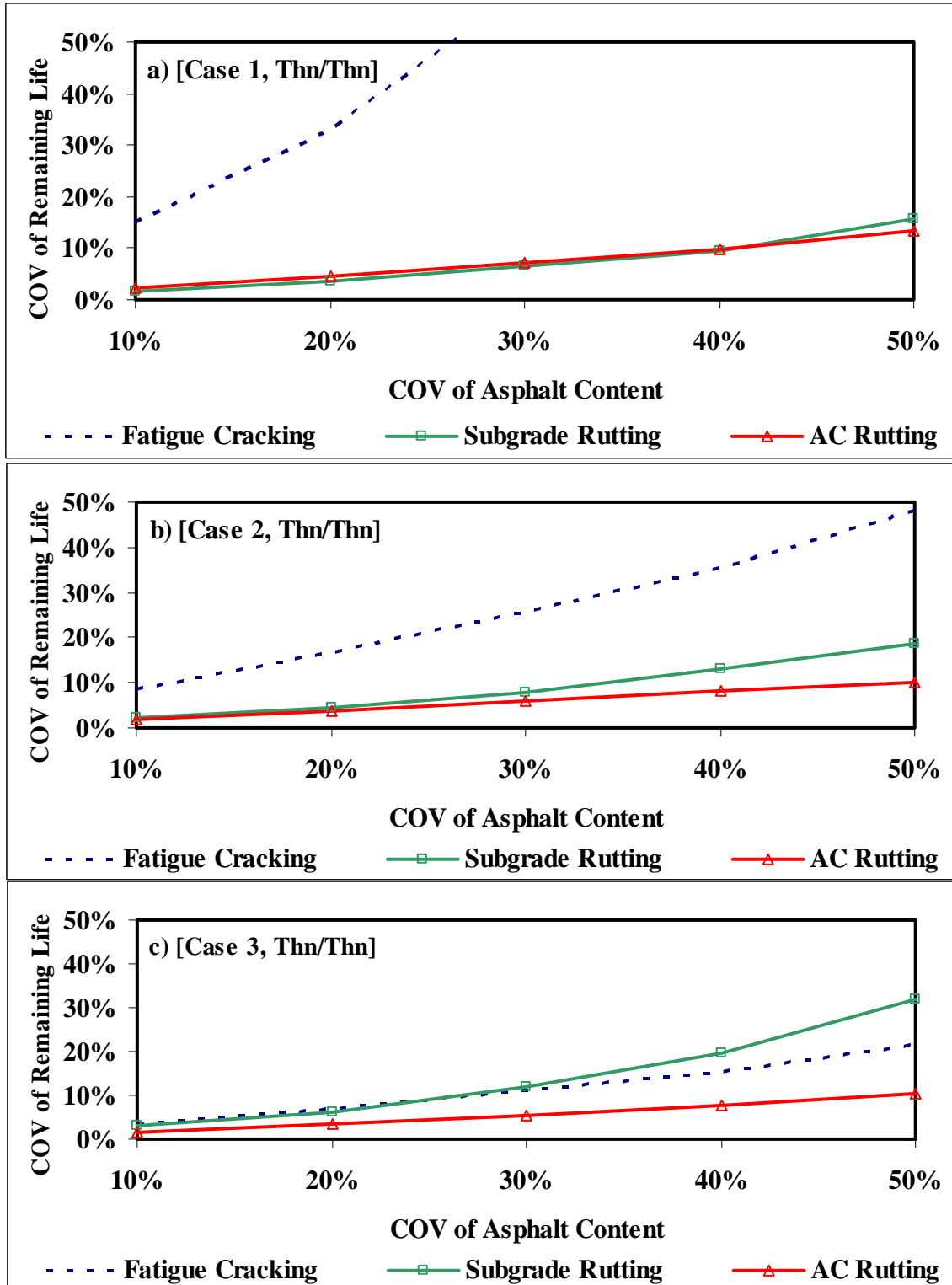


Figure A1 - Results of Impact of Variability of Asphalt Content on Remaining Life Varying AC Modulus for Thin-Thin Section

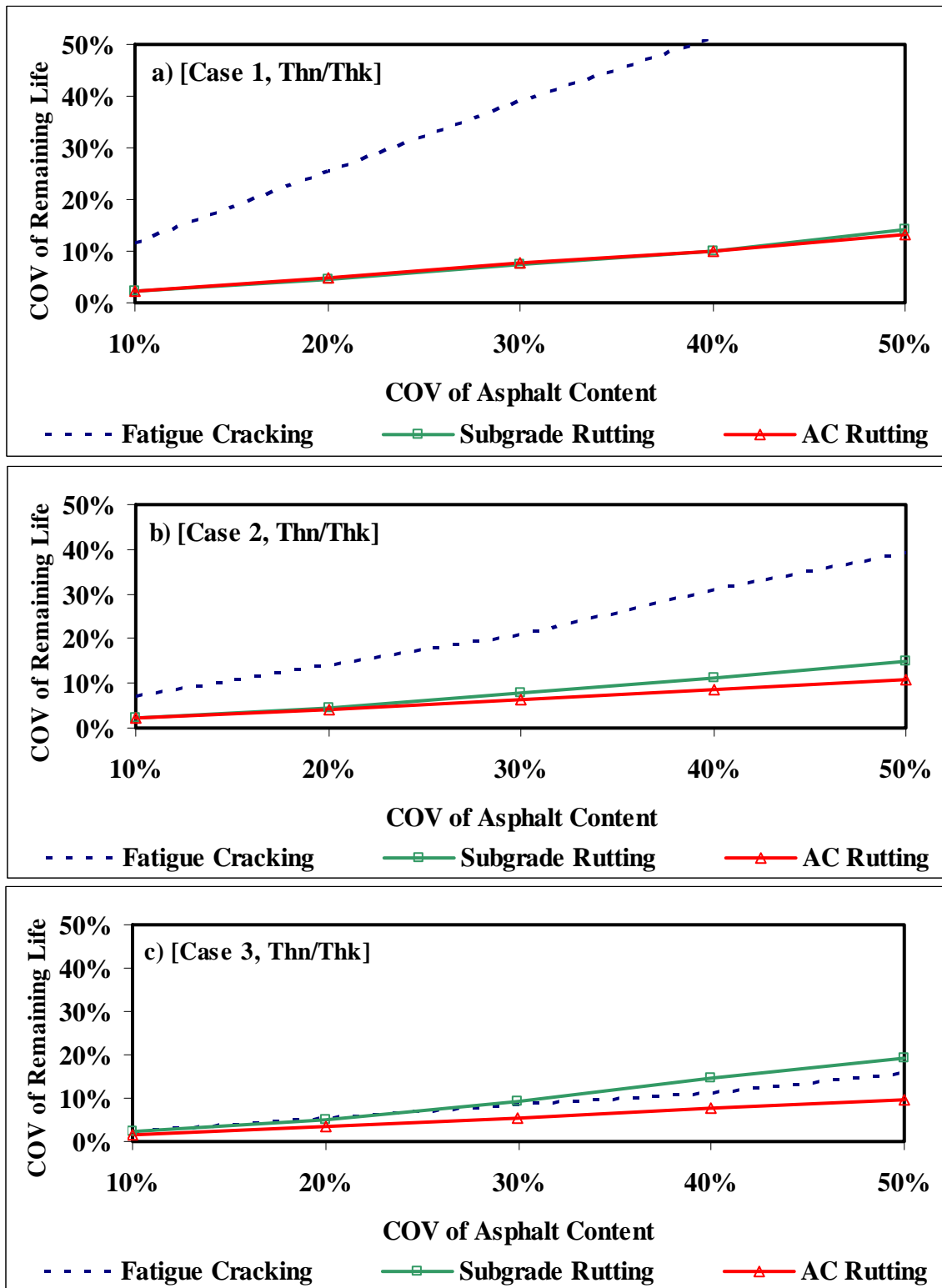


Figure A2 - Results of Impact of Variability of Asphalt Content on Remaining Life Varying AC Modulus for Thin-Thick Section

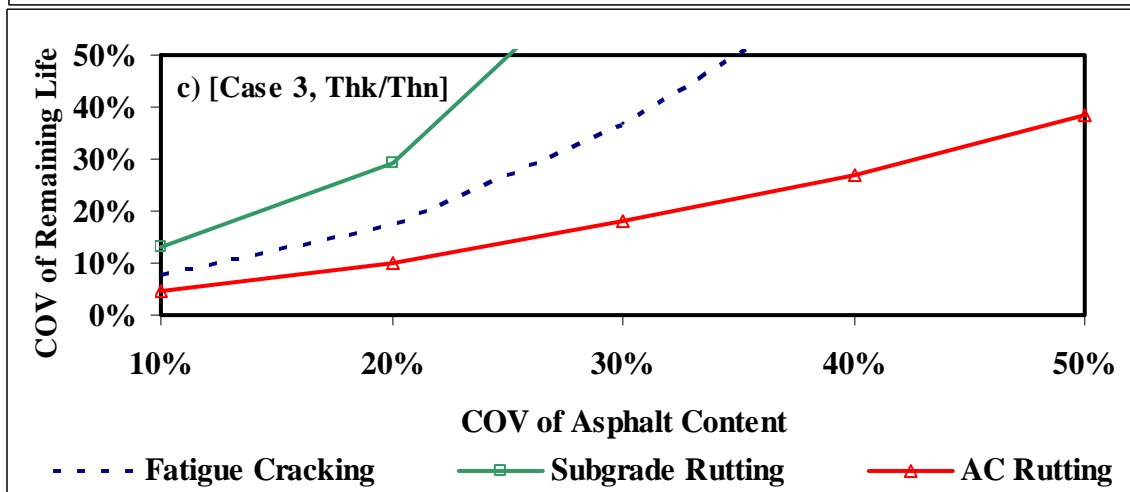
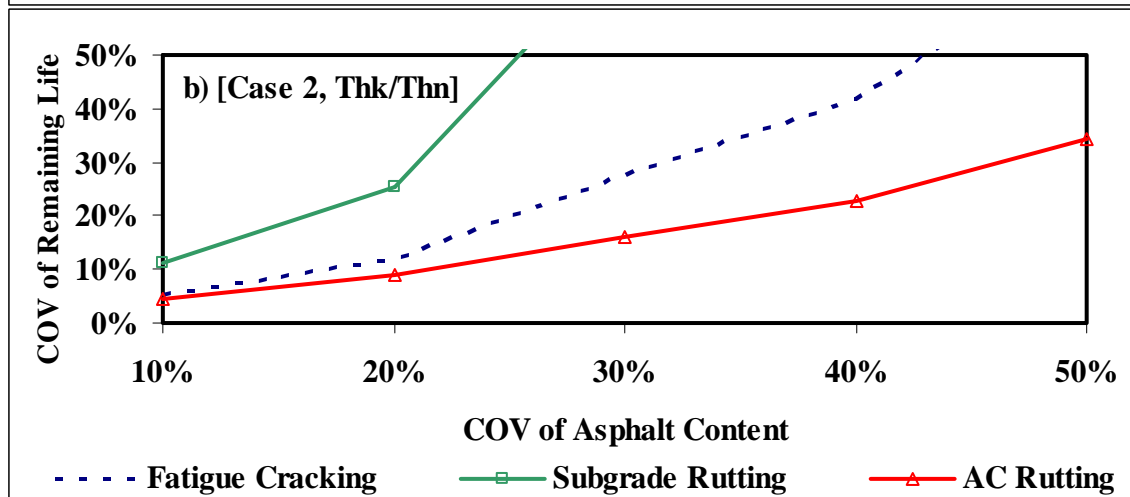
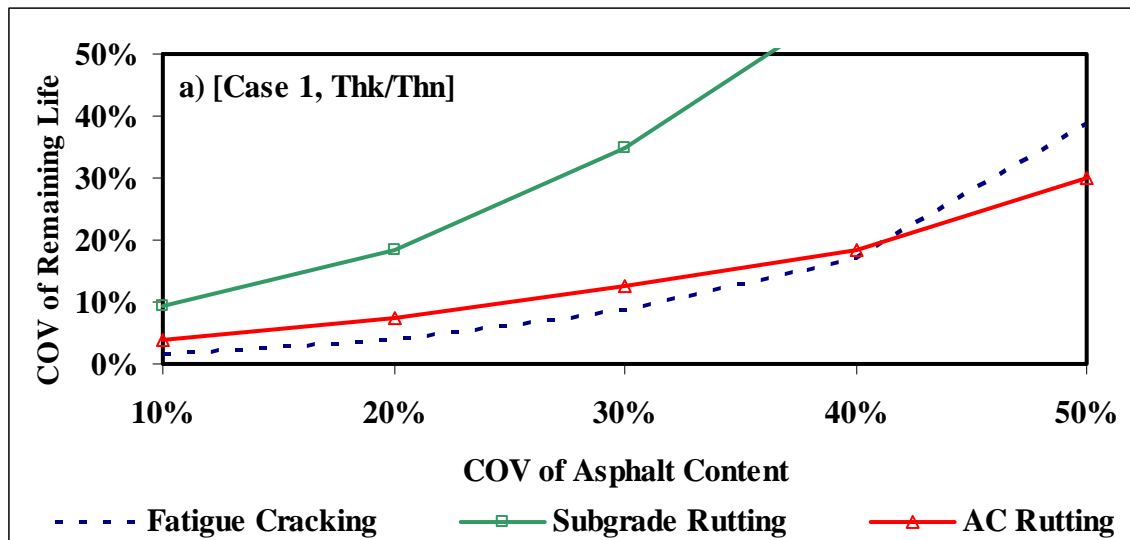


Figure A3 - Results of Impact of Variability of Asphalt Content on Remaining Life Varying AC Modulus for Thick-Thin Section

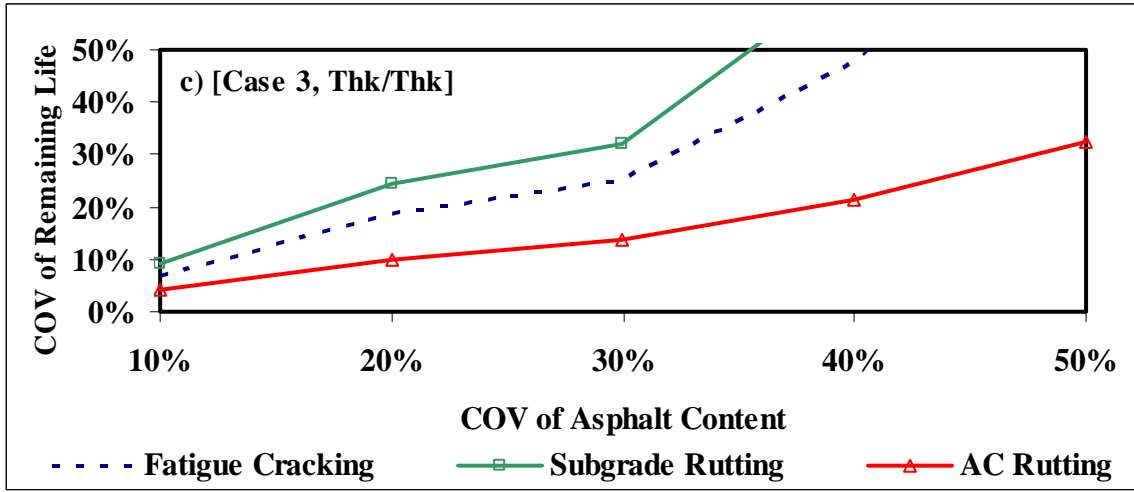
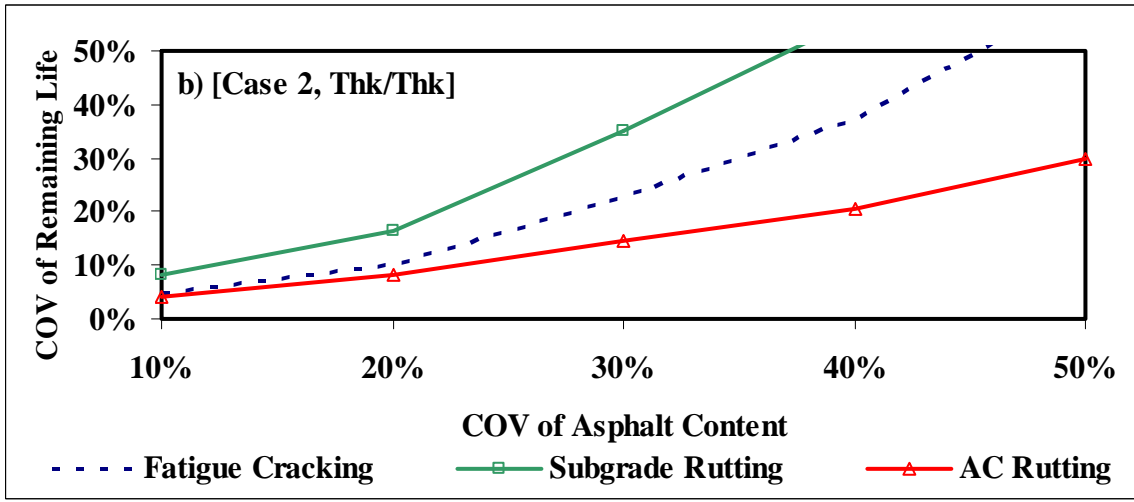
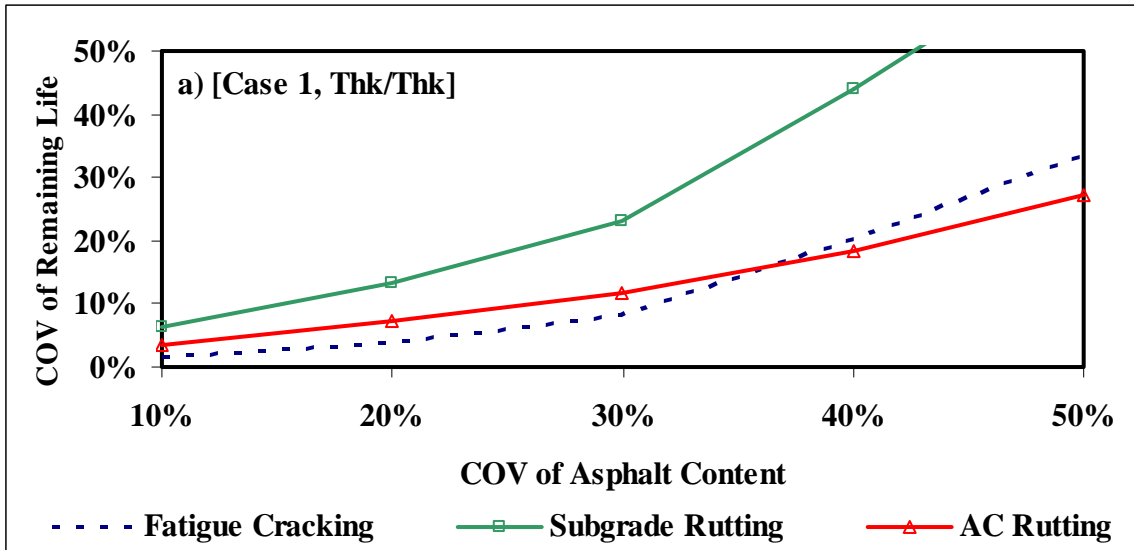


Figure A4 - Results of Impact of Variability of Asphalt Content on Remaining Life Varying AC Modulus for Thick-Thick Section

Table A1 - Summary of Results of Impact of Variability of Asphalt Content on Remaining Life Varying AC Modulus

Case	COV	Fatigue Cracking				Subgrade Rutting				AC Rutting			
		Tn/Tn	Tn/Tk	Tk/Tn	Tk/Tk	Tn/Tn	Tn/Tk	Tk/Tn	Tk/Tk	Tn/Tn	Tn/Tk	Tk/Tn	Tk/Tk
1	10%	15%	12%	2%	2%	2%	2%	9%	6%	2%	2%	4%	3%
	20%	33%	25%	4%	4%	4%	5%	18%	13%	5%	5%	8%	7%
	30%	60%	39%	9%	8%	6%	7%	35%	23%	7%	8%	13%	12%
	40%	87%	51%	17%	20%	10%	10%	59%	44%	10%	10%	18%	18%
	50%	108%	81%	39%	33%	16%	14%	116%	67%	13%	13%	30%	27%
2	10%	9%	7%	5%	5%	2%	2%	11%	8%	2%	2%	4%	4%
	20%	17%	14%	12%	10%	4%	5%	25%	17%	4%	4%	9%	8%
	30%	26%	21%	27%	23%	8%	8%	71%	35%	6%	6%	16%	14%
	40%	35%	31%	42%	37%	13%	11%	105%	56%	8%	9%	23%	21%
	50%	48%	39%	68%	61%	18%	15%	151%	90%	10%	11%	34%	30%
3	10%	4%	2%	8%	7%	3%	2%	13%	9%	2%	2%	5%	4%
	20%	7%	5%	17%	19%	6%	5%	29%	24%	3%	3%	10%	10%
	30%	11%	9%	36%	25%	12%	9%	70%	32%	6%	5%	18%	14%
	40%	15%	11%	64%	48%	20%	15%	146%	65%	8%	8%	27%	21%
	50%	22%	16%	90%	78%	32%	19%	177%	106%	11%	10%	38%	33%

APPENDIX B

RESULTS OF THE SENSITIVITY STUDY FOR AIR VOIDS OF AC LAYER

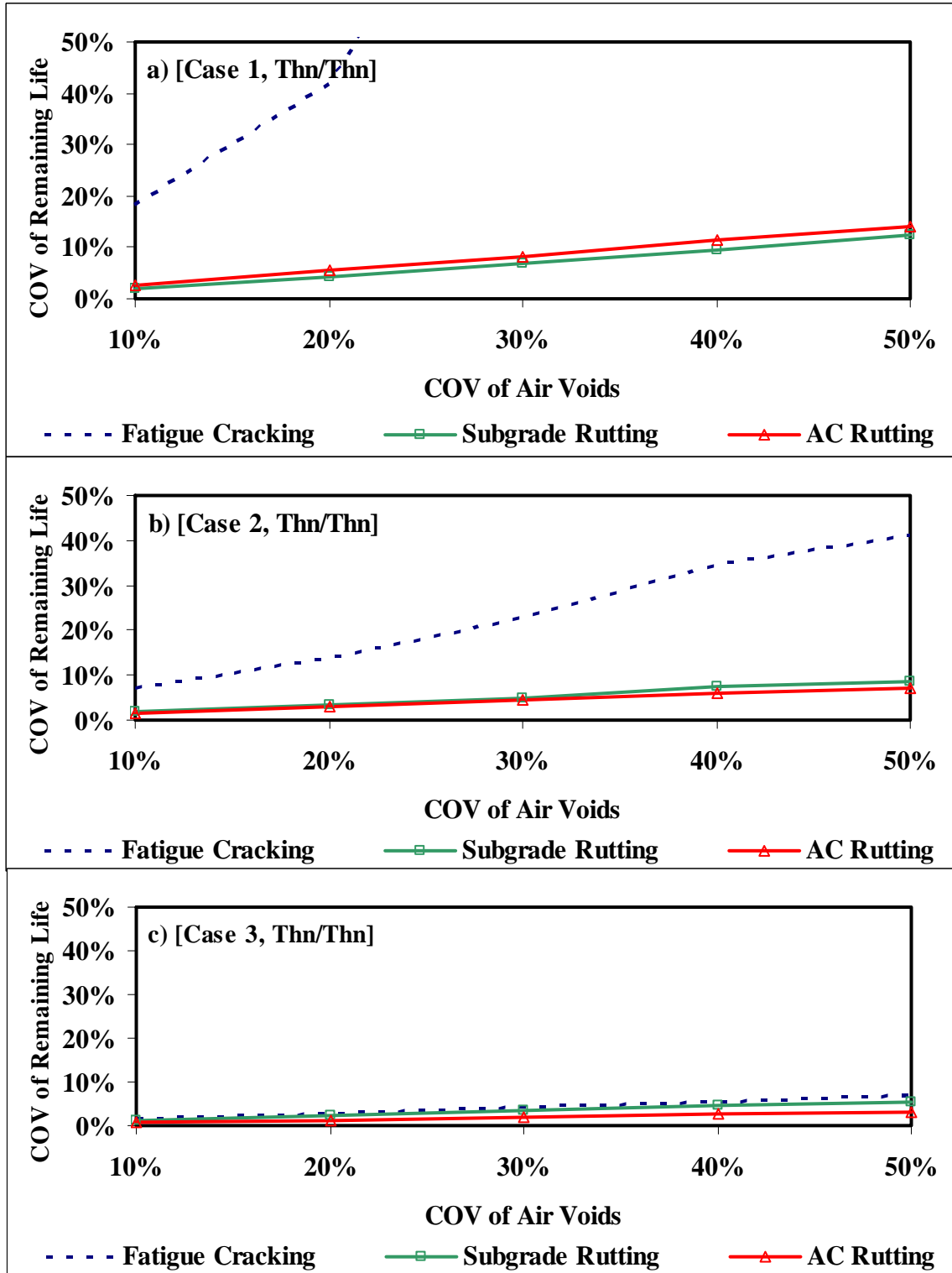


Figure B1 - Results of Impact of Variability of Air Voids on Remaining Life Varying AC Modulus for Thin-Thin Section

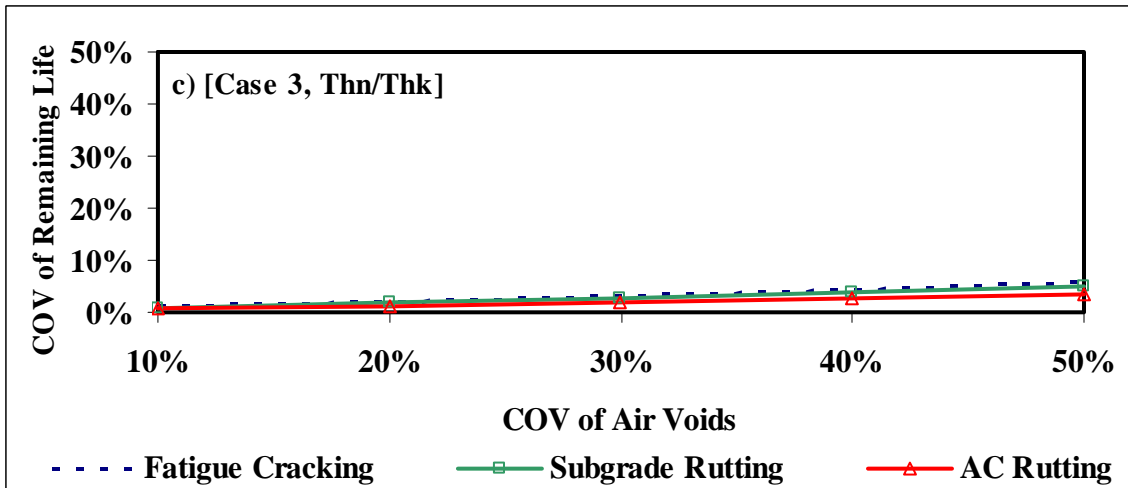
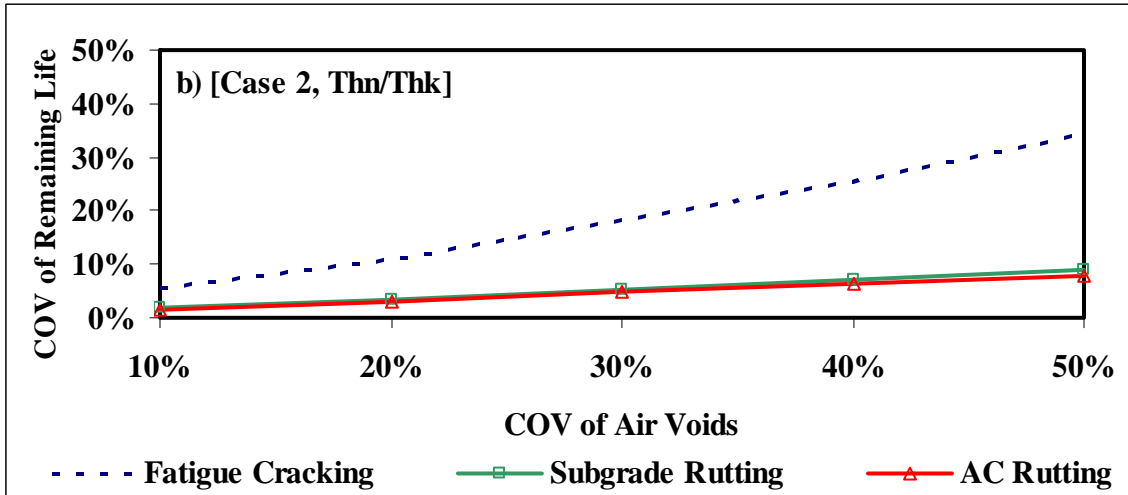
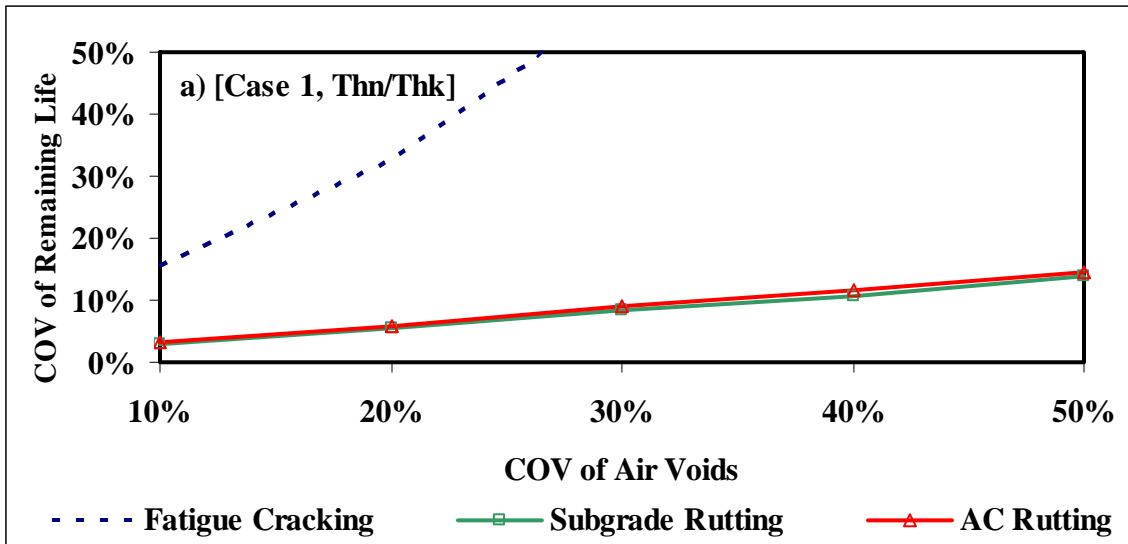


Figure B2 – Results of Impact of Variability of Air Voids on Remaining Life Varying ACP Modulus for Thin-Thick Section

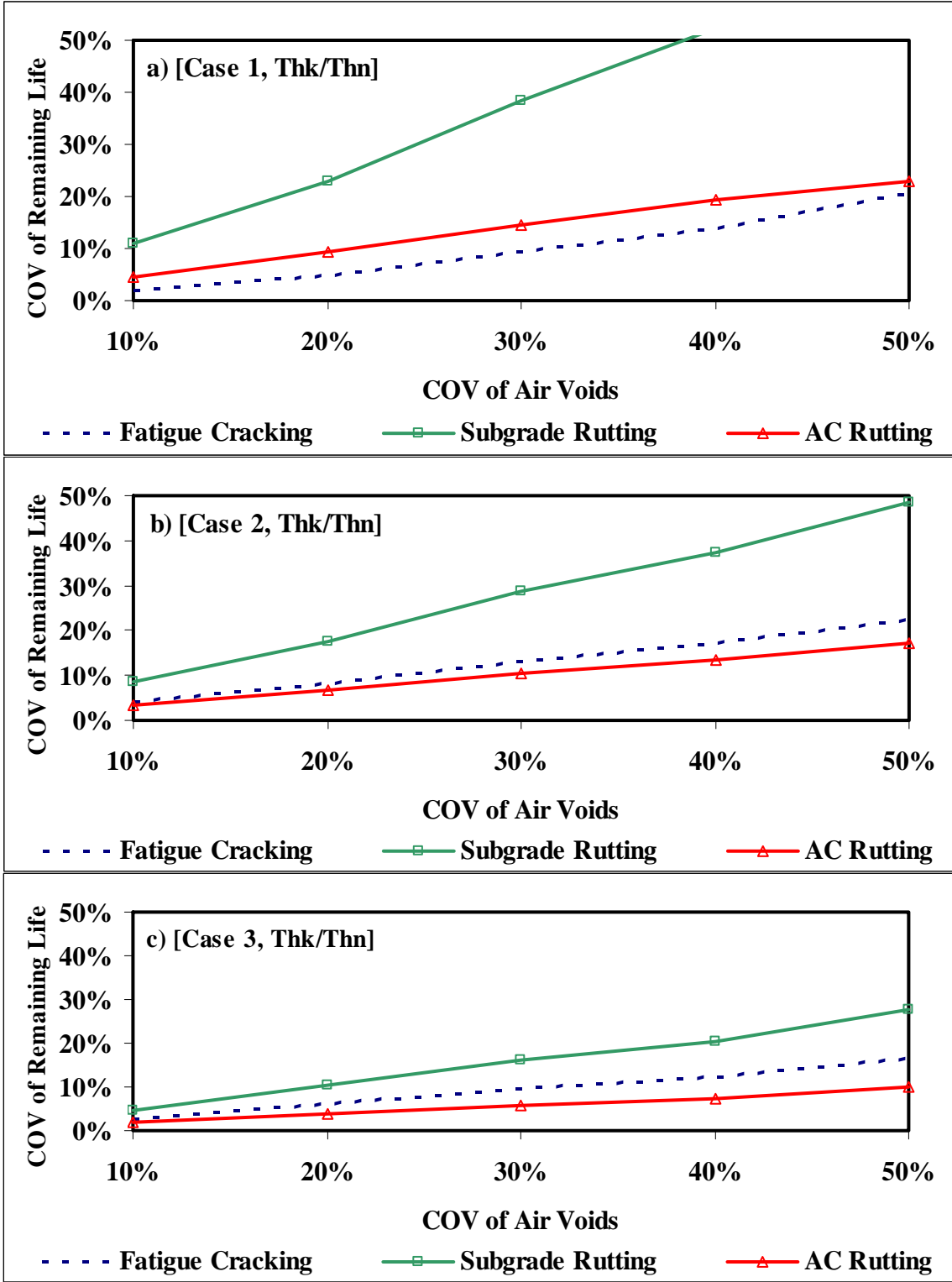


Figure B3 – Results of Impact of Variability of Air Voids on Remaining Life Varying ACP Modulus for Thick-Thin Section

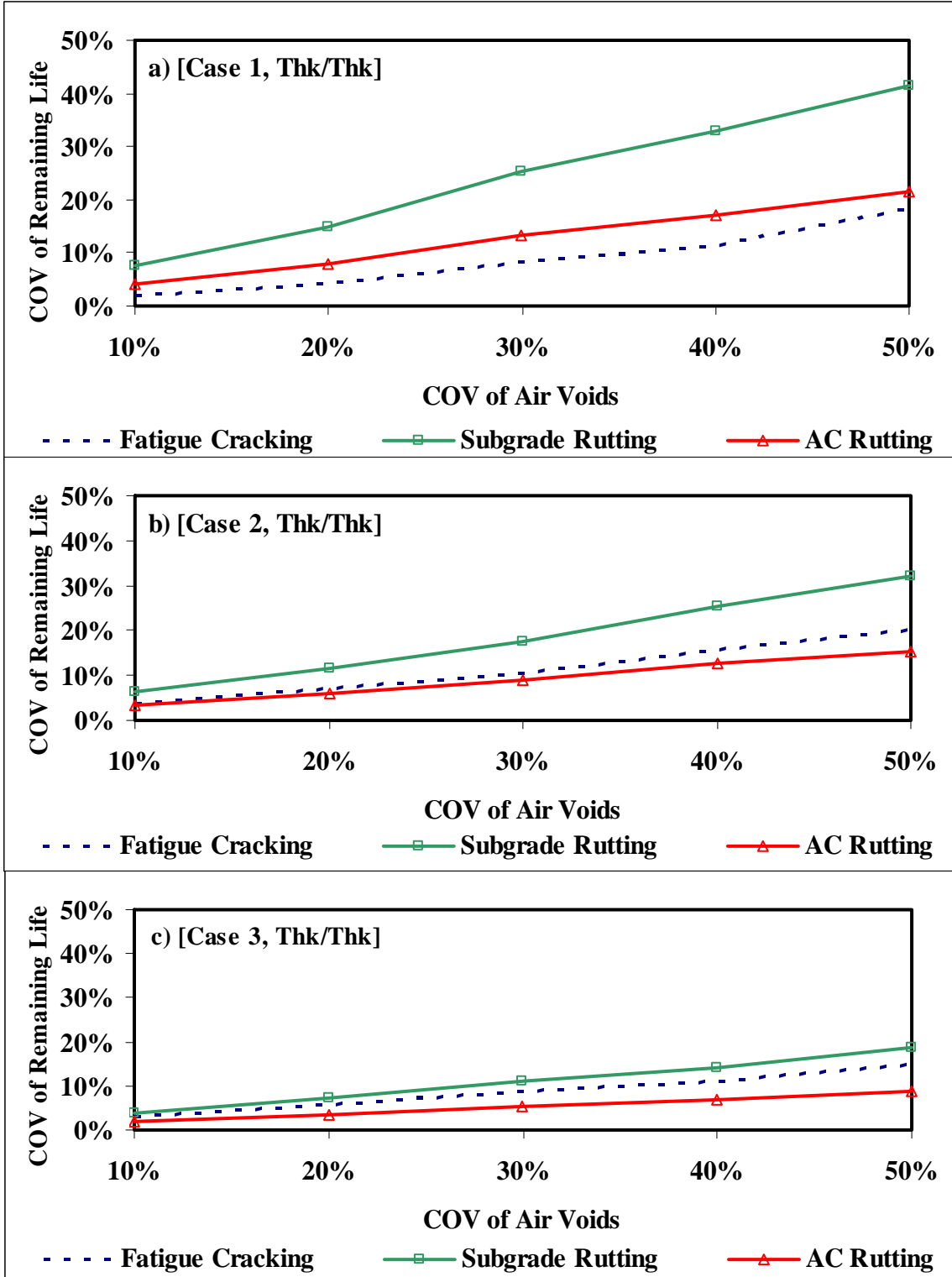


Figure B4 – Results of Impact of Variability of Air Voids on Remaining Life Varying ACP Modulus for Thick-Thick Section

Table B1 - Summary of Results of Impact of Variability of Air Voids on Remaining Life Varying AC Modulus

Case	COV	Fatigue Cracking				Subgrade Rutting				AC Rutting			
		Tn/Tn	Tn/Tk	Tk/Tn	Tk/Tk	Tn/Tn	Tn/Tk	Tk/Tn	Tk/Tk	Tn/Tn	Tn/Tk	Tk/Tn	Tk/Tk
1	10%	18%	16%	2%	2%	2%	3%	11%	8%	3%	3%	5%	4%
	20%	42%	32%	5%	4%	4%	5%	23%	15%	5%	6%	9%	8%
	30%	100%	59%	9%	8%	7%	8%	39%	25%	8%	9%	14%	13%
	40%	238%	120%	14%	11%	9%	11%	52%	33%	11%	11%	19%	17%
	50%	1728%	281%	21%	18%	12%	14%	62%	41%	14%	14%	23%	21%
2	10%	7%	5%	4%	4%	2%	2%	9%	6%	2%	2%	3%	3%
	20%	14%	11%	8%	7%	3%	3%	18%	12%	3%	3%	7%	6%
	30%	23%	18%	13%	11%	5%	5%	29%	17%	4%	5%	10%	9%
	40%	35%	25%	17%	16%	7%	7%	37%	25%	6%	6%	14%	13%
	50%	41%	34%	23%	20%	9%	9%	49%	32%	7%	8%	17%	15%
3	10%	1%	1%	3%	3%	1%	1%	5%	4%	1%	1%	2%	2%
	20%	3%	2%	6%	6%	2%	2%	10%	7%	1%	1%	4%	3%
	30%	4%	3%	10%	9%	4%	3%	16%	11%	2%	2%	6%	5%
	40%	5%	4%	12%	11%	5%	4%	20%	14%	3%	3%	7%	7%
	50%	7%	6%	17%	15%	5%	5%	28%	19%	3%	3%	10%	9%